Fall 12-20-2020

Development, Design, and Utilization of a Reflective Based Photoplethysmography Sensor

Madeline Mazjanis
University of Maine, madeline.mazjanis@maine.edu

DEVELOPMENT, DESIGN AND UTILIZATION OF A REFLECTIVE BASED

PHOTOPLETHYSMOGRAPHY SENSOR

By

Madeline Mazjanis

B.A. University of Maine Bioengineering, 2017

A THESIS

Submitted in Partial Fulfillment of the

Requirements for the Degree of

Master of Science in Biomedical Engineering

The Graduate School

The University of Maine

December 2020

Advisory Committee:

Dr. Michael Mason, Professor of Chemical and Biomedical Engineering, Advisor

Dr. Karissa Tilbury, Professor of Biomedical Engineering

Dr. Todd O'Brien MD, Doctor of Podiatric Medicine

DEVELOPMENT, DESIGN AND UTILIZATION OF A REFLECTIVE BASED PHOTOPLETHYSMOGRAPHY SENSOR

By Madeline Mazjanis

Thesis Advisor: Dr. Michael Mason

An Abstract of the Thesis Presented

in Partial Fulfillment of the Requirements for the

Degree of Master of Science

(in Biomedical Engineering)

December 2020

Plethysmography refers to the dynamic measurement of biological tissue volumes that, for example, may change due to fluctuations in blood volume. Photoplethysmography (PPG) makes use of the attenuation of light penetrating into vascular tissues to determine these changes in blood volume. Modern PPG is an optical technique involving low cost photosensors and light emitting diodes (LED), and is capable of measuring multiple biological vitals simultaneously. For example, in addition to heart rate determination, PPG devices can be used as pulse oximeters, capable of calculating the blood oxygen saturation (SpO_2) through a series of simple optical calculations performed on either reflectance or transmittance data. In this project, a reflectance-based PPG pulse oximeter was designed to collect blood volume measurements on the foot of a patient. This project also involves using the PPG sensor to determine the effect of vibrational signal on vasoconstriction in the tissue, to provide more information on biological properties, including diabetic nerve damage. The device is constructed via dual wavelength light sources and a phototransistor where the light sources are determined based on the isosbestic point, for oxygenated and deoxygenated hemoglobin.

ACKNOWLEGEMENTS

TABLE OF CONTENTS

LIST OF TABLES

LIST OF FIGURES

LIST OF ABBREVIATIONS

AC   ALTERNATING COMPONENT

AV   ATRIOVENTRICULAR VALVES

bpm   BEATS PER MINUTE

CPU   COMPUTER PROCESSING UNIT

DC   DARK COMPONENT

EDV   END-DIASTOLIC VOLUME

EKG/ECG   ELECTROCARDIOGRAPH

ETF   ELECTRONIC TUNING FORK

GUI   GRAPHICAL USER INTERFACE

IR   INFRARED

LED   LIGHT EMITTING DIODE

LPF   LOW PASS FILTER

MS   MICROPROCESSOR SYSTEM

O_2 OXYGEN

CO2   CARBON DIOXIDE

Hb   DEOXYHEMOGLOBIN

HbO_2 OXYHEMOGLOBIN

HR   HEART RATE

HPF   HIGH PASS FILTER

PaO_2 ARTERIAL PARTIAL PRESSURE OF OXYGEN

PCB   PRINTED CIRCUIT BOARD

Pco_2 PARTIAL PRESSURE CARBON DIOXIDE

POC   POINT OF CARE

Po_2 PARTIAL PRESSURE OXYGEN

$PtcO_2$ TRANSCUTANEOUS PARTIAL PRESSURE OF OXYGEN

PVC   PREMATURE VENTRICULAR CONTRACTION

RBC   RED BLOOD CELLS

SCD   SUDDEN CARDIAC DEATH

SD   STANDARD DEVIATION

SNR   SIGNAL TO NOISE RATIO

SO_2 SATURATION OF OXYGEN

SpO2   PERIPHERAL OXYGEN SATURATION

SV   STROKE VOLUME

WBC   WHITE BLOOD CELLS

CHAPTER 1

1.0   INTRODUCTION

The development design and utilization of a photoplethysmography sensor will be discussed throughout the extent of this thesis. In America and throughout the world there is an increasing number of health concerns. Some of the most common diseases such as cancer, heart disease and diabetes, can be fatal and often require constant medical monitoring to ensure good health. As technology advances, monitoring and assessing health is becoming easier and more accessible. The development of point-of-care medical tools, capable of monitoring and providing instant results, have led to the advance in medicine. These, small, compact, and easy to use medical devices can provide quick and easy monitoring of vitals as well as provide instant results for more advanced monitoring. Similarly, medical devices that are non-invasive and do not require skin penetration excel above the rest due to the decrease risk of infection. Designing medical devices should incorporate all of the described characteristics and should provide a tool that makes medical diagnostics and monitoring easier and more convenient.

Diabetes, a major medical disease and a growing concern in the United States, is incurable and if not treated appropriately can lead to adverse health effects. Continuous monitoring of the disease is necessary to track patient's health and monitor degradation. One of the most common effects of diabetes is nerve damage and degradation. An electronic tuning fork can be used to determine nerve damage caused by prolonged untreated diabetes. The tuning fork is an example of a medical device that can be utilized remotely and provide accurate instant results. There are many other medical devices widely utilized in the medical field, that monitor and evaluate vitals. The ease of use of the device and the time to results are critical when it comes to the effectiveness of these tools.

An electronic tuning fork is utilized as a point of care medical tool to evaluate nerve damage, in diabetic patients. The project goal is to incorporate a blood oxygen sensor into the electronic tuning fork, developing a device capable of evaluating the nerve damage and blood oxygen

levels. The device becomes more critical to doctors as it now provides two medical statistics instantaneously. Throughout the extent of this thesis the design and development of a blood oxygen sensor to incorporate into the electronic tuning fork, will be discussed in detail. The oxygen sensor is designed optimize the signal and provide doctors with more accurate results. The combined device will be beneficial to the medical field, and give doctors a faster and easier way to tests and evaluate patient health.

1.1   The Importance of Medical Device Technologies

As technology advances in all fields of science, the development of more versatile and compact medical diagnostic devices becomes available. Measuring biological vitals such as heart rate, body temperature and blood pressure are important indicators of one's health. A specific example of vital sign abnormality is heart rate variation, which can be an indication of many health concerns such as, the effects of disease, chemical imbalances, or other biological abnormalities. Monitoring heart rate can provide an indication of detrimental clinical health events, such as heart failure, or abnormal heart rates (e.g. Tachycardia, Arythmias, or premature contractions). If a patient is experiencing a continuous heart rate above 100 beats per minute, this is faster than normal, and known as tachycardia[1]. Monitoring patient vitals can be critical to determining health and can indicate serious medical abnormalities. According to a number of studies, changes in vital signs occur several hours before a serious adverse event[2]. It is important to constantly monitor vital signs; heart rate was provided as an example, but all health statistics are useful in determining the health of a patient. The importance of monitoring vital signs is evident, but the frequency and how best to monitor them is often disputed[2]. A study performed at a hospital in England determined that 31% of preventable deaths were a result of poor clinical monitoring[3]. Providing easy to use medical devices capable of monitoring vitals could lead to, earlier indication of a critical event, more extensive monitoring of disease progression, and better prolonged tracking of ill patients.

Diabetes causes degradation in many systems throughout the body, the disease is a result of high blood sugar which can lead to kidney failure, destruction of blood vessels and nerve damage.

2

The disease causes severe autonomic dysfunction leading to sudden cardiac death, continuous monitoring of heart rate can decrease this risk[4]. Many diseases can cause heart failure, often seen as abnormalities in heart rate, leading medical device companies to explore a number of approaches to continuous monitoring of vitals [1]. Over time this has resulted in increased device mobility and utility, tending towards decreased size and complexity.

Handheld devices such as personal digital assistants (PDAs) have become increasingly popular in the medical field[5]. Many PDAs involve recording and tracking information at point-of-care testing, allowing medical data to be stored throughout patient interaction. Point of care (POC) technologies have increased in popularity over the last 40 years, due to the changes in health care to deliver convenient and cost effective aid[6]. Most POC technologies are chemical diagnostic testing, such as blood glucose or other handheld fluidic testing devices, these usually require a finger prick or some invasive measure to acquire the biological material for testing. More popular POC devices include non-invasive technologies such as pulse oximeters, breathalyzers and other biological monitoring devices[7]. These compact non-invasive POC medical devices support growth in biological monitoring technologies. New non-invasive medical monitoring technologies give doctors easy to use testing devices with rapid results.

1.1.1 The Combination of Medical Devices to Advance Patient Care

As POC, and other medical devices become more capable, there is an increasing number of tools utilized to monitor and measure vital signs. Doctors will often evaluate multiple tests and vital monitoring to get a more in depth understanding of the patient's health. There are usually multiple devices needed to collect different vital statistics. For example, heart rate is measured using an ECG, blood pressure with a pressure cuff, temperature with a thermometer, etc. Combining various medical devices to incorporate all monitoring at once, not only reduces monitoring time, but provides paralleled medical results. For example, there are benefits of monitoring blood oxygen and heart rate simultaneously, as the blood oxygen decreases, heart rate might increase in attempts to provide more oxygen to the body. Measuring multiple vitals simultaneously provides doctors with more diagnostic information without needing to preform

multiple tests. A study evaluating patient vital signs found that patients with one abnormal value had an in-hospital mortality rate of 0.9% but if the patient had three abnormal values they had an in-hospital mortality rate of 24%[3]. Combining medical devices to monitor an assortment of biological vitals is efficient but difficult to execute. It is challenging to design a single accurate medical device with two separate devices that have varying points of contact, different biological collection processes and inconstant data acquisition techniques. All of those differences are important when designing handheld medical devices with numerous medical capabilities.

1.2   Diagnostics for Diabetic Neuropathy

Neuropathy of the lower extremities resulting from diabetes is a growing concern in the US with serious consequences. According to the CDC, 26.9 million people in the United States have been diagnosed with diabetes[8]. A result of prolonged untreated diabetes is neuropathy, where the nerves degrade due to lack of blood flow from increased blood glucose levels. Diabetic neuropathy usually starts as a loss of sensation in the extremities but can manifest into pain and inability to judge temperature. Further nerve damage can lead to atrophy (loss of muscle) in lower extremities resulting in loss of function and deformation[9]. Diabetic neuropathy is an extremely common disease, research suggests about 50% of those diagnosed with diabetes will develop peripheral neuropathy[6]. It is also suggested that it is impossible to accurately approximate the prevalence of the disease due to the variation in diagnostic criteria. A common practice for evaluating diabetic neuropathy involves vibratory sensation, where a 128-Hz tuning fork is held on the bottom of the foot. An abnormal response is recorded when the patient loses sensation and the examiner can still feel the vibration, the examiner will give a score between 0 and 3 depending on the extent of nerve damage[11].
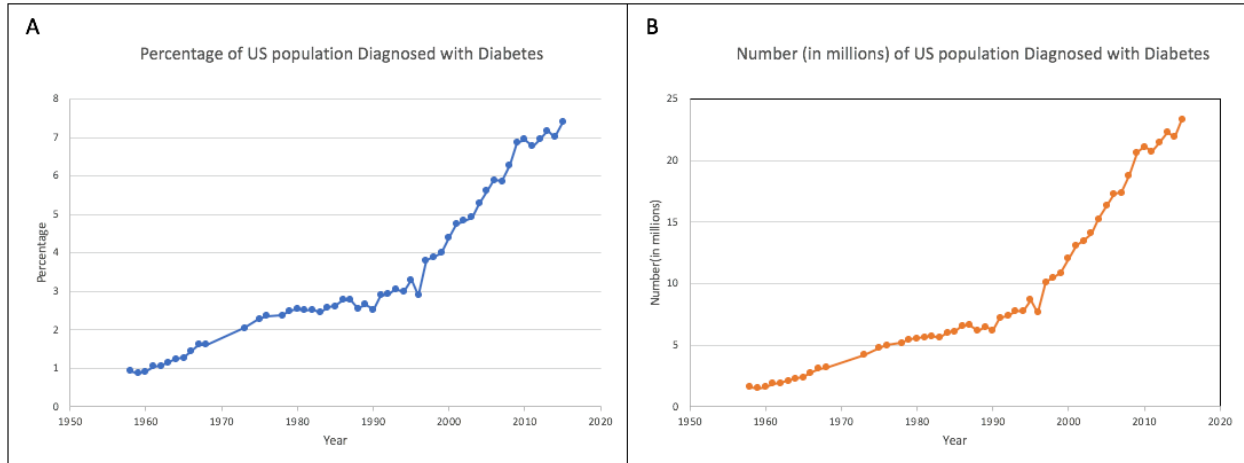
Figure 1.1: [A] Percentage of US population diagnosed with diabetes from 1958-2015. [B] Number of US population diagnosed with diabetes from 1958-2015. Image reproduced from [12]

Because diabetes is one of the most common diseases there are many methods to indicate how the disease is advancing in the body. As we discussed above neuropathy is a significant adverse effect of the disease measurable by a vibrational signal. Another result of diabetes is degradation of blood oxygen to the peripherals. Diabetes causes blood flow to decrease and many of the extremities to lose blood circulation, leading to the neuropathy. It is important to monitor blood oxygen in the extremities to evaluate the degradation of blood circulation. The combination of a tuning fork utilized on the foot of a diabetic patient that is also capable of monitoring the blood oxygen would be beneficial to further understand the extent of the diabetes in the patient.

1.3   Project Specific Aims

The Electronic Tuning Fork (ETF) is an example of a handheld medical sensor that can deliver POC diagnostics to a patient. The device is used to test the extent of neuropathy (damaged nerves) in patients who have diabetes. The ETF produces quantitative data to the extent of nerve damage and eliminates testing with tuning forks. The device is a small compact instrument that vibrates at specific frequencies, similar to the mechanical tuning forks. The ETF device is placed on the foot at a high vibrational amplitude, and slowly decreases until the patient can no longer feel the vibration. The time at which the patient lost vibrational sensation is recorded and represents the extent of nerve damage. The ETF provides a controlled and accurate way to define nerve damage. The device is designed to quantify the nerve damage and eliminate variation, seen

with the mechanical tuning fork, across doctors. Adding more medical diagnostic tools to the ETF would advance the device potential and usability in POC treatment.

Todd O'Brien, DPM the founder of O'Brien Medical LLC, launched the first Electronic Tuning Fork (ETF[128]) in 2015 and now has the more advanced ETF[MX]. O'Brien Medical LLC was looking to advance the ETF by addition of a blood oxygen monitor to the device. O'Brien connected with the University of Maine Bioengineering program to advance his device. I was tasked with the project to develop a blood oxygen sensor that could integrate into O'Brien's electronic tuning fork.

Aim 1: The first goal of the thesis is to design a pulse oximeter to fit into the ETF, allowing the examiner to collect information on the patients' diabetic nerve damage and blood oxygen saturation simultaneously using a single device. Construction of an operational blood oxygen sensor requires reverse engineering of current pulse oximeters and evaluation of optimal optical components. Research and evaluation of optical physics and light attenuation utilized to evaluate oxygen saturation in the blood is necessary to ensure accurate device construction. After research, optimal optical components, and device design are determined. The design of the device must allow for integration into the ETF. Further construction requires development of PPG boards created with the help from electrical engineers.

Aim 2: After designing an accurate blood oxygen sensor into the ETF, the final goal was to redesign the tuning fork cap to optimize the designed sensor. This involves research and understanding of light and it's physical properties through dermal material. The goal was designing a mechanical covering to optimize the amount of light that was penetrating into the skin and returning to the sensor. Testing requires changing the direction of light using various caps and evaluating the returned signal. 3D-printed caps must be designed to direct the light in different directions and the pulse signal should be evaluated to determine the optimal direction of light.

CHAPTER 2

2.0   BACKGROUND

For the body to maintain homeostasis, all biological components need to be preforming optimally adjusting to conditions and aiming for stability. There are many aspects of human life that can be monitored to determine the state of homeostasis for an individual, such as vital signs which are biological processes that can be observed. Therefore common vital signs are temperature, blood pressure, heart rate (pulse) and respiratory rate. Other vital signs include blood glucose levels, oxygen saturation, and pain. For example, a decrease in pulse, oxygen saturation or temperature can indicate the human body is not operating correctly. If this data is not captured quickly enough, further degradation can occur. This indicates that constant monitoring of vitals can be crucial for saving lives. There are many ways to monitor vitals, which have evolved over the years as technologies have likewise advanced. Today, there are a multitude of sensors utilized in medical facilities to provide constant monitoring of critical biological vitals.

Photoplethysmography(PPG) is an optical signal utilized in medical devices to monitor the heart rate. The signal is a technique that has become popular across the advancing medical technology field and is utilized across most hospitals today. PPG signal technique is applied in pulse oximeters, by means of light absorption and reflection through biological tissues. As the heart pumps blood throughout the body, it carries oxygen from the lungs to the tissues, and a pulsatile signal can be generated from obstruction of light due to increased blood flow. The PPG signal is a waveform which reflects the eb and flow of the heart pumping blood. The PPG signal is derived from Beer's law, where the incident of light exiting a material is proportional to the light entering and the optical characteristics of the material itself.

Understanding the biological and optical components of blood, as well as the components needed to optically record blood volume changes, a PPG signal can be generated. The PPG waveform is utilized in pulse oximeters and is capable of determining the difference between oxygenated and

deoxygenated blood, thus providing blood oxygen saturation. The PPG signal utilized in pulse oximeters is a critical tool to monitor and evaluate the health of an individual.

2.1   Significant Anatomy

Oxygen(O_2) is a vital element to the human body, without it, homeostasis is not maintained, and cells will begin to deteriorate. The process of supplying the body with oxygen relies on gas exchange, which first occurs within the respiratory system, where pressure differences in the lungs cause oxygen to be inhaled. Oxygen enters the blood and is transported throughout the body by means of the heart. The pumping action by specific chambers in the heart facilitates the movement of oxygenated blood from the lungs into the blood vessels, to transport it throughout the body. The heart is a vital organ that is capable of self-regulating to the body's cardiac output needs. The heart pumps blood from the lungs into first the arteries then the arterioles and finally capillaries. Once the oxygenated blood reaches the capillaries gas exchange occurs and oxygen from the red blood cells (RBCs) is transferred to the tissues.

2.1.1   Blood and Circulatory System

Blood makes up about 8% of the human body and aids in numerous functions to maintain homeostasis, including regulation of pH, maintaining body temperature, and transportation of vital nutrients throughout the body[13], [14]. Blood consists of two principal components, plasma and formed elements depicted in figure 2.1. Plasma makes up about 55% of the blood, and the formed elements account for the remaining 45%. The plasma portion of the blood is a water-based a yellowish fluid that contains <10% of plasma proteins, such as albumin, and other solutes[13], [14]. Of the formed elements in the blood, 95% are red blood cells (RBCs), the other 5% are white blood cells (WBCs) and platelets[14]. The WBCs provide protection against infections and disease, platelets coagulate to prevent bleeding, and RBCs transport nutrients and waste[15].
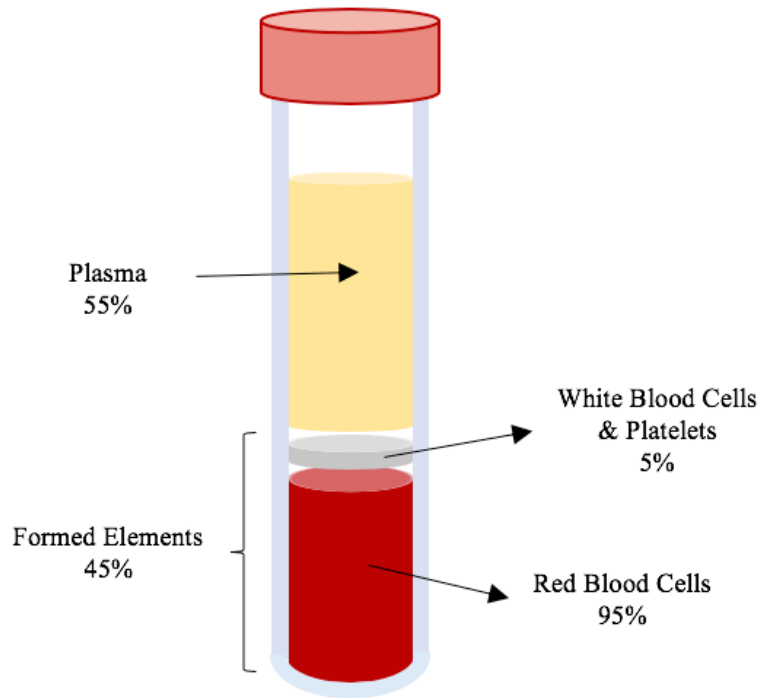
Figure 2.1: Separation of blood, and approximate values of components in a normal adult.

Erythrocytes, or red blood cells (RBCs), primary functions are delivery of O_2 to tissues and removal of carbon dioxide(CO_2) as waste[13]. RBCs shape is similar to a flat disc, but the outside edges are thicker than the inside center to increase the cell's surface area. The greater surface area allows O_2 and CO_2 to diffuse across the tissues more rapidly and the thin center adds flexibility to pass through smaller blood vessels[13], [14]. RBCs transport approximately 98.5% of the O_2 in the blood to the tissues, the other 1.5% is dissolved in the blood plasma[14].

The main component of RBCs is hemoglobin (Hb), which gives the cell the ability to transport oxygen. The hemoglobin molecule consists of four globin protein chains, each chain contains a non-protein heme group illustrated in figure 2.2. Iron, in the heme, facilitates the binding of oxygen (O_2) molecules to the RBCs, because the hemoglobin molecule contains four irons it has the capacity to bind four O_2 molecules to each hemoglobin molecule[13]. Hemoglobin on the

RBCs collect oxygen in the lungs and transport the gas to the tissues through the blood vessels. Once the oxygenated RBC reaches the systemic capillaries the O_2 molecule is released and a CO_2 molecule is collected. The RBC with bound CO_2 then travels back through the blood vessels to the lungs where the CO_2 is exhaled[13]–[15].

When oxygen is bound to hemoglobin it is referred to as oxyhemoglobin(HbO_2) and has a bright red appearance[14]. Another form of hemoglobin is deoxyhemoglobin (Hb) where no oxygen is bound to the heme group on the RBC. Some hemoglobin molecules have lost the ability to bind oxygen and lead to limited oxygen supply.
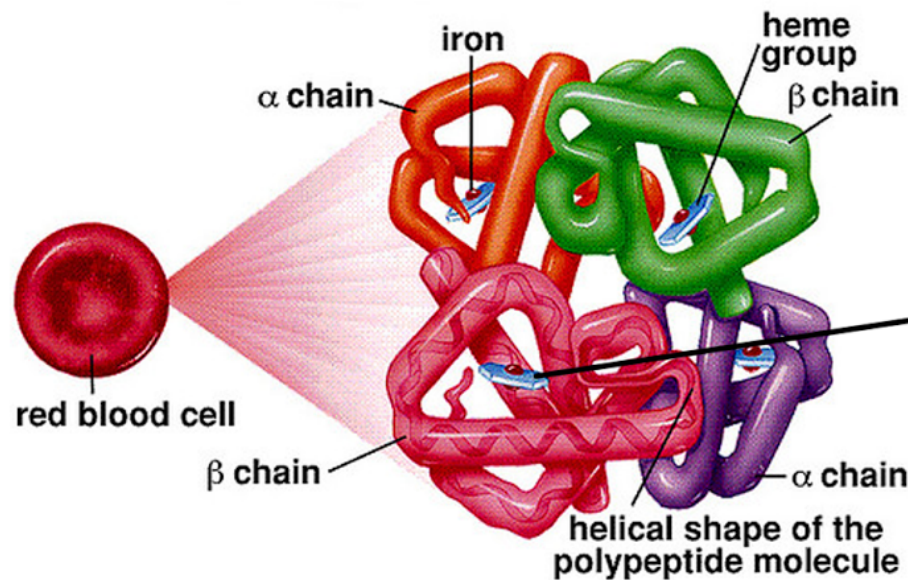
Figure 2.2: The Red blood cell is comprised of a hemoglobin molecule which contains 4 chains each with an iron group. The iron group on the chains binds to the oxygen in the lungs and transports it to the tissues.

All tissues utilize O_2 to operate and perform biological tasks, because of this RBCs are vital to maintain biological homeostasis, without them tissues would not receive oxygen, coincidentally diminishing functionality.

2.1.2 Respiratory System

The respiratory system in the body consists of an upper respiratory tract and a lower respiratory tract. The upper tract consists of the external nose, nasal cavity, pharynx, and associated structures, and the lower respiratory tract includes the larynx, trachea, bronchi, and lungs[13], [14]. Humans have two lungs located below the ribs in the upper trunk of the body. Each lung is branched off into lobes called lobar bronchi, which are further segmented into bronchioles, terminal bronchioles and finally alveoli[14]. Alveoli are small air filled chambers that facilitate gas exchange in the blood[14].
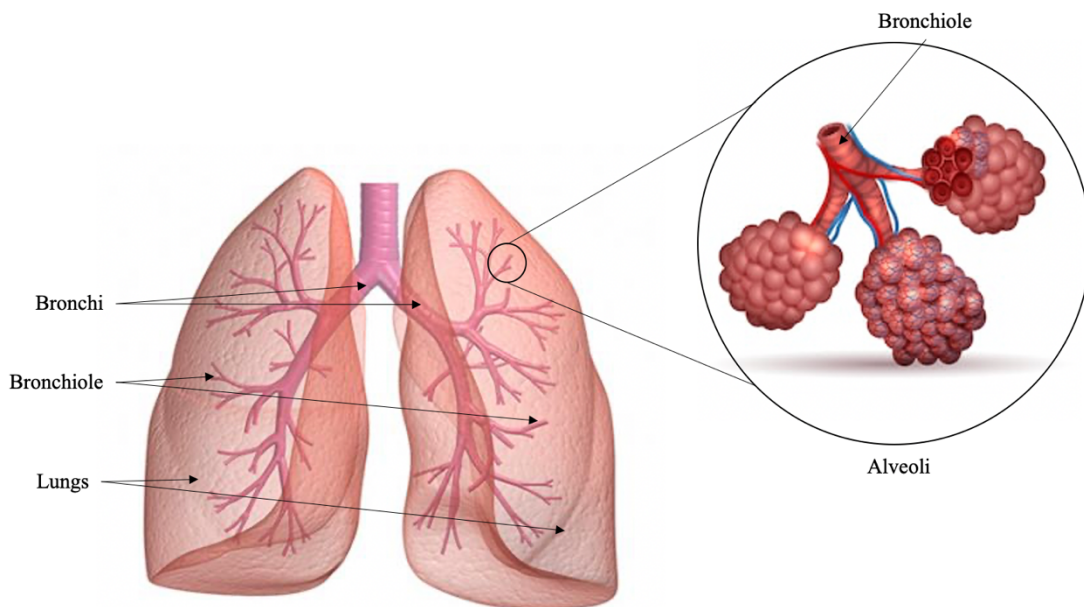
Figure 2.3: Anatomy of the lungs; two lungs a left and a right are separated from the trachea by the bronchi, within the lungs the bronchi segregate into bronchioles, leading to the alveoli. The alveoli are responsible for the gas exchange between lungs and the blood, facilitating CO_2 removal from blood to be exhaled and diffusion of O_2 inhaled into the blood.

Ventilation, the process of moving air in and out of the lungs, is divided into inhalation and exhalation[14], [15]. Respiratory ventilation is governed by principles of flow and pressure, the difference between the external pressure (atmospheric) and the pressure inside the lungs (intrapulmonary pressure) drives inhalation and exhalation[13]. Air enters the body and travels

through the lungs into the alveoli, where the O_2 readily transfers into the blood and CO_2 transfers from the blood to the lungs to be exhaled[13]. The alveoli have a thin membrane surrounded by pulmonary capillaries containing deoxygenated blood[15]. The transfer of gasses, or gas exchange is driven by the physics of partial pressure, where elements will flow to maintain equilibrium[13]. After inhalation the partial pressure of oxygen (Po_2) is higher in the alveoli then in the surrounding capillaries, thus driving the diffusion of oxygen from the lungs into the blood[16]. The reverse will happen for the CO_2 where the partial pressure of CO_2 (Pco_2) in the lungs is lower than the Pco_2 in the blood, thus the CO_2 from the blood will flow into the lungs and be exhaled[16].

Oxygen travels from the lungs into the blood and binds to the hemoglobin, once bound the oxygen is carried to the tissues where it released it in the systemic capillaries[15]. The hemoglobin binds or disassociates with the oxygen molecule depending on the surrounding partial pressure of oxygen[14]. In the systemic capillaries the Po_2 is lower than the Po_2 of the blood, causing the O_2 molecule to disassociate with the hemoglobin and move into the tissue. Partial pressure of oxygen and hemoglobin oxygen saturation (So_2) depict the bodies ability to use and transport oxygen.
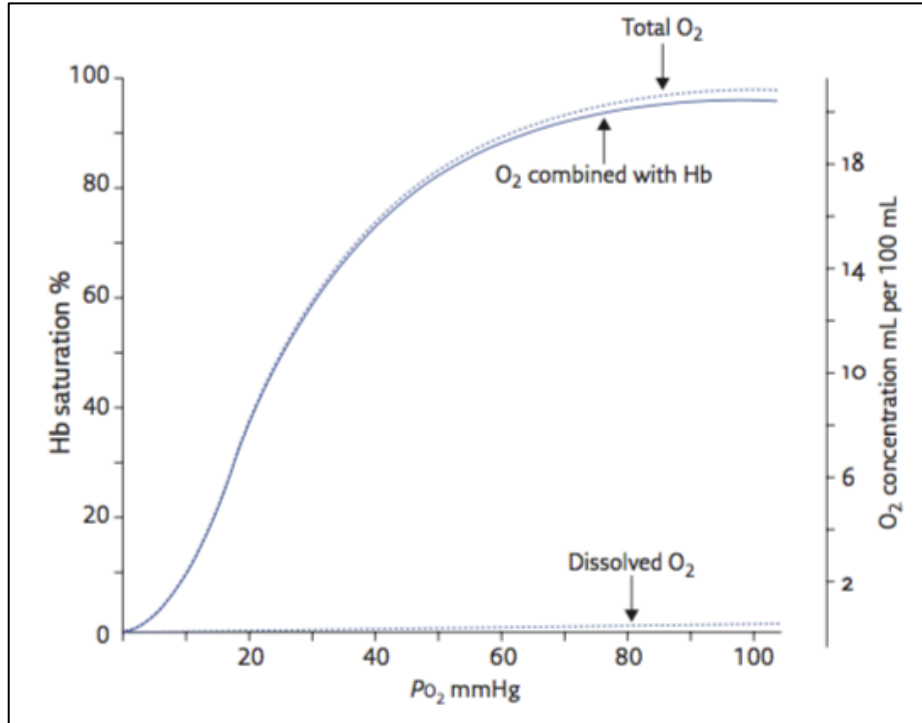
Figure 2.4: The oxygen-hemoglobin dissociation curve. Representing a healthy subject with a normal blood hemoglobin (Hb) concentration. The y- axis represents the hemoglobin saturation as a percentage, and the x-axis shows the partial pressure of oxygen in the blood. The Hb is highly saturated when the PO_2 is at high, and when the PO_2 is low the Hb saturation is low. The correlation is not and when the PO_2 is high the Hb saturation does not change significantly, but when the PO_2 declines the hemoglobin saturation fall rapidly. Image reproduced from[16].

The saturation of oxygen (So_2) is relative to the number of binding sites on a hemoglobin molecule[16]. Consequently, A hemoglobin macromolecule that is 100% oxygenated indicates that all four binding sites on the hemoglobin molecule are bound to oxygen, if only two O2 where bound the hemoglobin would be 50% and so on[13]. The oxygen-hemoglobin dissociation curve illustrates the percent saturation of hemoglobin to the partial pressure of oxygen shown in figure 2.4. Generally when the Po_2 increases this is followed by a rise in the oxygen saturation(So_2) [16]. Because the dissociation curve is considerably flat when the Po_2 is greater than 90%, an increase in Po_2 has minimal effects on the hemoglobin saturation. In contrast when the Po_2 is below 90% the hemoglobin saturation drops substantially[16]. The optimal oxygen saturation is between 94-98%[16].

2.1.3   Cardiovascular System

The cardiovascular system along with the circulatory system are responsible for the movement of blood through the body. The heart pumps oxygenated blood from the lungs to blood vessels which travel throughout the body to deposit oxygen. The heart and blood vessels are capable of regulating blood flow and optimizing oxygen transportation.

The heart consist of four chambers, two ventricles and two atria, left ventricle and left atria and right ventricle and right atria[13]. The ventricles are responsible for pushing blood out of the heart to the connecting arteries, thus the ventricles are of greater muscle mass than the atria. The left side of the heart acquires oxygenated blood from the lungs and pumps it throughout the body, whereas the right side of the heart obtains returning deoxygenated blood and pumps it to the lungs[14]. The atrioventricular valves (AV) regulate the opening between the atria and the ventricles.
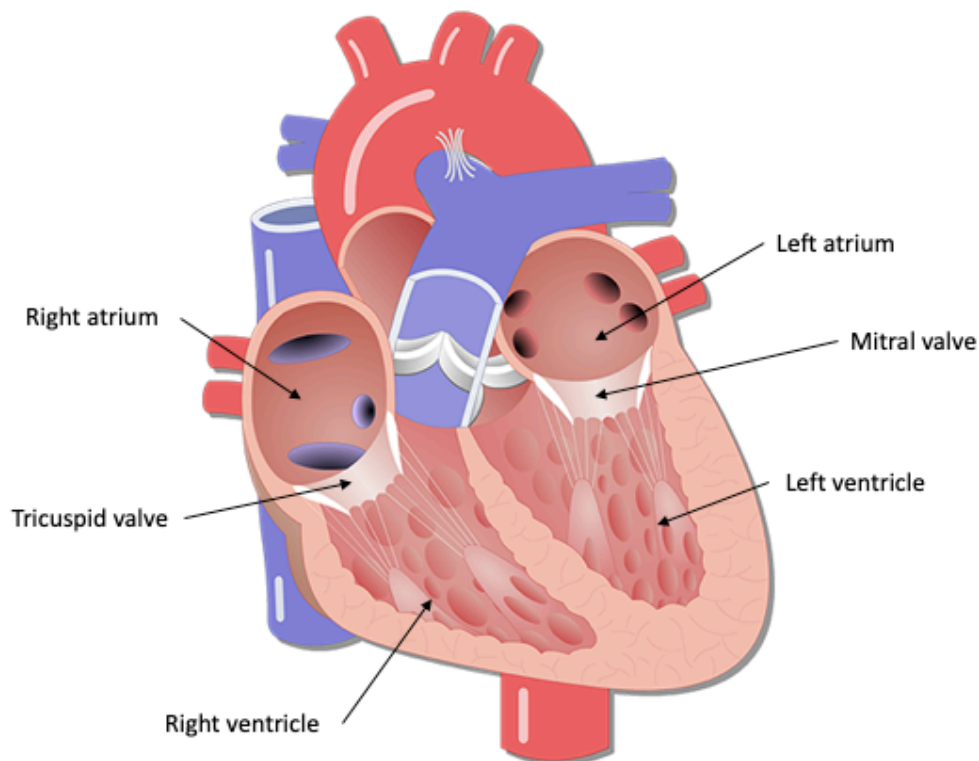
Figure 2.5: Anatomy of the heart, the left atrium fills with blood from the lungs and travels into the left ventricle, the two chambers are divided by the mitral valve. The left ventricle is responsible for contracting and forcing blood throughout the body. On the right side of the heart is the right atrium, responsible for collecting returned blood with CO2, and the right ventricle. The right chambers are divided by the tricuspid valve, the right ventricle contracts to send deoxygenated blood to the lungs to be exhaled.

The cardiac cycle refers to the continuous pumping action of the heart and consists of a complete contraction and relaxation of all four chambers[13], [14]. The cardiac cycle describes the movement of blood through the heart and consists of multiple phases but is often divided into systole and diastole. The terms systole and diastole refer to the contraction and relaxation of the ventricles [14]. Blood first enters the heart through the pulmonary veins, where blood oxygenated from the lungs flows passively into the left atrium. The first phase of the cardiac cycle is ventricular filling where the ventricles are relaxed (diastole) and the AV valves open causing blood from the atrium to flow into the left ventricle[13]. During ventricular filling the

atrium will contract to facilitate complete filling of the ventricle[13], [14]. At the end of this phase each ventricle contains an end-diastolic volume (EDV) about 130mL of blood[13]. The second phase in the cardiac cycle is isovolumetric contraction, where the atria relaxes, and the ventricles begin to contract. The slight contraction of the ventricles causes the AV valves to close and cease the blood flow from the atrium to the ventricle[13]. This forceful closing of the AV valves and vibrations from this cause the first heart sound often referred to as a "Lub" [13], [14]. The third stage of the cardiac cycle is ventricular ejection commonly referred to as systole. In this phase the ventricles forcefully contract increasing the pressure beyond that of the connecting arteries. The semilunar valves open and the blood in the ventricles is driven into the arteries, generating a spike in the aortic pressure[13].

Not all of the blood in the ventricles is ejected into the arteries, the EDV is about 130mL and only about 70mL is expelled, this is known as the stroke volume (SV)[13]. The amount of blood left in the ventricle after total ventricular ejection is the end-systolic volume (ESV), about 54% of the blood is ejected into the arteries[13]. During high intensity exercise the percent ejection can be as high as 90%[13]. The final phase of the cardiac cycle is isovolumetric relaxation, where the ventricles enter diastole and relax. As the ventricles relax a minimal amount of blood from the arteries flows back into the ventricles, this force prompts the semilunar valves to close creating a slight rebound in the aortic pressure, known as the dicrotic notch[13].
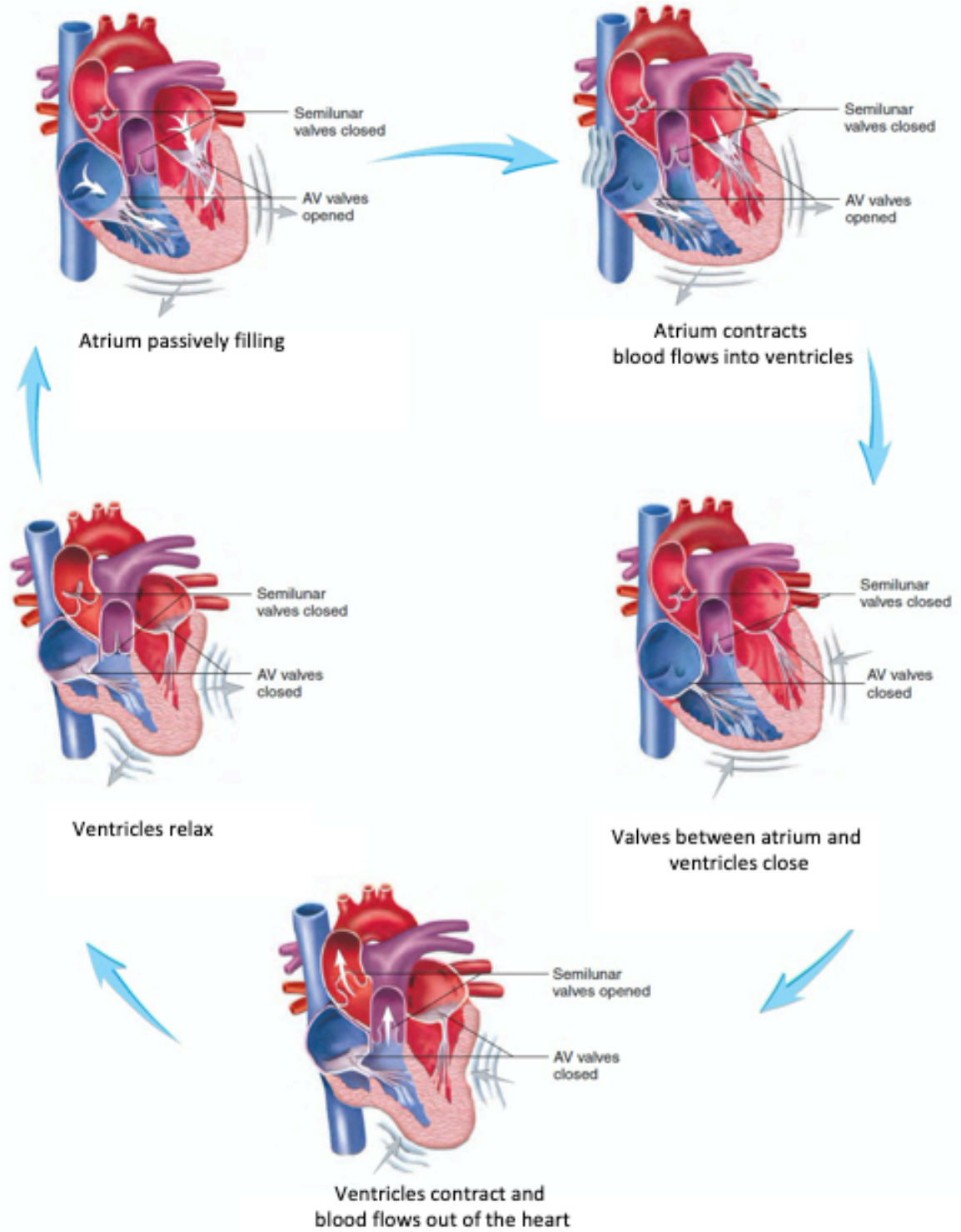
Figure 2.6: Heart contraction Cardiac Cycle starts with the passive flow of blood into the atrium once the blood fills, the atrium contracts forcing blood into the ventricles, the valves between the atrium and the ventricles close and the ventricles begin to contract, when the ventricles contract blood is forced out of the heart and into the body.

As the heart pumps, cycling through the cardiac cycle, blood is forced into the arteries. When the left ventricle contracts blood is forced out of the heart and into the circulatory system via the aorta. The increased blood volume into the aorta forces blood throughout the body, this increases the volume not only at the arteries but throughout all of the circulatory system components. The blood volume throughout the body pulses with the beating of the heart, allowing for heart rate monitoring in all locations with constant blood supply, even the capillary beds.

Variations occurring in the cardiac cycle, also known as arrhythmias, can be attributed to heart failures and lead to death. One benign example of this is premature ventricular contraction (PVC), which interrupts normal heartbeats and causes an irregular pulse. Although PVC can lead to more serious rhythm disturbances that are most often harmless, and detected as a miss beat or a "flip-flop" in the chest[17]. There are various other arrhythmias that are indications of harmful cardiac problems and can be detected as variations in the heartbeat.

2.2   Review of Clinical Techniques for Monitoring Blood Perfusion Vitals

Blood perfusion is necessary to sustain life, it is responsible for the transport of oxygen, nutrients and waste throughout the body[18]. Abnormalities in blood perfusion are used to identify and diagnose biological conditions, consequently monitoring this vital sign is important to sustained health. Blood flow or blood perfusion can be utilized to monitor many vitals such as, heart rate, blood oxygen saturation and blood pressure.

The observation of blood perfusion and blood monitoring techniques have been around for hundreds of years and are still utilized in modern medicine. The first measured heartbeat was said to have been discovered by Herophilus of Alexandria, Egypt (c. 335-280 BC) who designed a water clock capable of timing the pulse[19]. As technology and medical understanding advanced, so did the ability to monitor biological vitals and in the late 1800's the first ECG was

discovered by physician Willem Elbthoven[19]. Since then, the monitoring of pulse and other blood perfusion vitals have advanced throughout medical history. Today technology has advanced tremendously providing easy and affordable access to blood flow monitoring techniques.

2.2.1   Clinical Applications of Heart Rate Monitoring

The clinical need for compact, non-invasive, and easy to use, heart rate monitors has increased throughout medical history. Heart rate is the most important vital that can indicate biological failure, and although heart disease was the leading cause of death in the United States in 2017, there are many other diseases that affect heart rate[20]. Sudden cardiac death (SCD) accounts for 25% percent of the deaths in cardiac patients, monitoring heart rate variability can indicate problems before death occurs[21].

Heart rate is most frequently monitored using an EKG (ECG), in hospital settings, that records the pulsatile signals of heart contractions. Healthy heart beats are characterized as a "lub – dub" sound, but there are many instances where the heartbeat is abnormal. An abnormal heartbeat is referred to as an arrhythmia. There are many causes of arrhythmias, and they usually indicate that the heart is not functioning properly. The most common causes of out-of-hospital cardiac arrest are arrhythmias, specifically, ventricular tachycardia and ventricular fibrillation. If ventricular fibrillation goes undetected, and untreated the arrhythmia is usually fatal[22]. In the medical field monitoring heart rate is critical for patient care. There are many practices utilized for monitoring heart rate, as technology advances these devices have become increasingly more advanced and versatile.

2.2.1.1 Manual Heart Rate Measurement.

There are several techniques that exist for monitoring the heart rate, the most traditional is manually counting the beats at an artery that is close to the surface. The most common arteries that are used for this technique are the radial artery located at the wrist, and the carotid artery on the neck. The manual method requires placing two fingers on either artery and counting the number of pulses that occur in over 15 seconds, then multiplying this number by 4 to get the number of beats per minute(bpm). A healthy adult normally has a resting heart rate between 60bpm to 100bpm[14].
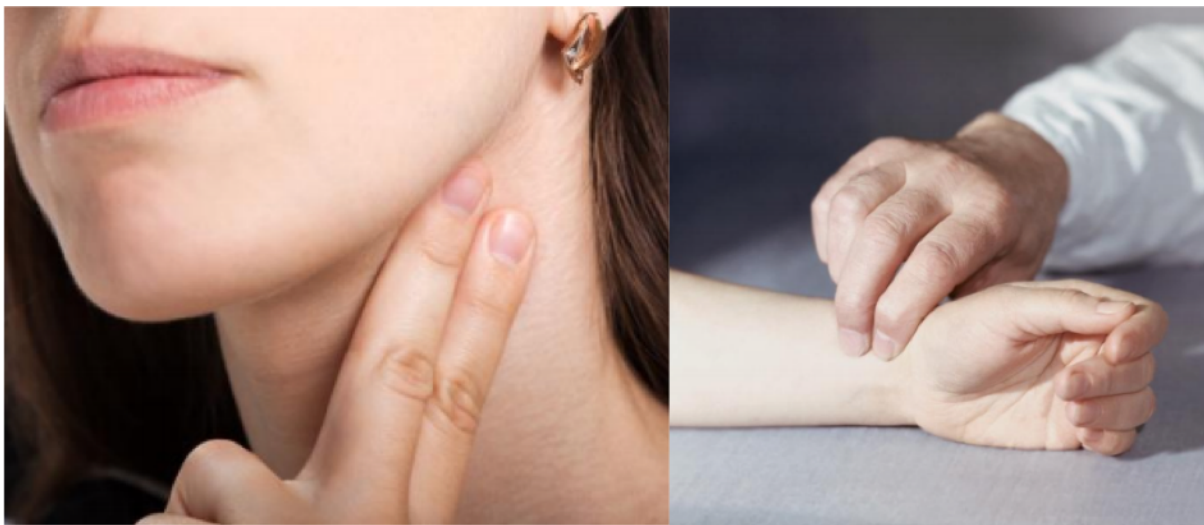
Figure 2.7: Visual descriptions of the manual heart rate measurement method on the carotid artery (left) and the radial artery (right). Image reproduced from [23]*.*

2.2.1.2 Digital Heart Rate Sensors.

The common method for measuring heart rate is digital heart rate sensors. Before the invention of pulse oximeters digital heart rate monitors were known as electrocardiograms (EKG or ECG). An ECG detects electrical changes in the heart using electrodes attached to the skin[13]. The electrodes pick up electrical impulses created by the heart during the cardiac cycle and then amplify the signal on an electrocardiograph[13]. The ECGs utilize the electrical impulses from heart contractions to detect heart rate, via electrodes that attach to the skin. These electrodes

from an ECG can cause irritation to the skin or burns. The ECG monitoring systems require multiple electrodes to be attached to the chest, back and abdomen, requiring time and effort to attach. Due to the limitations of ECG, this system is less optimal than optical non-invasive heart rate monitors in accessibility[24].

Instead of using electrical signals like the EKG, current pulse oximeters use optics: a less invasive technology to monitor the heart rate. The pulse oximeter device is usually applied to the finger and uses light perfusion across the tissue to measure heart rate. The pluses oximeters and other digital heart rate monitors use photoplethysmography(PPG) signals to interpret heart rate[23]. This method of monitoring heart rate is most commonly used today and can also be found in many commercially available technologies including watches and headphones.

2.2.2 Clinical application of Blood Oxygen Monitoring

As discussed in the previous chapter the blood oxygen saturation (SO_2) is a crucial vital sign that, when low, can indicate that oxygen is not readily being transported throughout the body. The brain is considered the most sensitive organ, if hypoxemia, or low SO_2, occurs, the brain does not get enough oxygen, and visual, cognitive and electroencephalographic changes can occur[25]. There are many methods to measure SO_2, or arterial blood oxygen saturation (SaO_2), the percentage of bound oxygen in the arteries. Some methods utilize the transcutaneous tissue or peripheral blood to estimate the SaO_2 by measuring the peripheral oxygen saturation (SpO_2). SpO_2 is often utilized for SO_2 measurement because of its similarities to SaO_2 and ease of measurement compared to arterial blood.

Blood oxygen saturation characterizes how blood is being transported and reaching the tissues. In June of 2017 the *BTS Guideline for Oxygen use in Adults in Healthcare and Emergency Settings* indicated that healthy individuals between the ages of 18 to 81 should have an arterial blood oxygen saturation (SaO_2) in the range of 94%-98%[26]. Throughout history there have

been many methods of measuring peripheral blood oxygen saturation (SpO_2) values including chemical methods, electrical PO_2 sensors, and other light attenuation oximeters.

2.2.2.1 Van Slyke Method

The Van Slyke Method is a means of measuring oxygen content using chemical reactions. The method requires a blood sample which is exposed to potassium ferricyanide which removes carbon dioxide from the sample. The sample is then compressed, and pressure is measured using a manometer[27]. After the CO_2 is removed sodium hydrosulfite is introduced to the sample to remove the remaining oxygen[28]. Van Slyke Method utilizes the Van Slyke apparatus to manipulate the sample and measure the pressure after the chemical reactions. The apparatus pictured in figure 2.8 uses mercury and a stopcock control to operate the chemical reactions and pressure measurements[29].
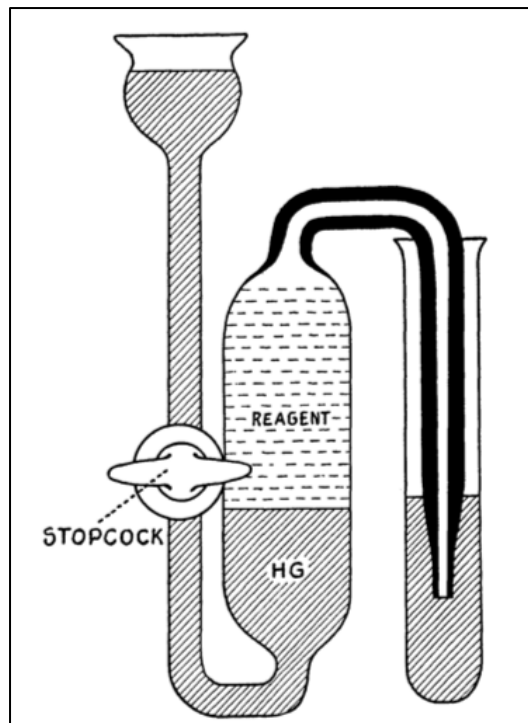
Figure 2.8: The Van Slyke apparatus contains a stopcock and mercury(Hg) to measure the chemical reaction and determine the oxygen saturation. Image recreated from [29]

2.2.2.2 Clark Electrode and Transcutaneous PO₂ Sensors

The Clark Electrode measures the partial pressure of oxygen PO₂ using chemistry. Oxygen dissolved in an aqueous solution is exposed to 0.7V. A silver anode in a potassium chlorine bath will attract (Cl⁻) producing a constant flow of electrons, and a platinum electrode in the same bath reacts turning oxygen to hydroxyl ions (OH⁻). The number of electrons used in the platinum cathode is proportional to the PO₂ value, thus the current across the electrodes corresponds to the PO₂ in the solution[28]. Later the Clark electrode was modified to be used, in vivo, as catheter electrodes. There are many downsides to the Clark electrode including the need to draw blood and the invasiveness of the vivo electrodes. There are often problems making sure the tip of the electrodes stays clean and clear of any debris or congealed blood, and the most challenging limitation of the device is the need for calibration using a separate blood gas analyzer.

Figure 2.9: Lenard Clark with his invention of defoaming in an oxygen bubbler that helped construct the Clark electrode. Image replicated from [30]

The Clark electrode can be placed on the outside of the skin to be utilized non-invasively. The transcutaneous partial pressure of oxygen ($PtcO_2$) can be measured to indicate the arterial partial pressure of oxygen PaO_2. The Clark electrode is heated on the skin, inducing hyperemia and increasing the blood flow to the affected area. The increased blood flow causes more O_2 to be diffused across the skin more easily, causing the $PtcO_2$ to approach PaO_2[28]. Although the transcutaneous sensor is less invasive than then Clark electrodes it still has some disadvantages. The heating of the sensor takes approximately 10mins and has risks of burring, in infants it is suggested to be moved every 4 hours[28].

2.2.2.3 Arterial Blood Gas Analyzer

The arterial blood gas test measures the concentration of gases like oxygen and carbon dioxide in the blood. The arterial blood gas analyzer was developed by Dr.Severinghaus and his technician in 1958, using the technology involved in the Clark electrode. Dr.Severinghas modified the Clark electrode and combined his own research, measuring pCO_2 and pH, into one analyzer to develop the arterial blood gas test[30]. The technology advanced throughout the years and by the 1960's the device was universally available. The analyzer requires arterial blood, usually withdraw from the radial artery but in some cases, it is extracted from the brachial or femoral arteries. The extracted blood must be kept warm and tested within 30 minutes of taking the sample. Since the 1960's the device has advanced and can be utilized today to measure oxygen saturation in cases such as shock, hypothermia, or kidney failure where other non-invasive oxygen monitors are less accurate. Although the oxygen saturation data from an arterial blood gas test is extremely accurate, the test takes time, and because the blood oxygen saturation within the body can change instantaneously, the results from the test can be skewed. Because of the tests's inability to perform instant measurements and requires a large blood gas analyzer, other non-invasive techniques have surpassed.

2.2.3   Pulse Oximeters

Pulse oximeters utilize light interaction to measure blood oxygen saturation and have become the most popular instrument to do so in medicine today. The first modern pulse oximeter was

developed in 1972 by Takuo Aoyagi and Muchio Kishi, who discovered the ratio of red to infrared light absorption through the tissue. After the discovery of the light ratio to measure oxygen concentration, and the tremendous advance in technology of that time, the pulse oximeter was constructed as an easy method for monitoring blood oxygen saturation. Monitoring real time oxygen saturation is critical to patient health, blood oxygen saturation can drop to critical limits within seconds. Pulse oximeters offer a convenient, non-invasive method for measuring blood oxygen saturation continuously[25].

Figure 2.10: Finger pulse oximeter, most commonly used in hospitals, the device is placed over the finger to read heart rate and blood oxygen saturation.

Current on market pulse oximeters are small enough to be placed over the finger, as seen in figure 2.10. The instrument contains micro lights which interact with the peripheral blood flow, as the heart beats the lights detect changes in blood volume. Pulse oximeters are a compact easy to use device that measures blood oxygen saturation and heart rate. Pulse oximetry continues to be a critical component of standard of care monitoring for critically ill patients[31].

2.3   Photoplethysmography

Photoplethysmography(PPG) is an optical signal, produced by blood perfusion at the microvascular bed of the tissue[32].   PPG signals are utilized by wearable non-invasive devices known as pulse oximeters[33]. Pulse oximetry and PPG are often confused, but pulse oximetry is an application of photoplethysmography[15]. A photoplethysmograph is the waveform generated by blood volume changes from the pulse signal[34]. Changes in the blood volume are synchronous with the heartbeat, so the device can be used to calculate the heart rate[32].

The PPG device utilizes light emitting diodes (LEDs) of different wavelengths and photodetectors, these components lead to the instruments small-scale and affordable characteristics[35]. Most PPG sensors are transmission-based, where the LEDs and the photodetector are located on opposite sides of the tissue. The relevant sensor in this thesis uses reflected-based PPG, where components are on adjacent sides. The LEDs beam light into the tissue where it interacts with biological material, and the light is either absorbed or scattered away. Scattered light can travel back to the sensor where the photodetector detects the light exciting the tissue[15].

A PPG signal can be obtained using two LEDs at different wavelengths, this signal is used to calculate peripheral oxygen saturation (SpO$_2$). Each wavelength of light interacts with materials differently, thus the SpO$_2$ can be calculated from the variation of the two LEDs' interaction with the tissue.

2.3.1   Photoplethysmograph Waveform

During the cardiac cycle the heart contracts pushing blood throughout the body[13], [14]. When the heart contracts this is known as systole, during this phase the blood is forced out of the heart and into the arteries. The force of the blood moving out of the heart causes a buildup in pressure throughout the arteries and an increase in blood volume in the capillaries[15]. As the volume in

26

the tissue increases the amount of light from the LED hitting the photodetector will decrease, thus causing the absorbance to increase. When the heart is relaxed in diastole the opposite will occur, the blood volume at the tissues will subside and more light will be detected on the photodetector, less absorbance[15]. This is the basic concept of the photoplethysmography waveform.

2.3.2 Theory of spectrophotometers

Spectrophotometry is the basis for all oximetry and the theory behind the PPG signal[28]. The spectrophotometer measures the absorption of light through a substance at a particular wavelength[28]. Spectrophotometers use a photodetector to measure the intensity of light that has passed through the substance.
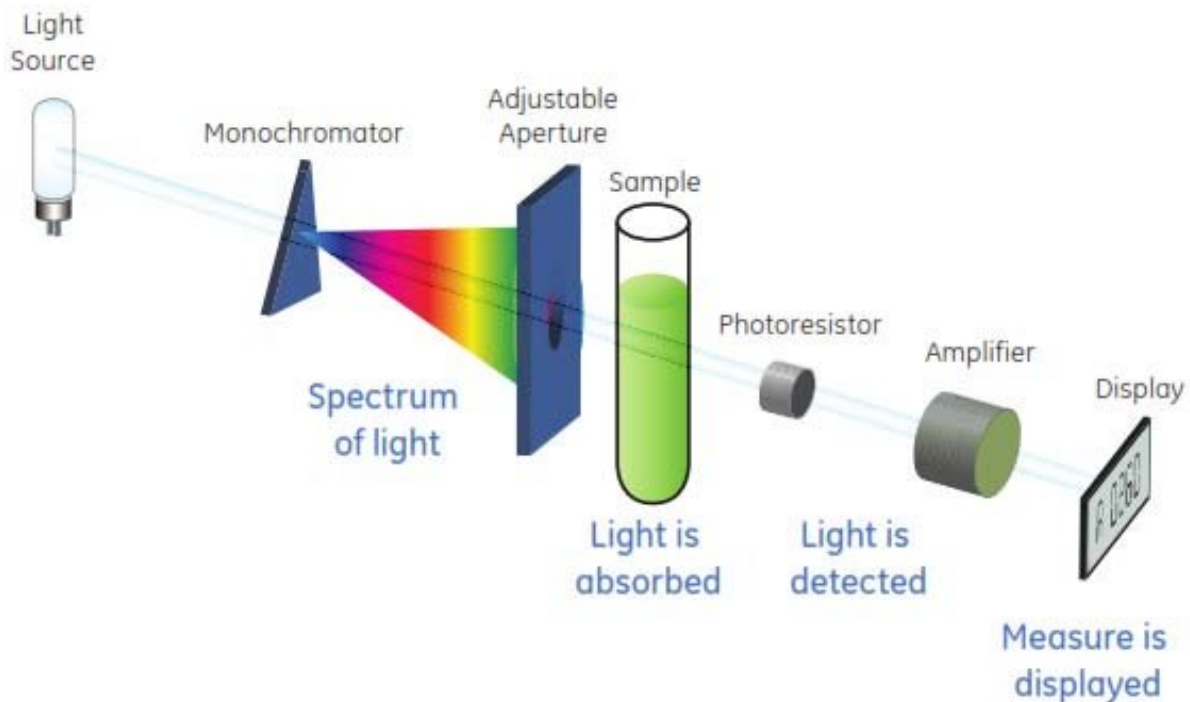
Figure 2.11: A spectrophotometer is comprised of a white light source which passes through monochromator scattering the light into all wavelengths, the spectrum of light then passes through an adjustable aperture to narrow the field of view. The light is then projected into the sample of interest, on the opposite side of the sample is a photoresist and an amplifier. Once the light hits the sample some is absorbed and some if reflected the reflected light is detected by the photoresistor amplified and displayed.

The transmission (T), the amount of light passing through the material, is a dimensionless quantity that can be calculated using equation 2.1 by dividing the intensity of incident light (I_0) by the intensity of light transmitted through the material (I).

$$T = \frac{I}{I_0}$$

Equation2.1

The absorbance (A), the amount of light absorbed by the material can also be calculated using the intensities of light before and after passing through a material:

$$A = log\frac{I_0}{I}$$

Equation 2.2

Beer's Law, which is derived from the absorbance and transmission equations, is utilized to calculate characteristics about the material light is passing through.

Beer's Law is as follows:

$$A = \varepsilon(\lambda)cd$$

Equation 2.3

Where $\varepsilon(\lambda)$ is the extinction coefficient of the substance at a given wavelength λ , c is the concentration of a substance and d is the path length the light travels through that substance[28]. Beer's Law is the fundamental governing equation for spectrophotometry and PPG sensors, as it provides a mechanism to calculate the concentration of a material. Spectrophotometry is the technique utilized in PPG sensors to calculate the concentration of oxygen in the blood. In the upcoming chapters the use of Beer's Law to calculate SO_2 will be discussed in greater detail.

2.3.3 Photoplethysmogram Correlation to Heart Rate

Although there are many devices to measure heart rate, such as ECG monitoring systems, PPG sensors are considered low cost, portable, non-invasive and applicable in various environments[36]. The PPG sensors are also capable of monitoring for heart rate variations to predict cardiac issues or abnormalities[36]. The PPG sensor can detect the pulsatile signal of blood volume changes due to the heart rate (HR) via the photodetectors modulation from the original light signal[24]. The attenuation of light energy is dependent on the transmission or reflection of light in the bloodstream, and correlates to systole and diastole in the cardiac cycle[24]. The PPG waveform derived from variations in light absorbance can be seen in figure 2.12.
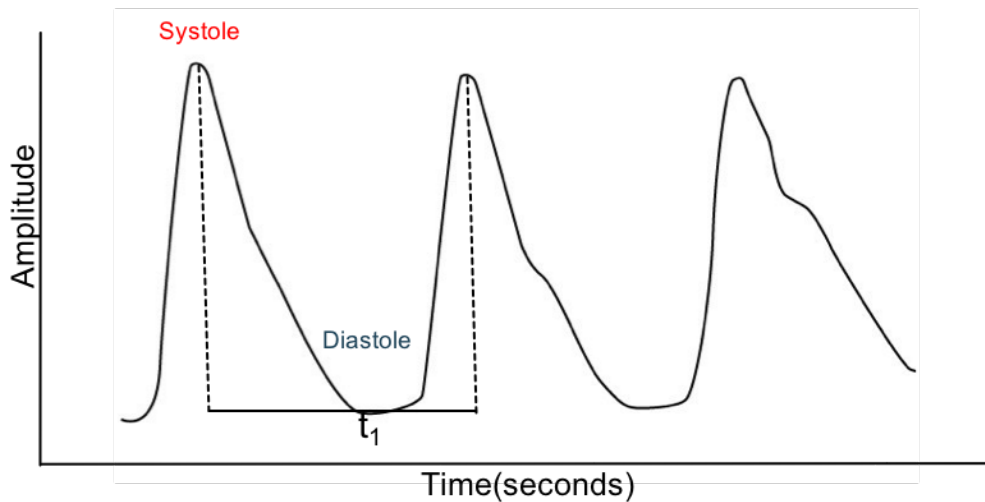
Figure 2.12: Photoplethysmogram where the amplitude correlates to the absorbance of light. The absorbance is related to the beating of the heart, when the hearts is in systole the absorbance is high and in diastole the absorbance is low. Image reproduced from [24]

From figure 2.12, illustrating the PPG waveform, the time interval between the systole pulses in the cardiac cycle (t_1) can be used to calculate the instantaneous heart rate in equation 2.4:

$$HR_{inst} = \frac{60}{t_1}$$

<div align="right">Equation 2.4</div>

The heart rate can be averaged over a period of time to increase accuracy of calculation.

$$HR_{med} = \frac{1}{Q_{nn}} \sum_{k \in [T_i, T_f]} NN[k]$$

<div align="right">Equation 2.5</div>

Where Q_{nn} is the number of samples of normal intervals NN over time interval $[T_i, T_f]$.

The PPG signal can use the pulses from the increased blood volume to calculate the heart rate. Most pulse oximeters or PPG devices today display not only SO$_2$, but also heart rate, because of its critical correlation to body health.

2.3.4 Acquisition of Photoplethysmography Signal

Light from the LED's in a photoplethysmography sensor interacts with biological tissues. This interaction can be complex involving scattering, absorption and/or reflection[37]. The technology utilized for collecting and evaluating a PPG signal can vary across devices. It is important that PPG signal devices use correlating components and wavelengths that interact with blood.

2.3.4.1 Measurement Modalities

Transmission and reflection are the two most prevalent types of PPG sensors. Transmission based sensors (Figure 2.13 (a)) are designed such that the LEDs are located above the finger, and project light through the extremity. These sensors are constrained to a clip, placed on the earlobe or finger where light can pass through the tissue [32]. On the contrary reflection based PPG sensors (Figure 2.13 (b)) do not utilize light passing through tissue, and theoretically can be positioned at any skin surface [32]. For the means of this thesis, the constructed PPG sensor utilized a reflection-based design.
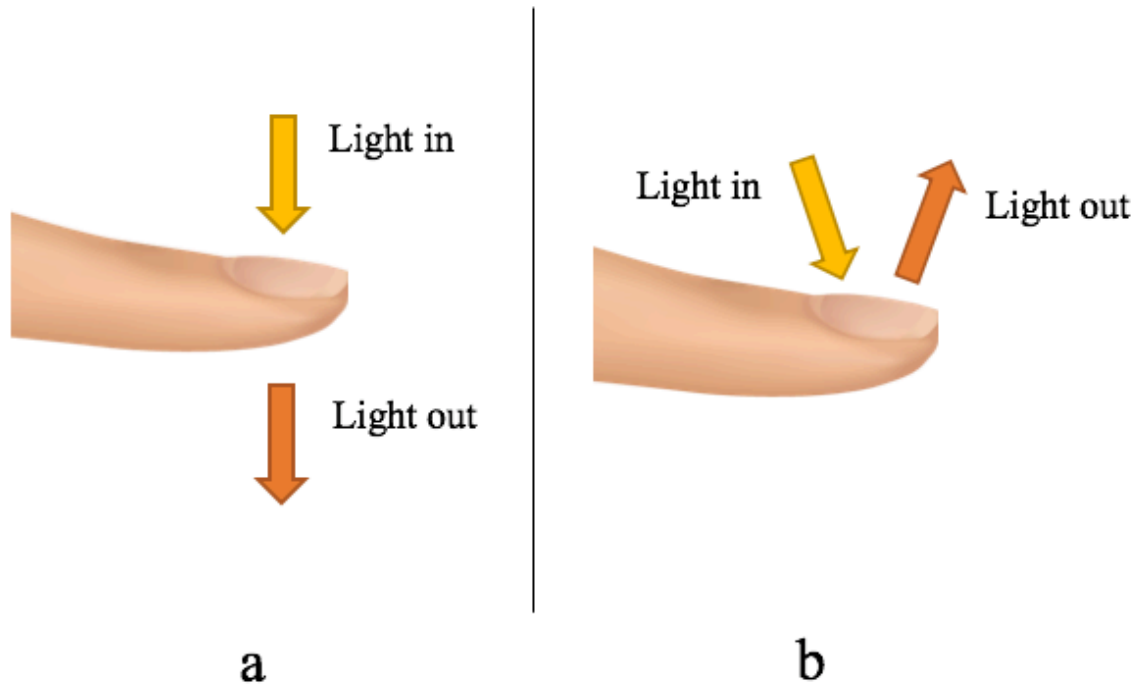
Figure 2.13: Two types of PPG sensors (a)Transmission based where the light source and the light detection component are on opposite sides of biological tissue and (b)Reflection based where the light source and the light detection component are on the same side of biological tissues. Image reproduced from [24]

As light passes through the tissues it reacts with materials in the body, causing light to scatter in different directions. For both types of sensors there are advantages and disadvantages, a transmission-based sensor must have enough light entering the tissue to ensure the light interacts with the blood and passes through the extremity. Because light travels through an extremity in transmission-based sensors, the results can be skewed from external light, and why most transmission sensors are designed to fully enclose the extremity, blocking out all light. The transmission sensor is widely utilized on the medical market today, the "clip" design eliminates variations that are found in a reflective PPG sensor.

Reflective PPG sensors detect scattered light that propagates back toward the light source, this allows for more compact and easier to use sensors. The reflective sensors can be used where

transmission sensors cannot, the sensors can be used virtually anywhere where vascular skin exists on the body, whereas the transmission-based sensors are limited to areas where light can attenuate through tissue i.e. earlobe, or finger[38]. The reflective based sensors do have some disadvantages including, movement of the tissue on the sensor, and pressure applied, both can cause variation in the PPG signal. Eliminating or decreasing the extent of the reflective sensor disadvantages could cause this sensor type to progress beyond transmission.

2.3.5 Components of the Photoplethysmograph

As light enters the tissue it is absorbed and reflected by all of the biological components in the tissue. The skin, bones and arterial/ venous blood are primary absorbers of light[28]. As the heart enters systole blood flows to the extremities and the incidence of light reaching the sensor is decreased, when the heart relaxes the blood volume in the extremities decreases and the light increases [37]. The PPG signal is formed from two components AC and DC [24]. The pulsatile signal produced from the PPG waveform is known at the AC component and can be seen in figure 2.14 superimposed on the DC component [39]. The DC component, or non-alternating component of the signal represents the constant components of the tissue like skin pigmentation and bone material. The AC component represents the blood volume changes from a heartbeat, each peak to peak signal represents a single heartbeat.
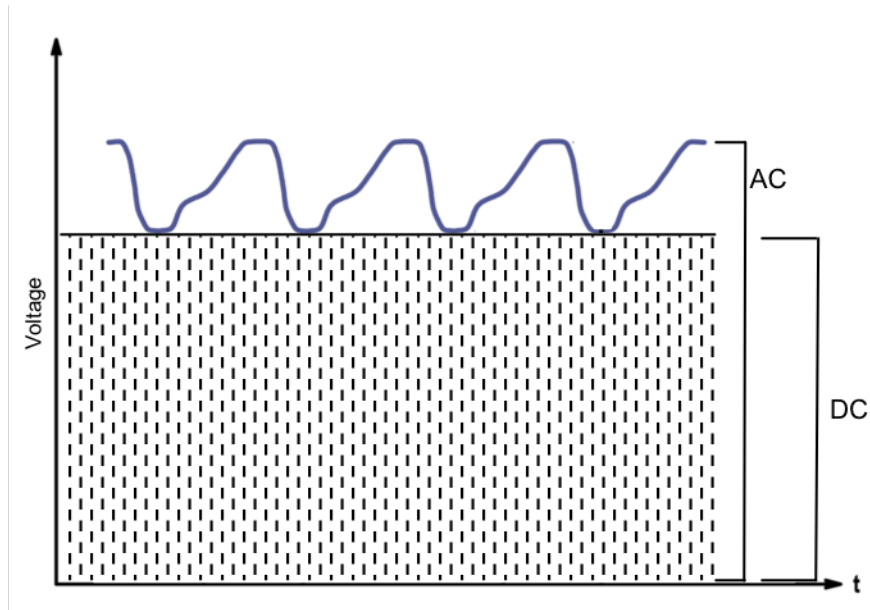
Figure 2.14: PPG signal from electrical components, the AC signal is the pulsatile variation due to changes in blood flow and the DC component of the signal is stagnant from the absorption of other biological components. Image reproduced from [23].

Within a single heartbeat the AC component is considered the maximum absorbance, and the DC as the minimum, therefore the AC and DC are the peak and baseline of the PPG waveform respectively[36]. In the past the variation in the AC and DC components generated a challenge for consistent detection of blood volume changes, but the use of two wavelengths of light and calculating a ratio of AC to DC signal components, the variation in the signal can be normalized for a reflective based PPG sensor[37]. Further analysis of the AD to DC ratio will be discussed in later chapters.

2.4   Optical Components of Photoplethysmography

Optics are the primary component in a PPG sensor, they are responsible for transmitting and detecting light through tissue. Blood in the vascular bed of the tissue contains oxyhemoglobin (HbO$_2$) a red blood cell fully saturated with oxygen molecules, and deoxyhemoglobin (Hb) blood without oxygen. The LEDs in the PPG sensor interact with the HbO$_2$ and Hb to determine the percentage of oxygen saturated blood.

2.4.1 Principles of Photoplethysmography Oxygen Saturation

Peripheral oxygen saturation (SpO$_2$) is an important biological reference characterizing oxygen content in the blood, and the ability to transport the oxygen throughout the body. Oxygen saturation calculation shown in equation 2.6, expressed as a percent the concentration of oxygenated hemoglobin (HbO$_2$) over the concentration of oxygenated hemoglobin plus deoxygenated hemoglobin (HbO$_2$ + Hb).

$$SpO_2 = \frac{HbO_2}{Hb + HbO_2} \times 100\% \qquad\qquad \textit{Equation 2.6}$$

Pulse oximeters use PPG signals to measure the blood oxygen saturation (SpO$_2$), by using Beer's Law to calculate the concentration of oxyhemoglobin (HbO$_2$) and deoxyhemoglobin (Hb) in the blood. The sensor uses two distinct wavelengths of light which interact with HbO$_2$ and Hb differently, in turn providing differentiation between the two concentrations. How various wavelengths of light interact with HbO$_2$ and Hb can be seen in figure 2.15, across the wavelength spectrum the interaction with the oxygenated and deoxygenated hemoglobin varies.
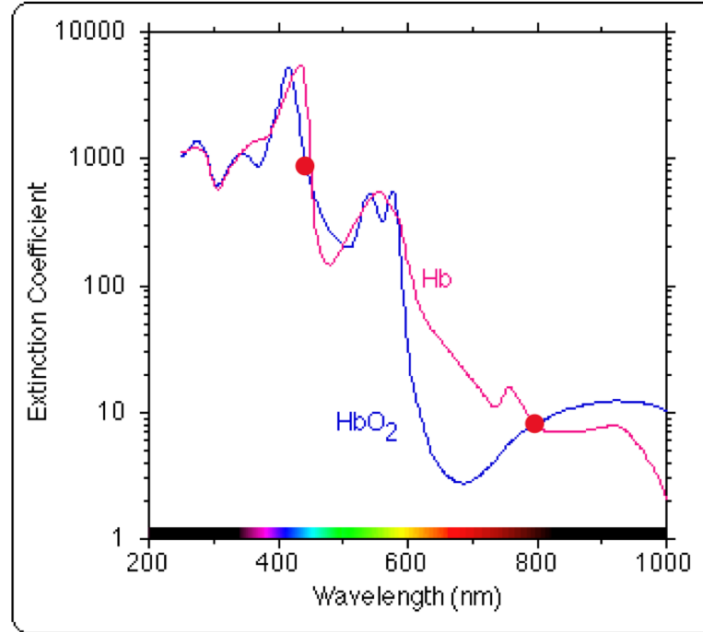
Figure 2.15: Extinction coefficient, related to absorbance, vs wavelength of light, for oxygenated (HbO₂) and deoxygenated (Hb) blood. The oxygenated and deoxygenated blood cross at two points throughout the light spectrum, these are indicated by red dots and are referred to as isosbestic points.

A similar graph illustrating the absorbance of HbO₂ and Hb for wavelengths in the 600-1000nm range can be seen in figure 2.16, where lower wavelengths of light (600-700nm) HbO₂ absorption is less than the absorption of Hb, and at higher wavelengths (850-1000nm) HbO₂ absorption is greater than Hb. The wavelengths between 600-700nm are in the red region of the spectrum, and the 850-1000nm wavelengths are in the non-visible infrared region. The variation in absorbances is due to the isosbestic point, around 805nm, where the absorption effect shifts.
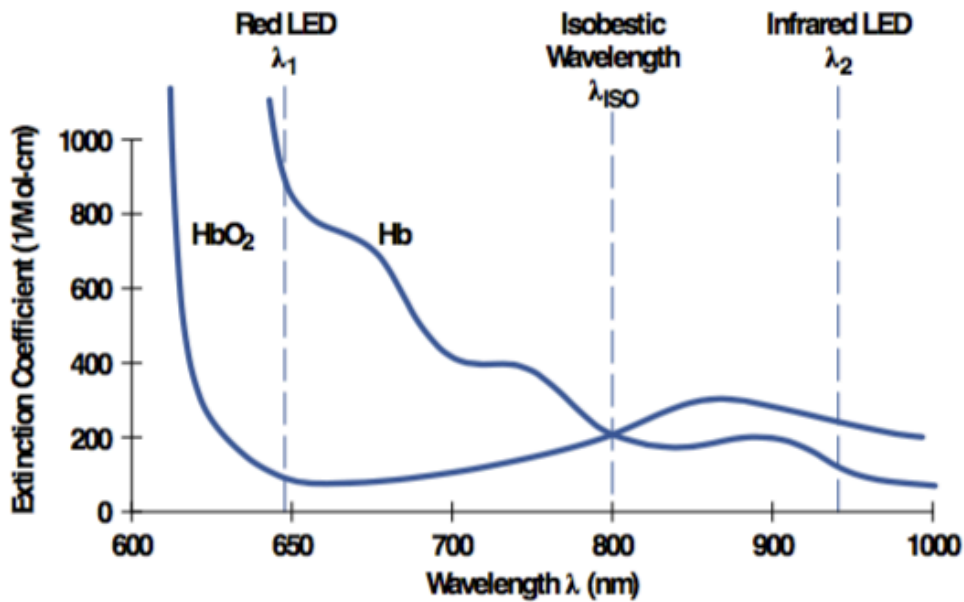
Figure 2.16: Extinction coefficient, related to absorbance, vs wavelength from 600nm to 1000nm, for oxygenated (HbO₂) and deoxygenated (Hb) blood. The isosbestic point is located at 800nm before this point Hb has a high extinction coefficient than HbO₂ and after this point Hb has a lower extinction coefficient than HbO₂. Image reproduced from [36]

In pulse oximetry the most common wavelengths of light utilized are 660nm and 940nm, any wavelengths can be used as long as they fall on either side of the isosbestic point. Beer's Law relates the concentration of a material to the absorption, using this concept the SpO_2 can be calculated. The concentrations of HbO_2 and Hb which make up the SpO_2 equation can be calculated using Beer's Law:

$$A = \varepsilon L c \qquad\qquad\qquad \textit{Equation 2.7}$$

Absorbance is equal to the extinction coefficient (ε) times the path length of light (L) times the concentration of the material (c). Using two wavelengths of light a ratio of absorbances can be calculated via Beer's Law (equation 2.7) the ratio becomes:

$$R = \frac{A_{\lambda 1}}{A_{\lambda 2}} = \frac{\varepsilon_{T1} C_{T1} L}{\varepsilon_{T2} C_{T2} L} \qquad\qquad \textit{Equation 2.8}$$

Where the ratio of light is equal to the absorbance of light at wavelength 1 ($A_{\lambda 1}$) over the absorbance at wavelength 2 ($A_{\lambda 2}$). From figure 2.16 the absorbance at λ_1 (red) for oxygenated blood is less than the absorbance at λ_2, thus when the blood is highly oxygenated (SpO$_2$=100%) the ratio (R) will be less than 1 (approximately 0.4). If the blood is not oxygenated (Hb) the absorbance at λ_1 is greater than the absorbance at λ_2 and the ratio will increase, a R=1 corresponds to an SpO2 value of approximately 85%.

2.4.2   Photoplethysmography Biologically Applied Absorbance Ratio

The light penetration depth in the skin depends on the tissue's absorption and scattering properties, also known as the extinction coefficient [32], [35]. Because absorption is dependent on the wavelength of light, the LED's in a PPG sensor require a specific wavelength to penetrate deep enough and acquire blood oxygen information. A PPG sensor measures the concentration of HbO$_2$ and Hb in the blood using specific wavelengths of light, so it is critical that the wavelengths penetrate through the tissue to reach the blood, and correlate to different HbO$_2$ and Hb absorbances.
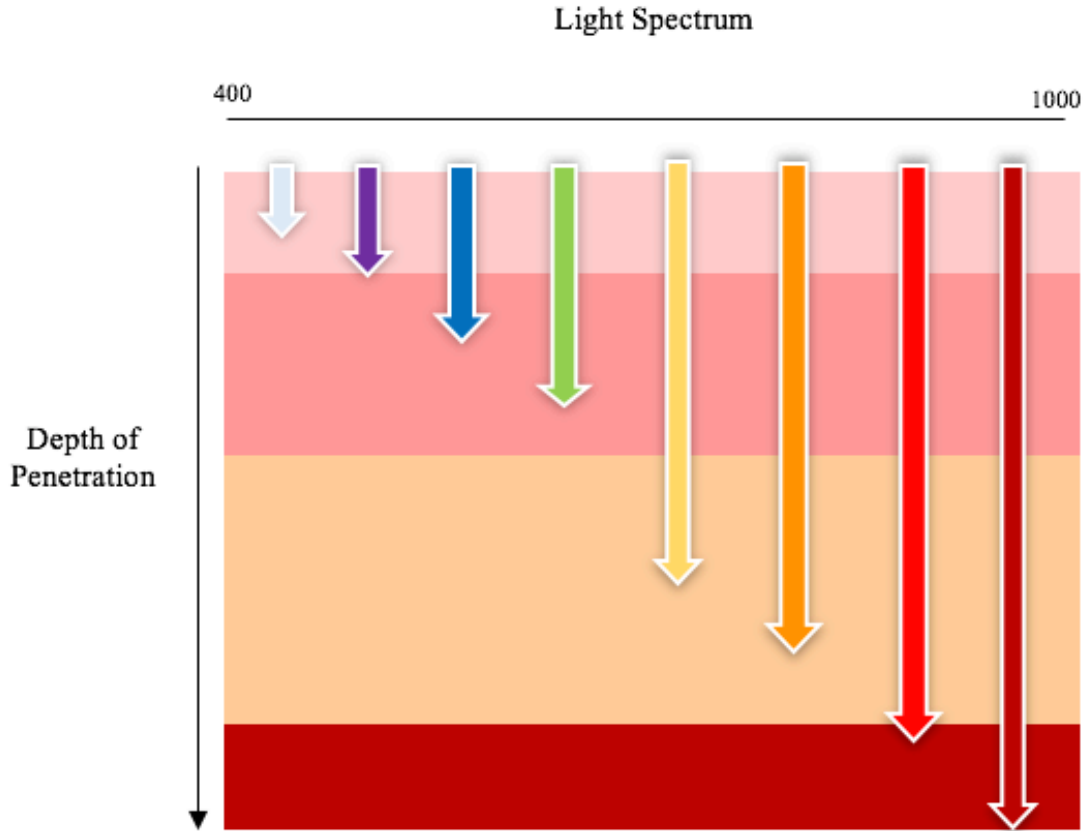
Figure 2.17: Depth of penetration vs wavelength of light, the wavelength of light directly correlates to the depth of penetration into the tissue. The larger wavelengths of light penetrate deeper than the lower wavelengths.

From figure 2.17 it can be noted that greater wavelengths of light penetrate through tissue to reach the layer of tissue containing blood. To collect PPG signals light penetrating the tissue must be of a wavelength capable of reaching the vascular tissue bed. Fortunately, as discussed in the previous section, the wavelengths of light utilized in PPG sensors are 660nm (red) and 940nm (infrared), two wavelengths capable of reaching the vascular bed containing blood.

2.4.3   Photoplethysmography Electrically Applied Absorbance Ratio

As discussed in the previous section a PPG signal is divided into two components, the pulsatile, AC component, and the constant background, DC component, or the maximum and minimum of a single PPG waveform respectively. The two LEDs utilized in a PPG sensor have distinct AC and DC components in the absorbance, seen in figure 2.18.
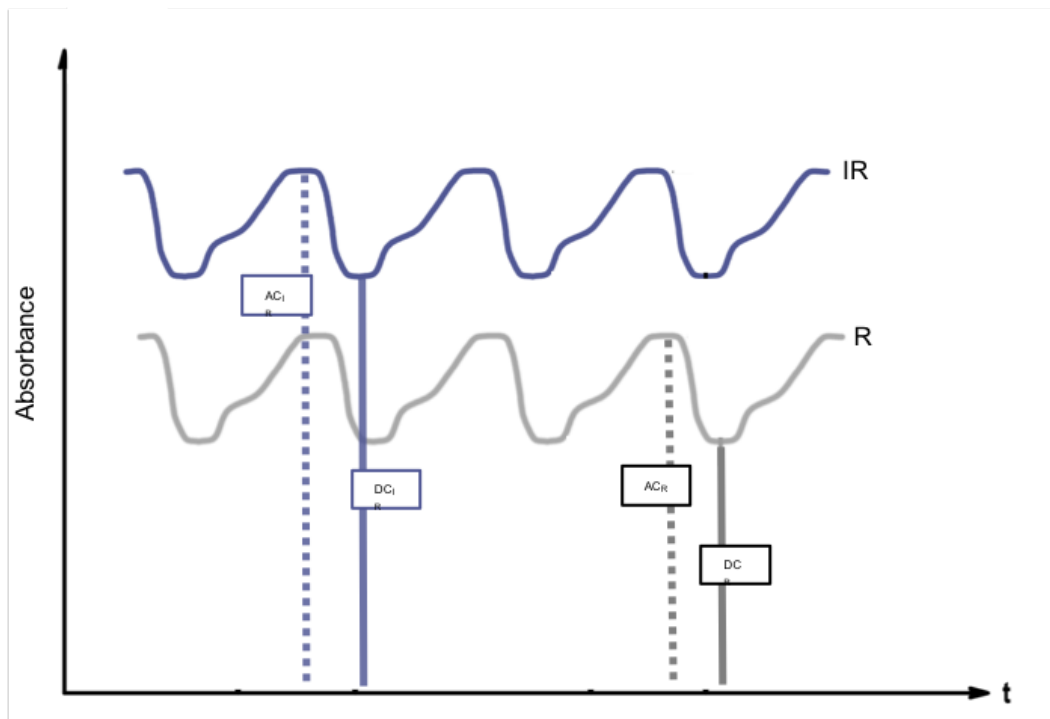
Figure 2.18: Dual PPG signal where one signal is from light in the infrared wavelengths(IR) and the other from red wavelengths (R). The AC and DC components of each signal are defined, AC(---) and DC (—).

Where there are two PPG waveforms one IR (infrared) and the other R (red), to calculate the ratio of absorbances the signal becomes:

$$R = \frac{(A_{max}/A_{min})_R}{(A_{max}/A_{min})_{IR}} = \frac{(AC/DC)_R}{(AC/DC)_{IR}} \qquad \textit{Equation 2.9}$$

The ratio of the AC and DC components cancels the absorbance of other components in the tissue such as bone or skin, and the ratio of the red light over the infrared light is used to calculate the SpO$_2$, discussed in later sections.

2.4.4 Oxygen Saturation and Beer's Law

Using Beer's Law and the ratio derived from the absorbance of light through the tissue the SpO2 can be calculated.

Peripheral oxygen saturation (SpO$_2$) is defined as:

$$SpO_2 = \frac{HbO_2}{Hb + HbO_2} \times 100\% \qquad \textit{Equation 2.10}$$

Where the SpO$_2$ is equal to the concentration of HbO$_2$ over the total hemoglobin concentration (HbO$_2$ + Hb) times 100. This equation is usually written as a concentration:

$$SpO_2 = \frac{C_{HbO_2}}{C_{Hb} + C_{HbO_2}} = \frac{C_O}{C_D + C_O} = \frac{C_O}{C_T} \qquad \textit{Equation 2.11}$$

The SpO$_2$ is represented as a concentration of the oxygenated hemoglobin (C_O) and deoxygenated hemoglobin (C_D) over the total concentration C_T in the blood. Using Beer's Law and equation 2.11 the oxygen saturation can be calculated from the absorbance of light in a PPG sensor.

The Beer's Law, equation 2.12, relates the concentration and extinction coefficient of a material at a specific wavelength to absorption of light.

$$A = \varepsilon L c \qquad \text{Equation 2.12}$$

Absorbance is equal to the extinction coefficient (ε) times the path length of light (L) times the concentration of the material (c). Beer's law can be represented with respect to oxygenated and deoxygenated blood in the following equation

$$A_T = A_O + A_D = \varepsilon_T C_T L = \varepsilon_O C_O L + \varepsilon_D C_D L \qquad \text{Equation 2.13}$$

Where the total absorbance (A_T) is equal to the absorbance of HbO_2 (A_O) plus the absorbance of Hb (A_D). Equation 2.13 can be expanded using equation 2.12, replacing the absorbances with extinction coefficients, concentrations and pathlengths. The path length of light is equivalent for Hb (D) and HbO_2 (O) and therefore does not require differentiation within the equation and can be eliminated from evaluation. Solving for ε_T in equation 2.13, the equation becomes

$$\varepsilon_T = \frac{\varepsilon_O C_O + \varepsilon_D C_D}{C_T} = \frac{\varepsilon_O C_D}{C_T} + \frac{\varepsilon_D(C_T - C_O)}{C_T} \qquad \text{Equation 2.14}$$

Where extinction coefficient total ε_T is defined by the HbO_2 and Hb extinction coefficient ε_O and ε_D respectively, the concentration of HbO_2 and Hb, C_O and C_D and, the total concentration which is the summation of C_O and C_D. rearranging the equation 2.14:

$$\varepsilon_T = \varepsilon_O \frac{C_O}{C_T} + \varepsilon_D (1 - \frac{C_O}{C_T}) \qquad \text{Equation 2.15}$$

Replacing C_O and C_T in equation 2.15 with SpO_2 from equation 2.11, the extinction coefficient total becomes:

$$\varepsilon_T = \varepsilon_O SpO_2 + \varepsilon_D(1 - SpO_2)$$

<div align="right">*Equation 2.16*</div>

Blood oxygen saturation is represented by the total extinction coefficient, a known value determined by the material and wavelength of light utilized.

Substituting Beer's law equation 2.12 into the ratio of light absorbances the equation becomes:

$$R = \frac{A_{\lambda 1}}{A_{\lambda 2}} = \frac{\varepsilon_{T1} C_{T1} L}{\varepsilon_{T2} C_{T2} L} = \frac{\varepsilon_{T1}}{\varepsilon_{T2}}$$

<div align="right">*Equation 2.17*</div>

Where the ratio of absorbances is directly proportional to the ratio of extinction coefficients, and it was determined equation 2.16 that the total extinction coefficient is equal to

$$\varepsilon_T = \varepsilon_O SpO_2 + \varepsilon_D(1 - SpO_2)$$

Substituting the equation for the extinction coefficient total, equation 2.16, into the ratio of extinction coefficients, equation 2.17, the ratio becomes:

$$R = \frac{\varepsilon_{T1}}{\varepsilon_{T2}} = \frac{\varepsilon_{O1} \varepsilon_{D1} + (1 - SpO_2)}{\varepsilon_{O1} \varepsilon_{D1} + (1 - SpO_2)}$$

<div align="right">*Equation 2.18*</div>

Solving equation 2.18 for SpO_2 the equation becomes:

$$SpO_2 = \frac{\varepsilon_{D1} - R \varepsilon_{D2}}{R(\varepsilon_{O2} - \varepsilon_{D2}) + (\varepsilon_{D1} - \varepsilon_{O1})}$$

<div align="right">*Equation 2.19*</div>

The blood oxygen saturation (SpO$_2$) is represented in terms of the ratio (R) of absorbances for the two wavelengths and the extinction coefficient of HbO$_2$ oxygenated hemoglobin (ε_O) and Hb deoxygenated hemoglobin (ε_D). Where the extinction coefficients of oxygenated and deoxygenated hemoglobin are known values for the wavelengths utilized.

The relationship between the measured absorbances of light and the calculated theoretical SpO2 value can be plotted as a calibration curve figure 2.15, where the normalized ratio, R, represents the ratio of absorbances of red to infrared wavelengths of light.
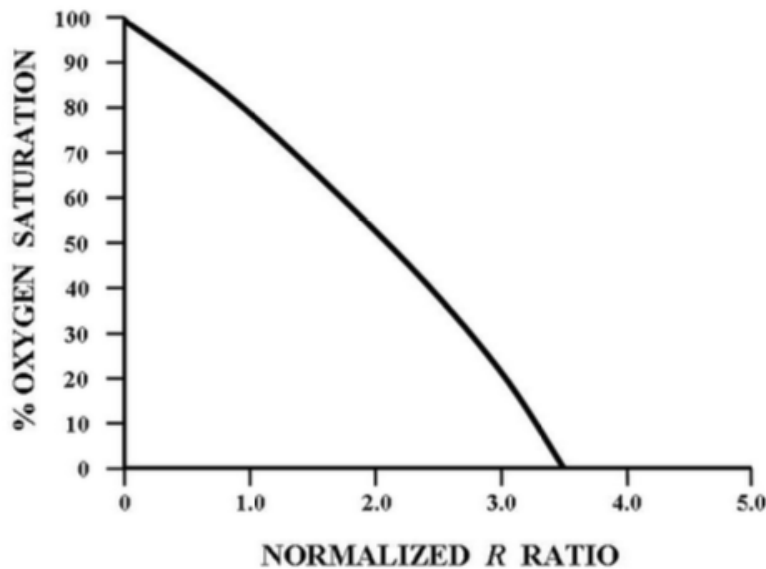
Figure 2.15: Oxygen saturation (SO$_2$) versus the normalized ratio R, described in equation 2.17 as the ratio of absorbances of two wavelengths of light through blood. Image reconstructed from [40]

The ratio of light absorbances to oxygen saturation is not a linear regression but is often represented as one because of the close correlation. Representing this correlation linearly yields the following linear equation:

$$SpO_2 = 110 - 25R \hspace{4cm} Equation\ 2.20$$

43

Where the oxygen saturation is equal to 110 minus 25 times the normalized ratio. R represents the ratio of absorbances, described above in equation 2.17.

CHAPTER 3

3.0 DESIGN OF REFLECTANCE BASED PHOTOTPLETHYSMOGRAPHY SENSOR

This thesis investigates the design and development of a reflective based photoplethysmography (PPG) sensor. A custom-designed sensor was constructed to acquire PPG signals. A PPG sensor or pulse oximeter consists of two LEDs and one photosensor. The two LEDs of different wavelengths penetrate the tissue, once the light reaches the blood it is either absorbed or scattered. The scattered light signal is then detected by the photosensor and the light absorption can be determined. For this thesis the PPG sensor was designed to be utilized on the foot no greater than 13mm in diameter. The dual-wavelength PPG sensor is designed with a red wavelength LED and an IR wavelength LED 660nm and 940nm respectively. Because the sensor is restricted to 13mm in diameter, it is critical that the LEDs are powerful enough to penetrate through the tissue and small enough to fit within the sensor. The absorption, determined from the light detected by the photo sensor, from the two LEDs are used to calculate peripheral blood oxygen saturation SpO_2. It is important to utilize LEDs with a narrow wavelength range to eliminate variation in the SpO2 calculations, this is especially critical for the 660nm LED, due to the steep slope of Hb in the extinction curve[28].

The absorbance of light, calculated from the PPG signal, is divided into AC and DC components, where the AC component is the pulsatile peak and the DC the steady valley. The 660nm and 940nm LED both have an AC and DC component, and the amount of light absorption correlates to the SpO2. The desire is to optimize the 660nm and 940nm signal by increasing the distance between the peak and valley of the signals, or AC and DC components. The layout of the optical components within the sensor greatly impacts the outcome of the PPG signal. If the optical components are too close together the light will saturate the photodetector and the signal will not have any pulsatile data, and if the components are too far apart the light signal reflected off the tissue will not reach the sensor. The distance between the LEDs and the photosensor directly relate to the signal to noise ratio of the PPG signal. Optimizing the distance between the optical components improves the signal to noise ratio by increasing the AC to DC signal ratio.

The physical distance between optical components is not the only design characterizing to advance the PPG signal, electronics resistance is altered to reduce noise. Depending on the sensor components the optimal resistance can be calculated and utilized to control the detected signal. Most pulse oximeters or PPG sensors contain photodiodes as the photosensor, but a phototransistor was selected due to its increased sensitivity[28]. A phototransistor operates varying current in response to light, this is then converted to a voltage signal.

Two dual-wavelength sensors were designed during the extent of this research, throughout the report I will refer to two PPG sensors as *Sensor-1* and *Sensor-2*. The major difference between the two sensors is the number of photodetectors, commonly referred to as a photosensor. The first design, *Sensor-1*, is designed with two photosensors, and the second design, *Sensor-2,* with a single photosensor. *Sensor-2*, the final sensor design, was constructed due to failures that occurred in Sensor 1, which are discussed in more detail throughout the chapter. *Sensor-2* is also a dual-wavelength PPG sensor, but only contains 1 photosensor.

3.1 Photoplethysmography *Sensor-1*

Sensor-1 is designed with two photosensors to simultaneously detect both wavelengths of light reflected light from the LEDs. *Sensor-1* contained four optical components divided into visual light emission and detection and infrared light emission and detection. These 4 components were printed on a 10mm printed circuit board (PCB), with intention to connect to an external motherboard. The LEDs on the PPG sensor project light at wavelengths in the visual light spectrum(380nm-740nm) and the infrared light spectrum(700nm-1000nm), with photosensors capable of detecting the light reflected from those LEDs. In *Sensor-1*, two photosensors were utilized, one to detect the visual light emission and the other to detect the IR light emission. This would provide two signals for both wavelengths of light, and optimal for calculating SpO_2.

3.1.2 Optical Components of *Sensor-1*

The PPG sensor or pulse oximeter is designed with optical components to emit and acquire light signals. The sensor contains light emitting diodes (LEDs) which emit light into the tissue, and two phototransistors which detect the reflection of light. The PPG *Sensor-1* is a dual-wavelength sensor containing two LED's of different wavelengths, one at 660nm and the other at 940nm. As the LEDs emit light into the tissue the phototransistors detect the specific wavelength of reflected light, which is converted into absorbance. The sensor is designed with two phototransistors, one capable of detecting wavelengths of visible light and the other capable of detecting wavelengths of infrared (IR) light. Because the ratio of absorbances is calculated from two pulsatile signals, it is critical that the reflected light is detected as separate signals. If the PPG sensor had one phototransistor capable of detecting both visible and IR light the result would be one signal contains of both wavelengths of light seen in figure 3.1. The two photosensors allow the device to detect both LED signals simultaneously. On the contrary a sensor with a single phototransistor is designed to switch the LEDs on and off to accommodate for the sensor's inability to distinguish between IR and RED wavelengths.
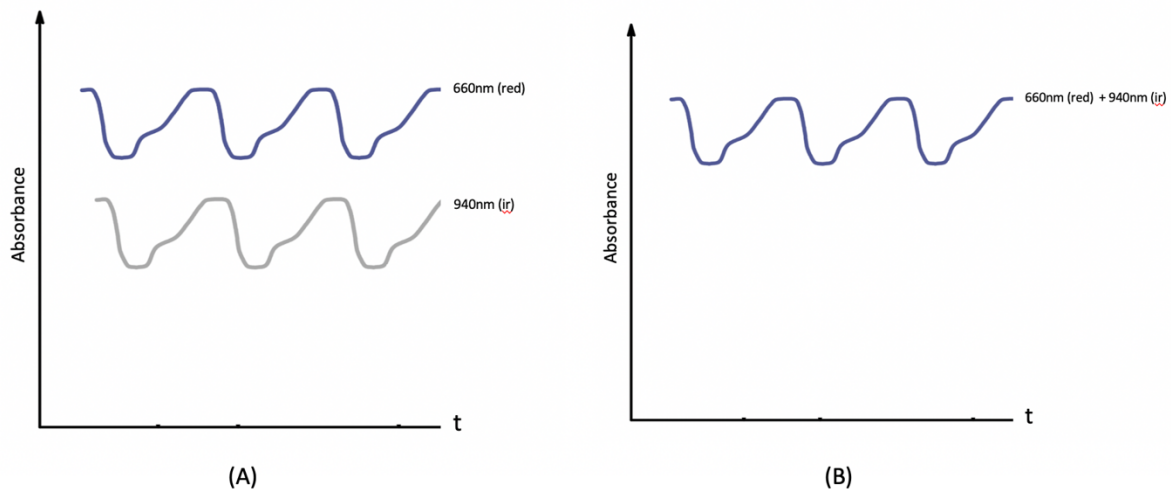
Figure 3.1: (A) two photosensors capable of detecting light from two different LED wavelengths, resulting in two separate absorbance signals. (B) one photosensor that detects both light wavelengths resulting in one signal comprised of both wavelengths.

The optical components utilized in Sensor-1 can be divided into visual light acquisition and infrared light acquisition. For visual light acquisition, *Sensor-1* consists of a red LED and an

ambient light sensor. The red LED (AP2012HD, Kingbright©, USA) has a peak wavelength at 660nm shows in figure 3.2, and the ambient light sensor (ALS-PT19-315C/L177/TR8, Everlight Electronics Co Ltd., Taiwan) utilized can detect reflected emissions from the red LED. The spectrum for the ambient light sensor, a phototransistor, can be seen in figure 3.3, having a peak absorbance at 630nm and a sensitivity range from 390nm to 700nm. It is important to note that the ambient light phototransistor has a sensitivity maximum of 700nm, indicating that the photosensor will not be able to detect wavelengths of light greater than 700nm. Comparing the emission and detection spectrums for the red LED and the ambient light sensor, figure 3.2 and figure 3.3 respectively, it can be concluded the ambient light sensor will detect the 660nm signal emitted from the LED.
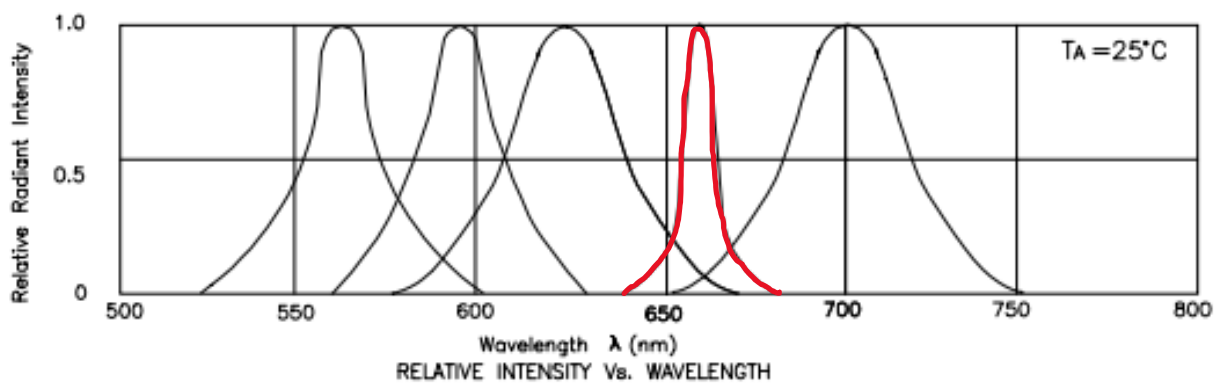
Figure 3.2: Optical emission graph of the red LED in Sensor-1, (AP2012HD, Kingbright©, USA) labeled is red. Relative intensity on the y-axis and wavelength on the x-axis, the red LED has a peak wavelength at 660nm.
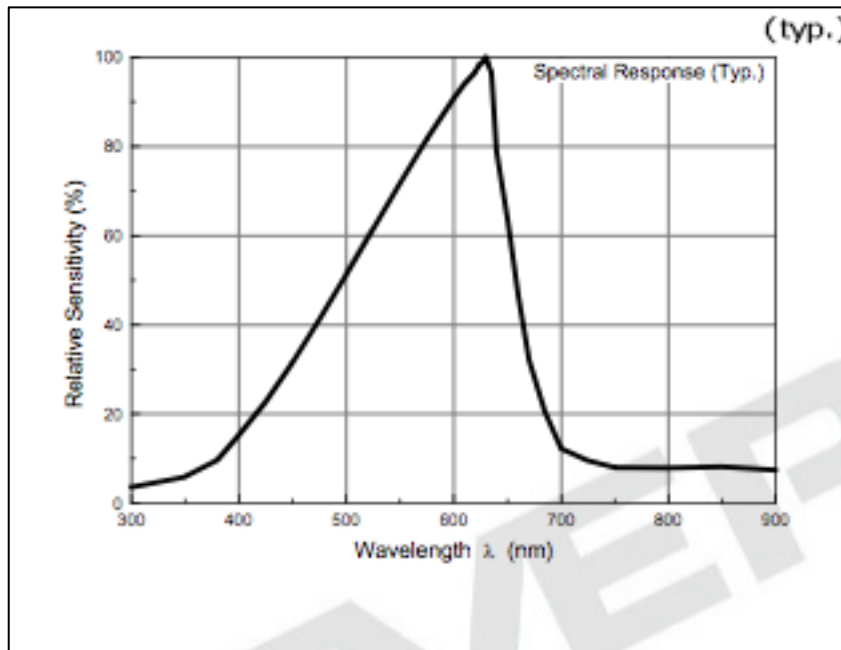
Figure 3.3: Absorption graph of the ambient light sensor utilized in Sensor-1, (ALS-PT19-315C/L177/TR8, Everlight Electronics Co Ltd., Taiwan). On the y-axis is relative sensitivity and on the x-axis is wavelength of light. The ambient light sensor has a peak sensitivity at 640nm.

Sensor-1's infrared (IR) light acquisition consists of an IR LED and an IR phototransistor. The IR LED (APT1608F3C, Kingbright©, USA) has a peak wavelength at 940nm illustrated in figure 3.4. The IR phototransistor (PT15-21B/TR8, Everlight Electronics Co Ltd., Taiwan) is a light sensor capable of detecting light emissions in the IR wavelengths. The IR phototransistor has a peak detection wavelength of 940nm and a range from 730 to 1100nm figure 3.5, indicating that the photosensor will not detect any wavelengths less than 730nm.
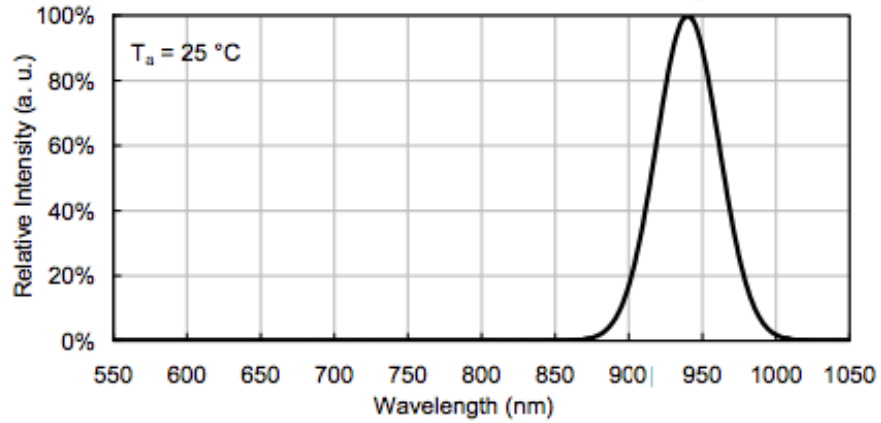
Figure 3.4: Optical emission graph of the infrared LED in Sensor-1, (APT1608F3C, Kingbright©, USA), with relative intensity on the y-axis and wavelength on the x-axis The infrared LED has a peek emission at 940nm.
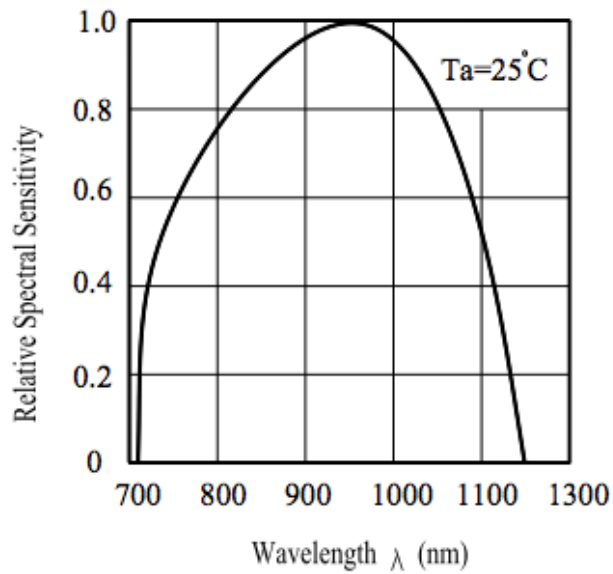
Figure 3.5: Absorption graph of the infrared light sensor utilized in Sensor-1, (PT15-21B/TR8, Everlight Electronics Co Ltd., Taiwan), with relative sensitivity on the y-axis and wavelength on the x-axis. The infrared light sensor has a peak sensitivity at 940nm.

The specs, including dimensions and operating conditions for the LEDs and photosensors can be seen in table 3.1 and 3.2 respectively.

Table 3.1: Optical specifications for red 660nm LED and IR 940nm LED

Parameter	Red (660nm) LED	IR (940nm) LED
Dimensions	2.0 mm x 1.2 mm x 1.1 mm	1.6 mm x 0.8 mm x 0.75 mm
Peak Wavelength (IF=20mA)	660 nm	940 nm
Spectal Line Halfwidth (deltaY ½)	20 nm	50 nm
Luminous Intensity	1.2 mcd	-
Forward Current	40 mA	20 mA
Forward Voltage (IF=20mA)	1.85 V	1.2 V
Capacitance	95 pF	90 pF
Power Dissipation	100 mW	90 mW
Reverse Voltage	5 V	5 V
Operating Temperature	-55 to +85 ºC	-40 to +85 ºC

Table 3.2: Optical specifications for visual photosensor and IR photosensor

Parameter	Visual Photosensor	IR Photosensor
Type	Phototransistor	Phototransistor
Dimensions	1.7 mm x 0.8 mm x 0.6 mm	3.2 mm x 1.5 mm x 1.1 mm (1206)
Peak Wavelength Absorbance	630nm	940nm
Sensitivity Wavelength range	390nm – 700nm	730-1100nm
Half angle	-	-
Emitter-collector-voltage	Voltage range 2.5V to 5.5V	5 V
Collector-emitter voltage	-	30 V
Collector Current	-	20mA
Dark Current	100nA	100nA
Rise and Fall Time	0.11 ms – 0.22 ms	-
Power Rating	75mW	75mW
Operating Temperature	-40ºC – +85ºC	-25ºC – +85º C

Sensor-1 is designed with visual and infrared light subdivisions, each subdivision contains an LED and a phototransistor. The visual light and infrared subdivisions contain the LED: red 660nm and IR 940nm, respectively. The visual light phototransistor has a detection range of 390nm – 700nm, allowing the photosensor to detect the emissions from the 660nm red LED but not the 940nm IR LED. In contrast the infrared phototransistor has a range of 730nm – 1100nm, facilitating the detection of the 940nm IR LED but not the 660nm red LED. The emission intensity and the detection intensity of the LEDs and the phototransistors can be seen overlain with respect to wavelength in figure 3.6. The visual light sensor detects the emissions from the red LED but does not detect any emissions from the IR LED, and the IR light sensor detects emission from the IR LED, but not the red LED. This is optimal for the data acquisition of the sensor, allowing both emissions to be detected simultaneously, as separate signals.
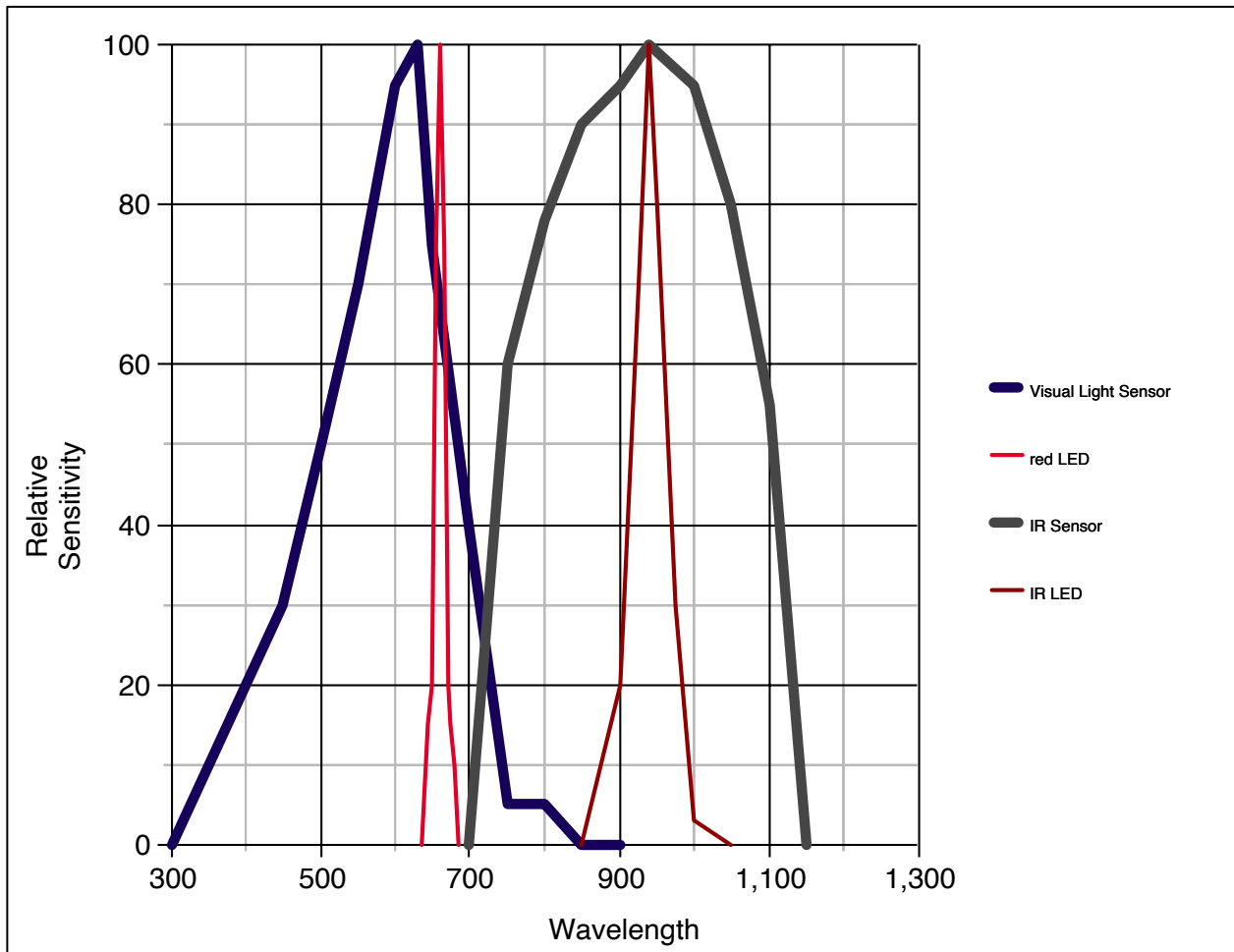
Figure 3.6: Absorbance and emission spectrum of the optical components utilized in Sensor-1, The visual light sensor is indicated by the thick navy blue line, the red LED, the thin red line, the IR sensor the thick gray line and the IR LED, by the thin dark red line. The graph illustrates the IR LED emissions are detected by the IR sensor, and the red LED emissions are detected by the visual light sensor.

3.1.3 Electronic Development of *Sensor-1*

Sensor-1 electronics are implemented within a printed circuit board (PCB), containing through-holes and padding shown in figure 3.7. The padding is designed with specific dimensions to allow the soldering of the SMD (surface mount device) LEDs and photosensors. The through-holes in the PBC are implemented to solder wires through the sensor and control the device remotely. *Sensor-1*'s design meets the 11 mm diameter requirement and includes all 4 SMD

optical parts with the appropriate connections. Not pictured, is the back side of the PCB, which contains the resistors needed to operate the sensors and LEDs. The back of *Sensor-1* is designed with similar padding to solder the resistors needed to operate the sensor.
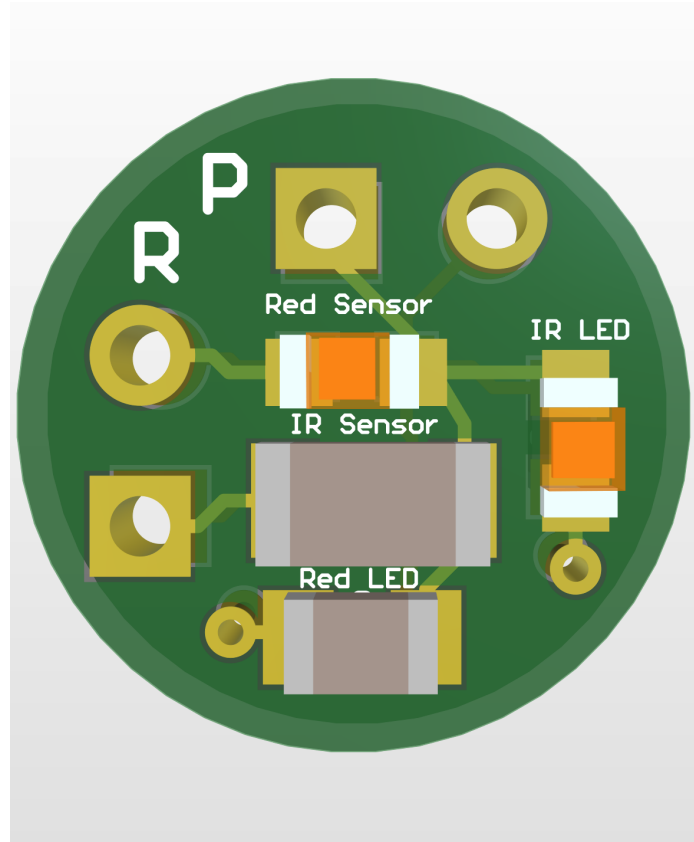
Figure 3.7: 3D -rendering of sensor-1 PBC, there are 4 optical components, two sensors and two LEDs, labeled on the board. There are 4 pin- out holes in the board to wire each component.

The electronic schematic for *Sensor-1* can be seen in figure 3.8, as mentioned above the back of the PCB is designed with padding to accommodate the resistors, illustrated in the schematic below. The sensor is designed to receive 5 volts of power, which is altered depending on component requirements. The red LED and IR LED have a forward voltage 1.85V (at 40mA forward current), and 1.40V (at 20mA forward current) respectively. Both LEDs require a resistor to supply optimal voltage to the components, a 820ohm resistor is implemented between the 5v and the LED leads. The phototransistor detection signal was optimized for both the visual

and IR photosensors, a 10kOhm resistor was added between the provided power and the photosensor.

The visual and IR photosensors are phototransistors, operate by changing current in response to changes in light. The electronics involved with a phototransistor will be discussed in future chapters, but it is important to note that a voltage divider is needed to acquire voltage signal changes from a phototransistor. A voltage divider is implemented for both phototransistors with a 10kOhm resistor utilized, seen in figure 3.8
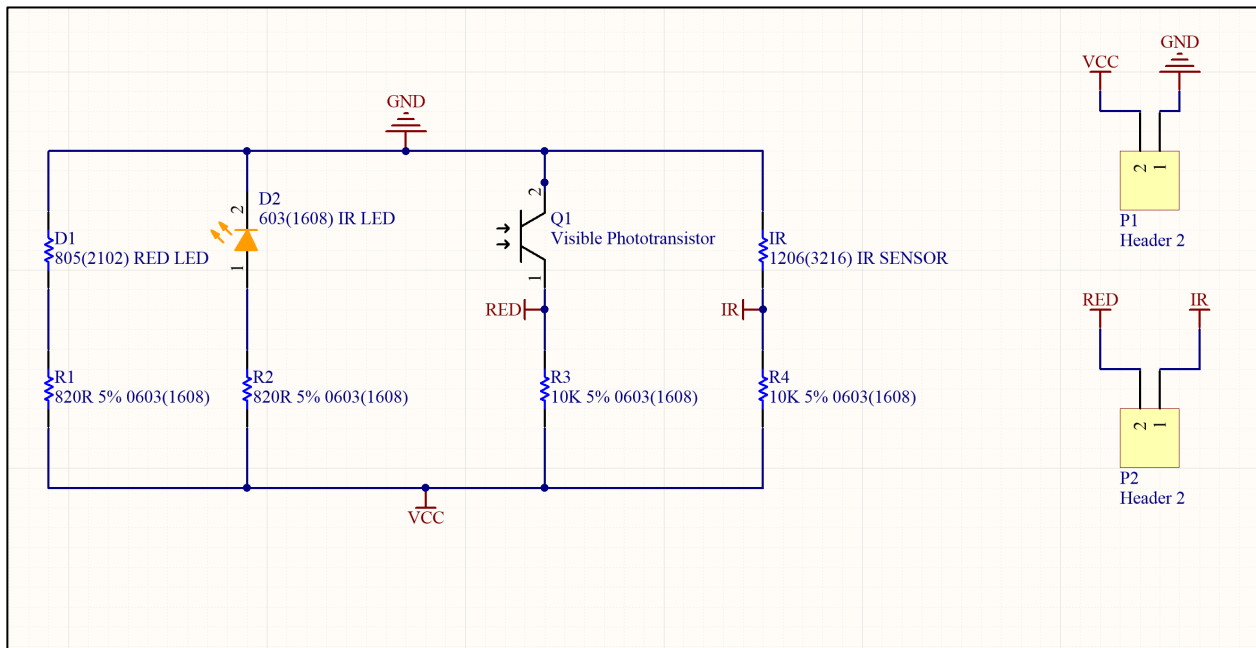
Figure 3.8: Schematic of electronics for sensor 1. D1 and D2 are the Red and IR LEDs respectively, both LEDs require an 820ohm resistor, R1 and R2. The phototransistors Q1(visible phototransistor) and Q2(IR phototransistor) require a 10kohm resistor; R3 and R4. All components are wired to ground.

3.1.4   Failures and Limitations of *Sensor-1*

Sensor-1 was connected to an oscilloscope to evaluate and optimize the signal. Throughout the oscilloscope testing it was discovered that the visual light sensor (ALS-PT19-315C/L177/TR8, Everlight Electronics Co Ltd., Taiwan) was able to detect not only the red 660nm LED but also the 940nm IR LED. The visual light sensor did specify that it had a range of 390nm-700nm and would not be able to detect light greater than 700nm. Because the visual light sensor can detect the IR (940nm) emission the sensor is unable to successfully differentiate between the emitted IR signal and the red signal. Although it is optimal to have two separate photosensors capable of detecting contrasting wavelength spectrums, it was difficult to find a photosensor with such a limited detection range capable of fitting on a 10mm PCB. After evaluation of Sensor-1 design and components it was determined the best method is to reconstruct the sensor utilizing smaller electronic components and a single photosensor. It was decided to utilize the current ambient light sensor as the sole phototransistor in the design of *Sensor-2*, because it was able to detect both the IR 940nm and 660nm LEDs being utilized. With only one photosensor the new sensor would have to utilize a sample and hold signaling technique to acquire signal from both LEDs. The sample and hold signaling technique allows the sensor to quickly alternate between collection of red and IR LED emissions and storing the data to generate a fluid emission graph. When using the switch and hold signaling it is important to note the frequency of rise and fall time of the phototransistor, as well as the rate of emission of the LEDs.

Further testing of *Sensor-1* identified that the visual light sensor actually acquired a higher-quality signal from the IR LED emission than the red LED emission. The red emission was noisy and low because the LED was not as bright as the IR(940nm) LED. Re-evaluating the LEDs utilized in *Sensor-1*, it was determined that the IR LED has a greater luminosity than the red LED. For S*ensor-2* a higher luminosity red LED with the same wavelength was utilized to provide more light penetrating the tissue and returning to the sensor.

Even though it was decided that the IR photosensor would not be utilized in *Sensor-2* it was discovered, when the IR LED and the IR photosensor were enabled the PPG signal exhibited

high amplitude, and high noise. The noisy signal from the IR phototransistor, was most likely a result of the component distance. When designing a reflective biased PPG sensor, the distance between the photosensor and the LED is critical to the acquired PPG signal. If the sensor and the LED are too close the light emitting from the LED will be directly absorbed by the photosensor before reaching the tissue, and the photosensor will be over saturated. If the LED is too far from the photosensor there will not be enough reflected signal from the LED to reach the photosensor, resulting in a low intensity noisy signal. The goal is to determine the optimal distance between the photosensor and the LED to optimize and refine the PPG signal.

3.2   Photoplethysmography *Sensor-2*

The PPG sensor or pulse oximeter is designed with optical components to emit and acquire light signals reflected from the tissue. The PPG sensor developed is a dual-wavelength sensor containing two LED's of different wavelengths. As the LEDs emit light into the tissue the phototransistor detects the reflected light, which is converted into absorbance. *Sensor-2*, the final sensor design, contains three optical components, two LEDs, with emissions in the visual and IR light spectrum, and one photosensor. The photosensor utilized is a phototransistor, which fluctuates current in response to changes in light. Most pulse oximeters or PPG sensors contain photodiodes as the photosensor, but a phototransistor was selected due to its increased sensitivity[28]. *Sensor-2* components are implemented on a 10 3/8 mm dimeter circle printed circuit board (PCB). The sensor components are controlled using an NI myDAQ with compatible LabVIEW software. The software is capable of powering the LED's, collecting the signal from the phototransistor and evaluating the signal to calculate and produce an SpO_2 value. Emissions from the LEDs enter the tissue, respond to blood volume changes and backscatter to be detected by the phototransistor. Once the reflected light is detected by the phototransistor, the response is converted from current to voltage and collected into the mDAQ for further signal manipulation.

3.2.1   Optical components of *Sensor-2*

Similar to *Sensor-1*, *Sensor-2* contains a red and IR LED, with emission at 660nm and 940nm, respectively. *Sensor- 2* contains a signal photosensor, the visual light sensor from *Sensor-1* is

utilized in *Sensor-2*, due to the ability to detect both the IR and red LED emissions. The schematic of the *Sensor-2* can be seen in figure 3.9, including the two LEDs, and the visual light phototransistor. The system consists of optical, electrical and signal processing components, all of which are designed together to generate a PPG signal and determine the SpO$_2$.
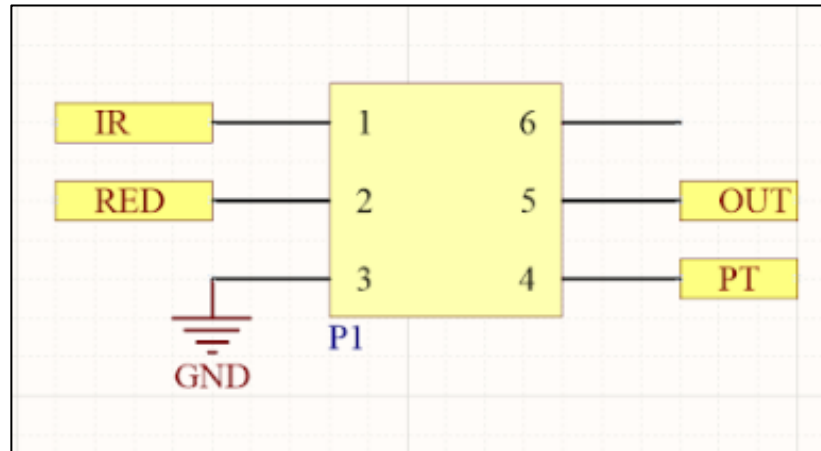
Figure 3.9: Sensor-2 circuit board schematic, there are 6 pin-out connections from the board, pin-1 is power to the IR LED, pin-2 is power to the red LED, pin-3 is ground, pin-4 is power to the phototransistor, pin-5 is acquisition from the phototransistor and pin-6 is open.

The 660nm red LED (SML-LX0603SRW-TR, Lumex Opto/Components Inc., USA) selected for *Sensor-2* has a peak wavelength at 660nm and a 0805 surface mounting package (1.6 mm x 0.8 mm x 0.60 mm). The 940nm IR LED (APT1608F3C, Kingbright, Taiwan) selected for *Sensor-2* has a peak wavelength at 940nm and a range of 50nm. The specifications for the IR and red LEDs are indicated in table 3.3.
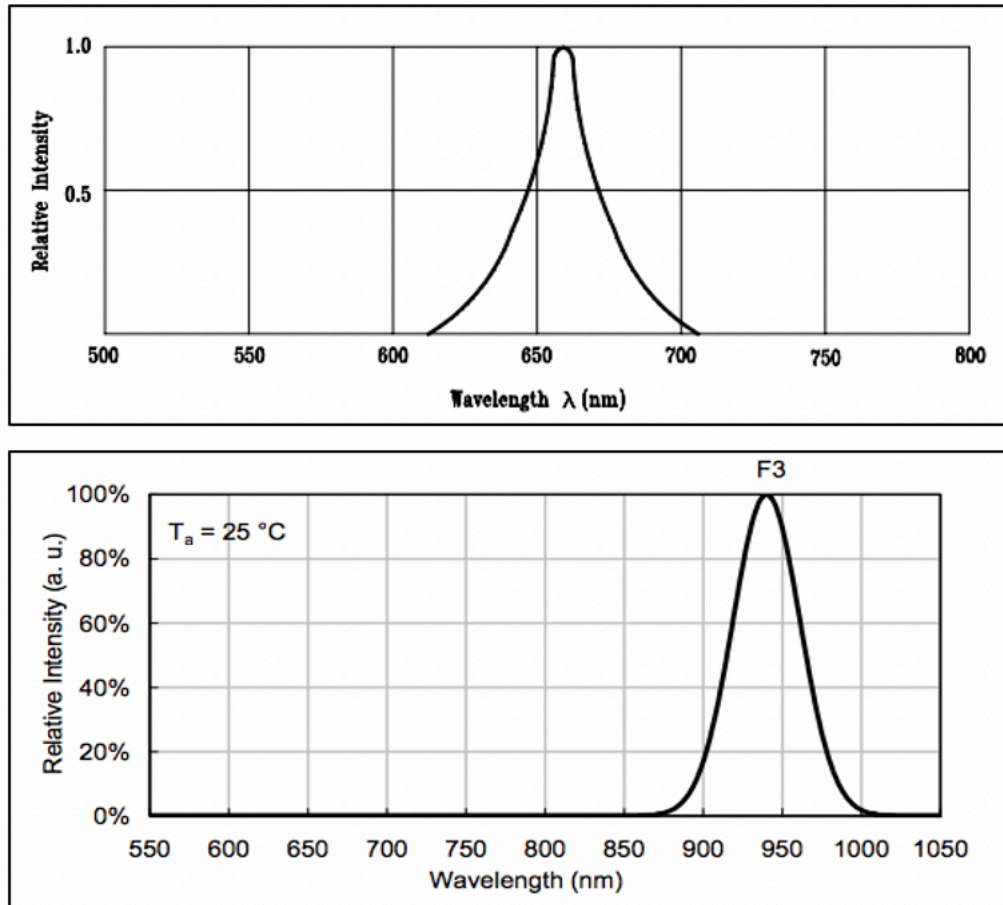
Figure 3.10: Emission spectrum of the red and IR LED respectively, with relative sensitivity on the y-axis and wavelength on the x-axis. The red LED has a peak wavelength of 660nm and the IR LED has a peak wavelength of 940nm.

Table 3.3: Optical and electrical characteristics of the red (SML-LX0603SRW-TR) 660nm LED and the IR (APT1608F3C) 940nm LED respectively

Parameter	Red LED	IR LED
Dimensions	1.6 mm x 0.8 mm x 0.6 mm	1.6 mm x 0.8 mm x 0.75 mm
Peak Wavelength (IF=20mA)	660 nm	940 nm
Spectal Line Halfwidth (deltaY ½)	-	50 nm
Luminous Intensity	15 mcd	-
Forward Current	40 mA	20 mA
Forward Voltage (IF=20mA)	1.7 V	1.2 V
Capacitance		90 pF
Power Dissipation	50 mW	90 mW
Reverse Voltage	5 V	5 V
Operating Temperature	-40 to +85 ºC	-40 to +85 ºC

The phototransistor in *Sensor-2* detects light reflected from the tissues and in response the current traveling across the component changes. The PPG sensor contains the surface mount ambient light sensor (ALS-PT19-315C/L177/TR8, Everlight Electronics Co Ltd., Taiwan) utilized in Sensor-1, capable of sensing a wide range of emissions. The spectral range for the phototransistor is unknown but, discovered from failures in *Sensor-1*, is capable of detecting both 940nm IR LED and 660nm red LED emissions.

Table 3.4: Optical and electrical characteristics of the (ALS-PT19-315C/L177/TR8) phototransistor

Parameter	Phototransistor
Peak Wavelength	630 nm
Sensitivity Wavelength range	-
Half angle	390nm - ~1100nm
Emitter-Collecter- voltage	2.5 V – 5.5 V
Dark Current	100 nA
Rise and Fall Time	0.11 ms – 0.22 ms
Saturation Output Voltage	4.5 V
Power Rating	75mW
Reverse Voltage	5 V
Operating Temperature	-40ºC to +85 ºC

3.2.2   Electrical Development of *Sensor-2*

The PPG sensor is an optoelectronic sensor containing a dual wavelength light emission, a photodetector and a microprocessor system (MS). The PPG sensor developed in this thesis utilizes a National instruments myDAQ and LabVIEW as the microprocessor system. The optical components are mounted onto a custom printed circuit board (PCB) no greater than 11mm in diameter. Within the 11mm maximum diameter the board contains two LED's and a phototransistor, which are separated to an optimal distance. The design of the PCB and the orientation of the components is crucial to the PPG signal. In reflective-based PPG sensors the distance between the LED's and the photosensor must be optimized to ensure the most accurate data is collected. The absorbance of the light will change as the distance between the optical components changes. The distance should be such that the maximum(AC) and minimum(DC) components of the PPG signal can be differentiated[28]. If the LEDs are too close to the

phototransistor, light from the LED will be detected by the phototransistor before reaching the tissues, thus producing a PPG signal with no information about the blood volume and high background noise. The background noise is known as the DC component of the PPG signal, or the valley produced by the heartbeat as seen in figure 2.18. When the DC amplitude is greater than the AC amplitude (peak) noise will saturate the signal and the AC signal will be indistinguishable. A study was done by Mendelson and Ochs, investigating the optimal separation distance between the components and the results are shown in figure 3.11 [40].
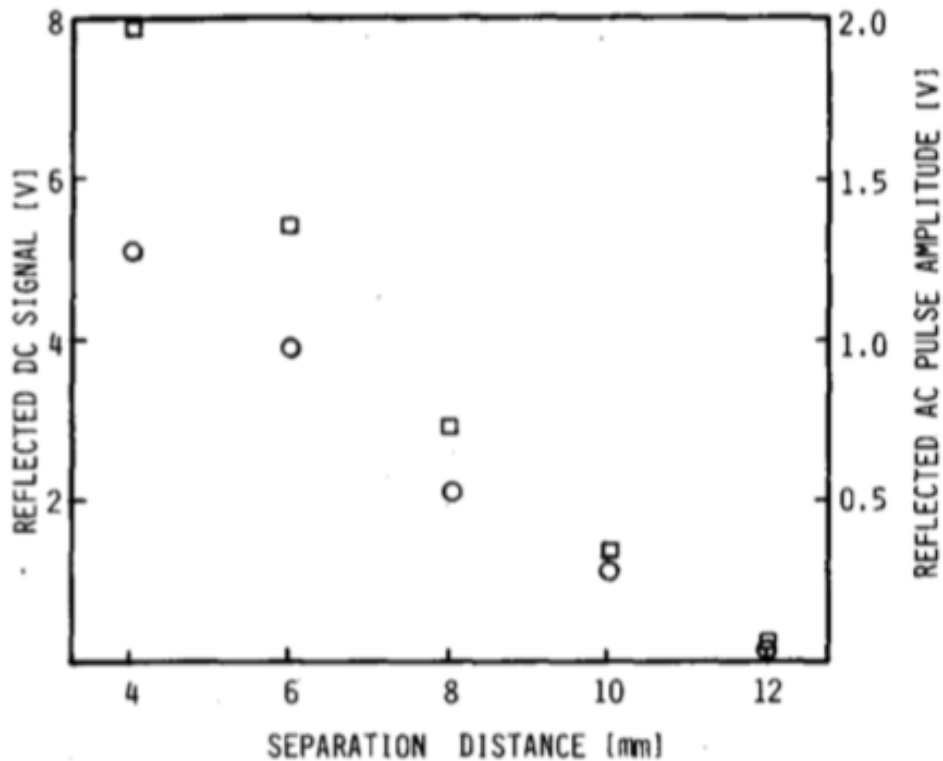
Figure 3.11: The separation distance of the photosensor relative to the LEDs on a PPG sensor with respect the AC (○) and DC (□) components of the PPG signal. The y-axis represents the amount of reflected AC and DC signal as a voltage from a photosensor. The distance between the light sensor and the LEDs should be no less than 4mm and no greater than 11mm. Image recreated from [38].

Figure 3.11 indicates that if the LED and photosensor are 12mm apart the amplitude of the AC and DC component is low, and no light is reaching the phototransistor. As the separation

distance between the components decreases the AC amplitude increases and becomes distinguishable from the DC component. The graph also illustrates, the DC intensity increases over the AC component as the separation distance is minimized, indicating saturation of the phototransistor. The study suggests a minimum of 4mm and a maximum of 11mm separation distance between the optical components is capable of increasing the PPG amplification two-fold[38].

A printed circuit board (PCB) contains of copper-based layers between non-conductive materials, the model supports electronic components and connections made through etching track or pads in the PCB. Altium Designer (Altium Ltd, Australia) was utilized to design and construct the PCB. After the PCBs were designed the boards were ordered through OSHPARK (Oshpark LLC, United States), a PBC board manufacturer. Figure 3.12 contains two CAD images, (A) and (B), illustrating the front and the back of *Sensor-2's* PCB design, respectively. The front of the PCB (figure 3.12-A) contains four padding sites on the right and two padding sites on the left. The right padding sites are for the IR and red LEDs and the left is for the photosensor. The back of the PCB (figure 3.12-B) contains six padding locations, implemented for the addition of a SMD conn Header (TSM-103-01-T-DV-TR, Samtec ©) seen in figure 3.13.
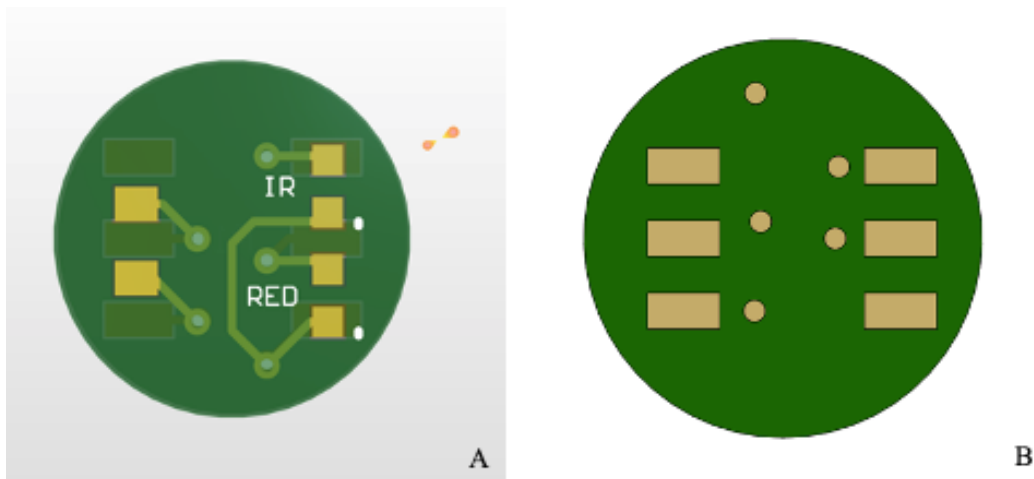
Figure 3.12: Printed Circuit Board layout for Sensor-2. (A) the top/front of the board indicating the soldering pads for the LEDs and photosensor. (B) The back of the board illustrating the 6 pads for the SMD header, to facilitate wiring to the board and components.

Figure 3.13: The SMD 6position conn Header (TSM-103-01-T-DV-TR, Samtec ©) soldered to the back of sensor-2 PCB.

A computer-aided design (CAD) model of *Sensor-2* can be seen in figure 3.14, containing the phototransistor and both the IR and red LED. The model was designed in SolidWorks to visualize the size and dimensions of the final sensor. The LEDs are approximately 4mm from the phototransistor, the maximum distance attainable within the 11mm diameter board. As discussed previously the distance between the photosensor and the LEDs is critical to the PPG signal obtained. Anything less than 4mm would saturate the photosensor, so it was optimal to use the extent of the board to maximize the distance between the components.
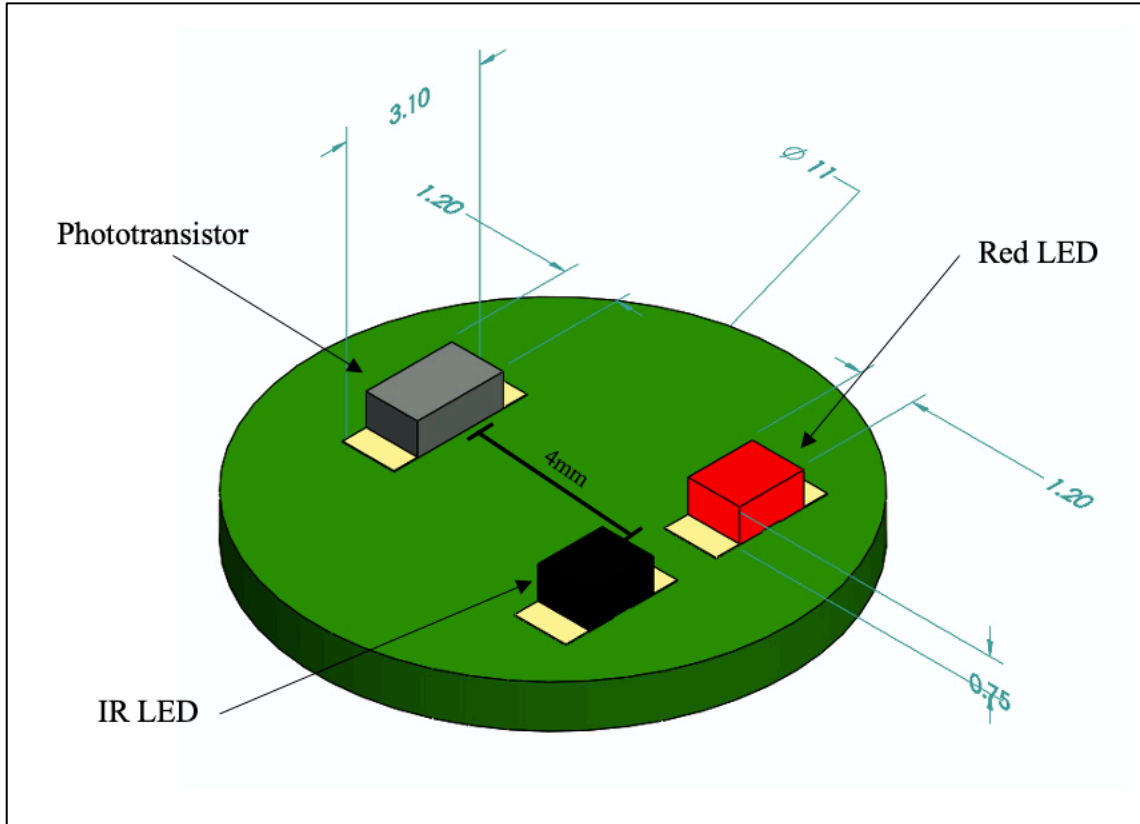
Figure 3.14: 3D rendering of Sensor-2 housing the optical components, the two LEDs are located on the right side of the sensor and the phototransistor on the left. The red LED is red, the IR LED is black, and the phototransistor is gray. The phototransistor is located 4mm to the left of the LEDs, the maximum distance that the 11mm diameter sensor could accommodate.

The final sensor with the soldered optical parts is seen in figure 3.15, the phototransistor is soldered to the padding on the left and the LEDs on the right. The distance between the two LEDs is insignificant because they will be alternating power, due to the use of a single photosensor.
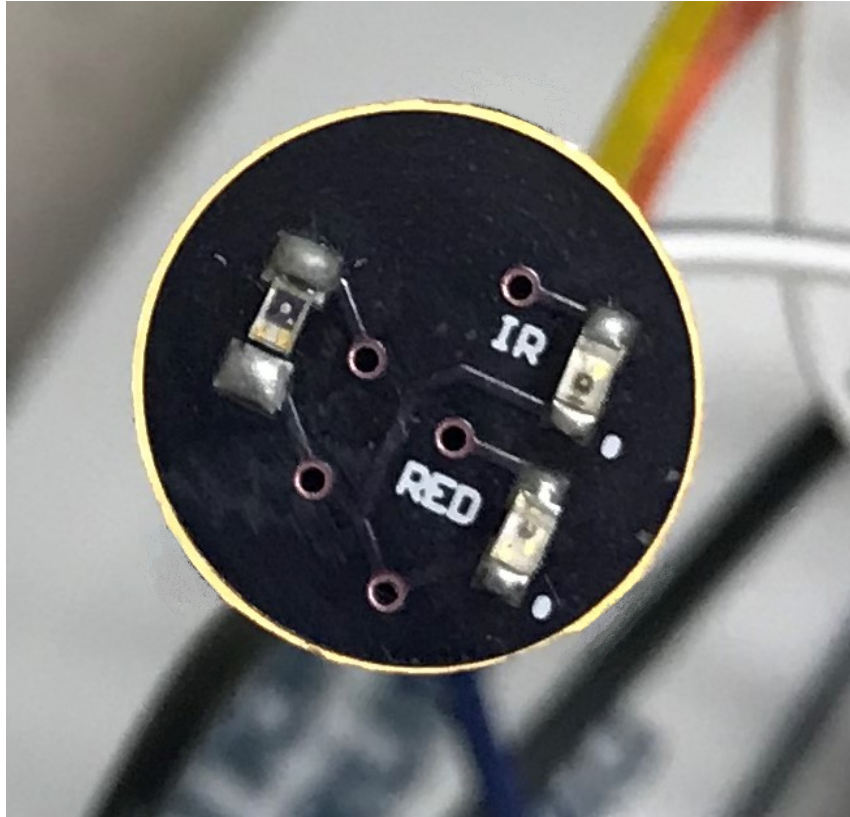
Figure 3.15: Visual image of the front of the final sensor design (Sensor-2) with optical components soldered on, the two LEDs are located on the right side of the board 4mm away from the phototransistor which is located on the left. The LEDs are labeled on the board with "IR" and "RED" correlating to the IR LED and the red LED respectively.

Sensor-2 electronic connection schematic, depicted in figure 3.16, houses 6 pins connected from the back of the PCB to terminals to control the components. The six pins consist of power to both of the LEDs, power to the phototransistor, signal out from the phototransistor and ground. An NI myDAQ is used to control the components from the pins and signal acquisition, from the phototransistor.
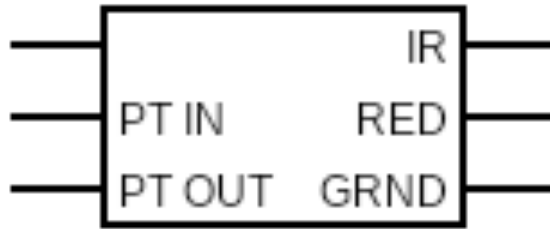
Figure 3.17 is the circuit diagram for the two LEDs, 3v supplied from the NI MyDAQ passes through a 2.2kΩ resistor before passing through the LED and connecting to ground. This schematic is the same for the IR (940nm) and red (660nm) LEDs.
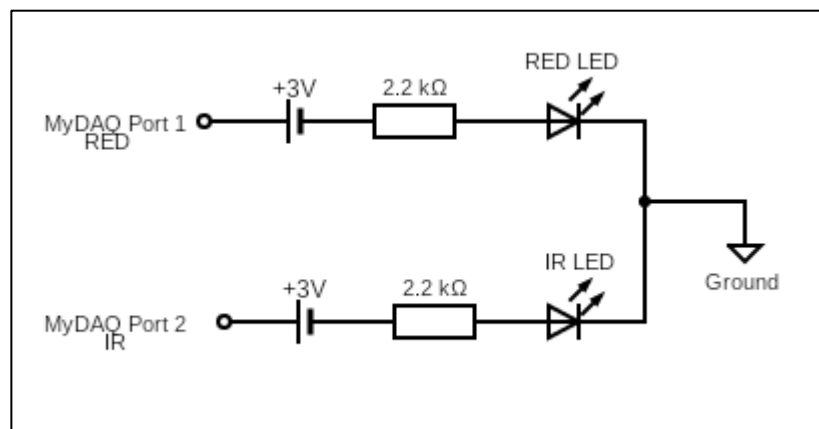
Sensor-2 utilizes a phototransistor as the photosensor, as mentioned above the phototransistor changes current in response to light. Because of this a voltage divider is needed to receive a voltage signal from the phototransistor. The schematic for this component can be seen in figure 3.18 where 5v is supplied to the phototransistor. The 5v passed through the phototransistor, to a

10kΩ resistor and then connecting to ground to close the circuit. The phototransistor output signal is measured between the phototransistor and the 10kΩ resistor.
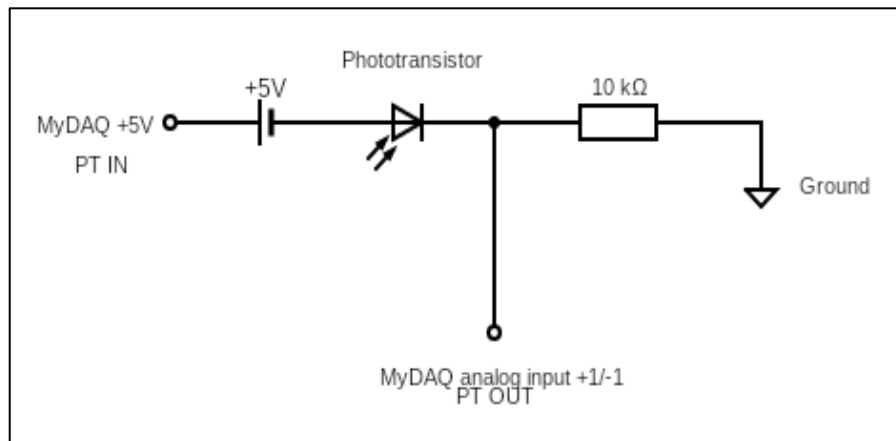
Figure 3.18: Phototransistor electronic schematic +5v is supplied to the phototransistor from the myDAQ 5v pin, the PT is powered and connected to ground via a 10kΩ resistor. The out signal from the phototransistor is collected between the phototransistor and the 10kΩ resistor. The signal is acquired on the myDAQ via the analog input +1/-1.

The phototransistor circuit operates using the voltage divider, when there is minimal light hitting the phototransistor, the voltage out signal will be low, as more light begins hitting the sensor the voltage out will increase toward Vcc in this case +5v form the NI nyDAQ. The voltage out signal will change as more or less light is hitting the sensor. Measuring the voltage out provides a signal in response to more or less light hitting the sensor, representing the increase and decrease in blood perfusion from the heart beating.

3.2.3   Signal acquisition and Processing (LabVIEW) of *Sensor-2*

The majority of signal processing is performed using National Instruments (NI) LabVIEW suite. The LabVIEW suite contains a powerful graphical block coding software and compatible external microcontrollers. The myDAQ, an external microcontroller in the LabVIEW suite, is utilized to control the components of *Sensor-2*. The myDAQ is responsible for powering the LEDs and the phototransistor, as well as receiving and analyzing the phototransistor signal. The LabVIEW software processes the signal and relays controls to the myDAQ. figure 3.19 illustrates the signal flow from the sensor components to the LabVIEW software. One of the

reasons LabVIEW is such a powerful software is because of its integrated graphical user interface (GUI). For Sensor-2, a GUI created in the LabVIEW software, relays signals to the NI myDAQ, which is connected to the sensor and controls the optical components (figure 3.19).
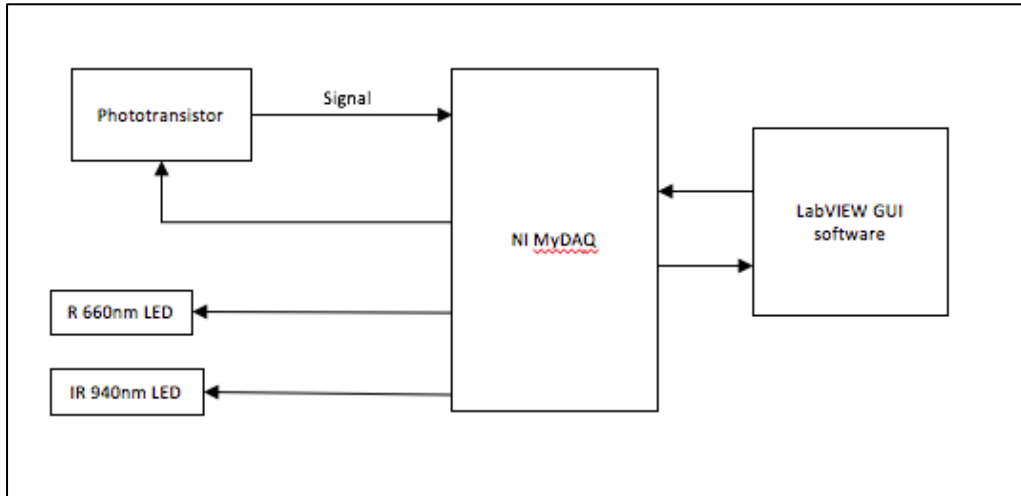
Figure 3.19: The schematic diagram for the PPG sensor processor includes a National Instrument myDAQ which receives and feeds information to the LabVIEW GUI and software. The myDAQ not only powers the two LEDs and the phototransistor, but also acquires signal from the phototransistor.

The majority of PPG sensors utilize an external motherboard that controls the components, but for the extent of this thesis it was optimal to utilize the LabVIEW suite to optimize the signal. In a PPG sensor signal processing is a critical component, the control of the LEDs, the signal transmitted to the phototransistor, the signal acquired from the phototransistor as well as the signal calculations all need to be optimized to generate a selective PPG sensor.

CHAPTER 4

4.0   SIGNAL PROCESSING

As blood volume changes due to the heart rate, more blood reaches the extremities and the phototransistor reacts to more or less light hitting the sensor. This signal can be manipulated to optimize the information. There are many signal manipulation processes utilized in PPG sensors, the majority are applied utilizing a variety of electronic components, and a microprocessor. In some sensors additional electronic components are designed to amplify, filter and sort the data appropriately before the signal is processed by an external microprocessor. Figure 4.1 is a general signal manipulation flow diagram for a PPG sensor, for each component in the schematic the signal is optimized for the ratio calculation. The phototransistor signal is processed through an initial amplifier to reduce the signal to noise ratio (S/N). As discussed in previous chapters the phototransistor cannot differentiate between the red and IR LED signals, so a sample and hold mechanism is utilized to separate the signals. The sample-and-hold mechanism is triggered by the LED states, for example when the IR LED is on the sample-and-hold is collecting the IR signal, and vice versa. The separate components are individually processed through a filter, and the DC offset is determined. The separate signals are then amplified individually and compared to calculate the AC/DC ratio.
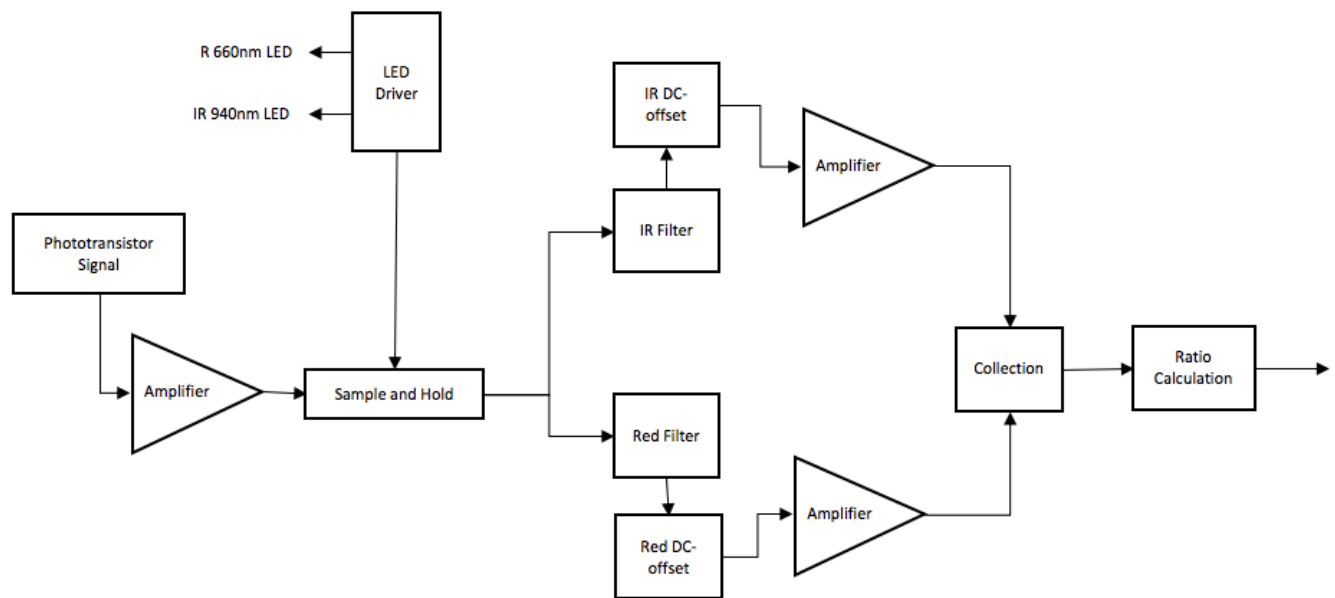
Figure 4.1: General PPG signal manipulation, signal received from the Phototransistor enters an amplifier to increase the signal received, the signal is then manipulated using the sample and hold technique were the signal is divided into IR and Red signals. Both signals are filtered and normalized by evaluating the DC off-set, after normalization the AC component of the signals are amplified, the data is then collected, and the ratio is calculated.

The majority of PPG sensors manipulate the signal via electronic components, for the sensor in this thesis all of the signal optimization and calculation is executed using the NI myDAQ and LabVIEW processing suite. The NI myDAQ and LabVIEW software are capable of controlling the PPG sensor components as well as manipulating the signal similar to electronic components.

4.1 LabVIEW and My DAQ Component Control

LabVIEW™ stands for Laboratory Virtual Instrument Engineering Workbench and is a system-design platform for visual programing from National Instruments©. All of the necessary components for signal manipulation described in figure 4.1 are processed using LabVIEW. The NI package uses a myDAQ™ an external data acquisition device to acquire signals. The myDAQ™ is paired with the NI LabVIEW™ software, where the signals acquired from the myDAQ™ are processed. The schematic in figure 4.2 describes the signal processing for the PPG sensor.
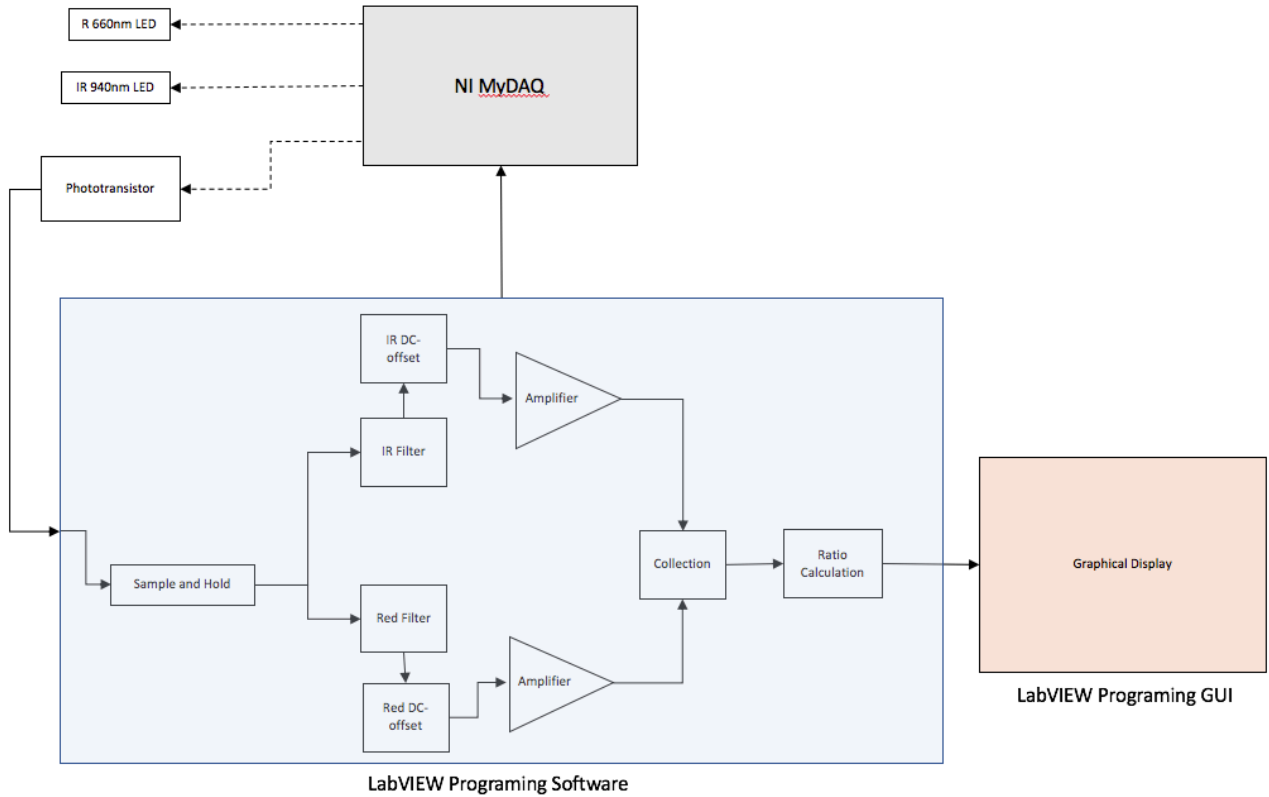
Figure 4.2: The LabVIEW Programing suite is responsible for relaying information the NI myDAQ which provides power to the LEDs and the phototransistor. Data from the phototransistor is acquired through the myDAQ and processed in the programing software. The signals and controls are processed and viewed through the LabVIEW GUI.

The LabVIEW program encompasses all of the signal manipulation involved in a PPG sensor, the signal manipulation in figure 4.1 is indicated in figure 4.2 as LabVIEW software. Signal from the LabVIEW software is sent to the NI myDAQ where the signal is relayed to drive the LEDs and the phototransistor. The information received from the phototransistor is collected through the myDAQ and processed in the programing software and displayed through the programs graphical user interface (GUI).

4.1.1 NI myDAQ Sensor Component Control

The NI myDAQ is a powerful signal acquisition device capable of a variety of electrical signal drivers and acquisitions. The myDAQ is equipped with analog signal acquisition input (+/- 10v), 7 digital IO pins (0-5v), a common ground, and a 5v power supply. The DAQ also incorporates audio in and out as well as a digital multimeter.

The NI myDAQ is utilized as the digital driver to control components and acquire the phototransistor signal. The electronic control of the PPG sensor via the myDAQ is illustrated in figure 4.3, the wire connections from the myDAQ to the sensor are connected to the front of the board, this is done to provide a more comprehensive understanding of the electrical components, but it is important to note that the PPG sensor is wired via pins on the back of the board. The PPG sensor seen in figure 4.3, consists of the IR LED (black), the red LED (red) and the phototransistor(grey), each element on the sensor is connected to the myDAQ. The myDAQ controls the red LED via the DIO port1 and, the IR LED via DIO port2, both LEDs require a 2.2kΩ resistor to optimize the emission signal. The phototransistor is supplied 5v of power from the myDAQ and then wired to ground to close the circuit. Between the phototransistor and ground is a 10kΩ resistor, the signal is collected between the component and the resistor, depicted in figure 4.3. The myDAQ collects the phototransistor signal via the analog 1+ port, which is used for signal acquisition by the myDAQ.
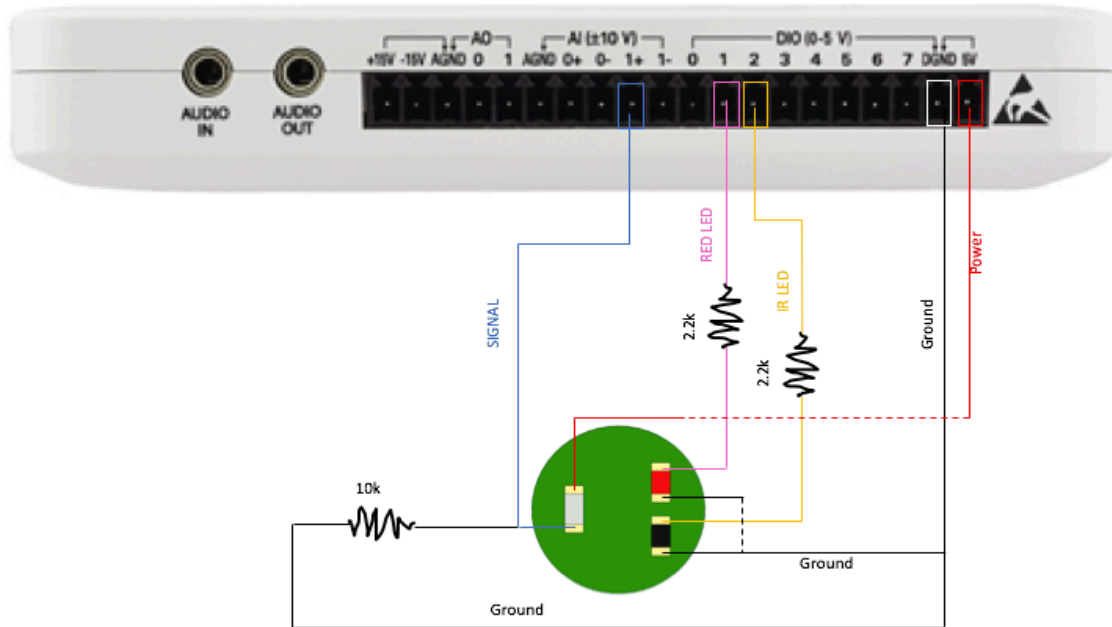
Figure 4.3: NI myDAQ (the white box) wiring diagram to the PPG sensor, the figure shows wiring on the front of the sensor, this is for comprehension of the electronics in the actual sensor the connections are from the back. The red(red) and the IR LED(black)s are connected to pins 1 and 2 on the myDAQ DOI out pins. The myDAQ pins providing power to the LEDs pass through a 2.2kΩ resistor before powering the LEDS. The myDAQ 5v pin supplies power to the phototransistor, and the signal out from the phototransistor is collected by the AI pin 1+ on the myDAQ. The phototransistor out passes through a 10kΩ resistor before connecting with the LEDs and closing the circuit to ground.

4.1.2 LabVIEW Software Component Control

As discussed above the digital outputs (DIO pins) on the myDAQ are wired to the LEDs on the PPG sensor, and control power to the LEDs. The LabVIEW software controls the myDAQ and thus regulates the power supplied to the LEDs. The software is designed to drive the LEDs, similar to how a LED driver circuit would operate in stand-alone PPG sensors. The PPG sensor contains two LEDs and one phototransistor, and the phototransistor reacts to light from both the 660nm LED and the 940nm LED, because of this a sample-and-hold technique is needed to collect signal from the LEDs nearly simultaneously. The sample-and-hold technique works when the LEDs are rapidly alternating, so the phototransistor is never exposed to both LED emissions simultaneously.

74

An example of the LabVIEW software components needed to drive the LEDs, is illustrated in figure 4.4, contains a series of local variable controls (A), timers (B) and DAQ controls (C). The local variable control, figure 4.4-(A), is utilized to send information indicating the state of the LEDs to other components of the LabVIEW software. The timers or wait controls, figure 4.4-(B), are utilized to provide a pause in the sequence. The final component in the PPG sensor component control, figure 4.4-(C), is the myDAQ control, the signaling between the software and the myDAQ which provides power to the components and supplies the LEDs with power. The DAQ controls, the blue square in figure 4.4-(C), are wired a Boolean true or false, correlating to turning the LED on or off.
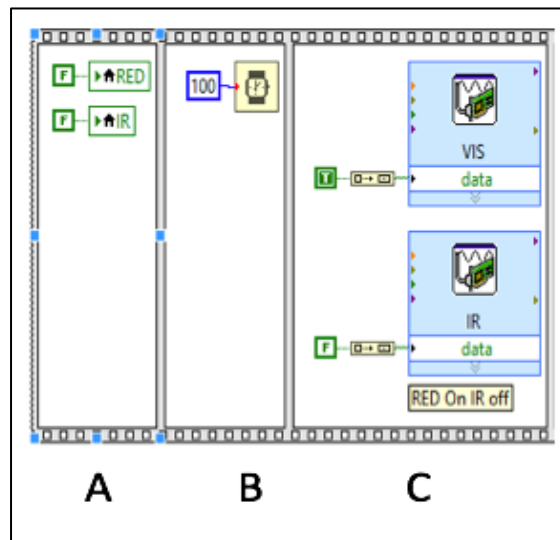
Figure 4.4: Example of sequence components in the LabVIEW software to drive the LEDs via the myDAQ. (A)Variable controls which change the state of digital variables that represent the LEDs, this is utilized to relay information about the LED states to other aspects of the software. (B)A timing sequence to delay the time between software actions. And (C) the blue blocks are express Vis that relay information to the NI myDAQ and provide power to specific pins, the express Vis are controlled with true and false Boolean commands.

The software to control the LEDs, utilizes a structure known as a sequence event, where each component in the sequence will operate in succession (figure 4.5). The sequence begins at left and moves from left to right through each segment in the sequence. If the sequence is placed in a while loop, once the sequence is completed it will go back to the first segment and start over.
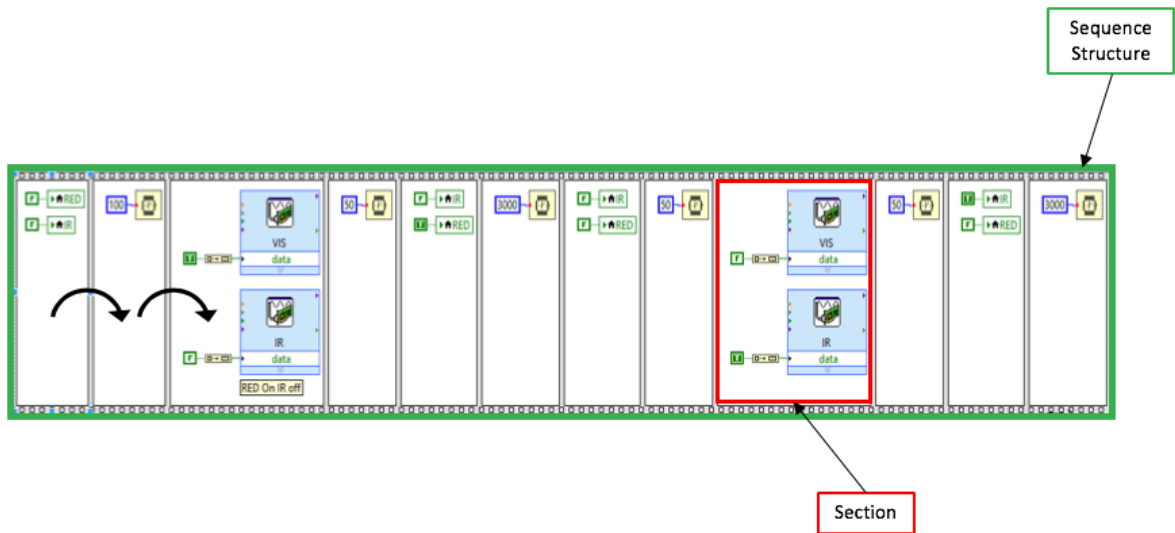
Figure 4.5: An example of a sequence designed in the LabView software; the green box encompasses the full sequence structure which is divided into sequence sections outlined with the red box. The arrows are the beginning of the sequence structure represents the path of the processes, the software will complete the task in each section in sequence.

Power to the LEDs is controlled by the LabVIEW program which relays signal to the DAQ and drives the LED states. The diagram above is an example of a sequence that can be utilized to control the LED states, and rapidly turn on and off the LEDs.

4.2   LabVIEW Signal processing

The LabVIEW software components needed to drive the LEDs was discussed above, the rapid switching of the LED states is used in the sample-and-hold technique. This technique is utilized so the phototransistor can collect emissions from the two LEDs, at virtually the same time. The myDAQ receives a signal from the LabVIEW software to control the components of the PPG sensor. The myDAQ also provides power to the phototransistor and acquires the returning signal from the phototransistor at the analog input. Data received from the phototransistor is manipulated in the LabVIEW software to optimize the signal. The received signal is processed through a sample and hold technique to separate the red and IR LED data collected by the phototransistor. The signal is amplified and filtered to exhibit the signal components and calculate the heart rate as well as the SpO_2.

4.2.1   Sample and Hold Technique

The sample-and-hold technique is needed in the PPG sensor, because it is designed with two LEDs and one phototransistor, capable of detecting both wavelengths of light. The technique works by driving the LEDs to alternate states rapidly, when one LED is on the other is off. For example if the red 660nm LED is powered on the IR 940nm LED must be off, this allows the phototransistor to pick up light emissions from only one LED. The other processing components of the sample-and-hold technique involves the signal being received by the photoresistor. If the signal was not divided into two separate signals the phototransistor would detect rapid switching between the LEDs and nothing about the red or IR LED signal could be differentiated. The sample-and-hold technique collects the "sample" or data from the phototransistor when indicated, and "holds" that data, until indicated to collect more data. For example when the red LED is powered on, signal from the LED will reflect off the tissue and become detected by the phototransistor, the signal will then be transported to the myDAQ and LabVIEW software. The signal received will be flagged as a "red LED" signal, and stored to a "red LED" signal data location. The "red LED" flagging will then turn off as the IR LED on the PPG sensor turns on and the LabVIEW software flags the new incoming data as "IR LED". An example of the incoming PPG signal with the sample-and-hold technique is graphed in figure 4.6 below.
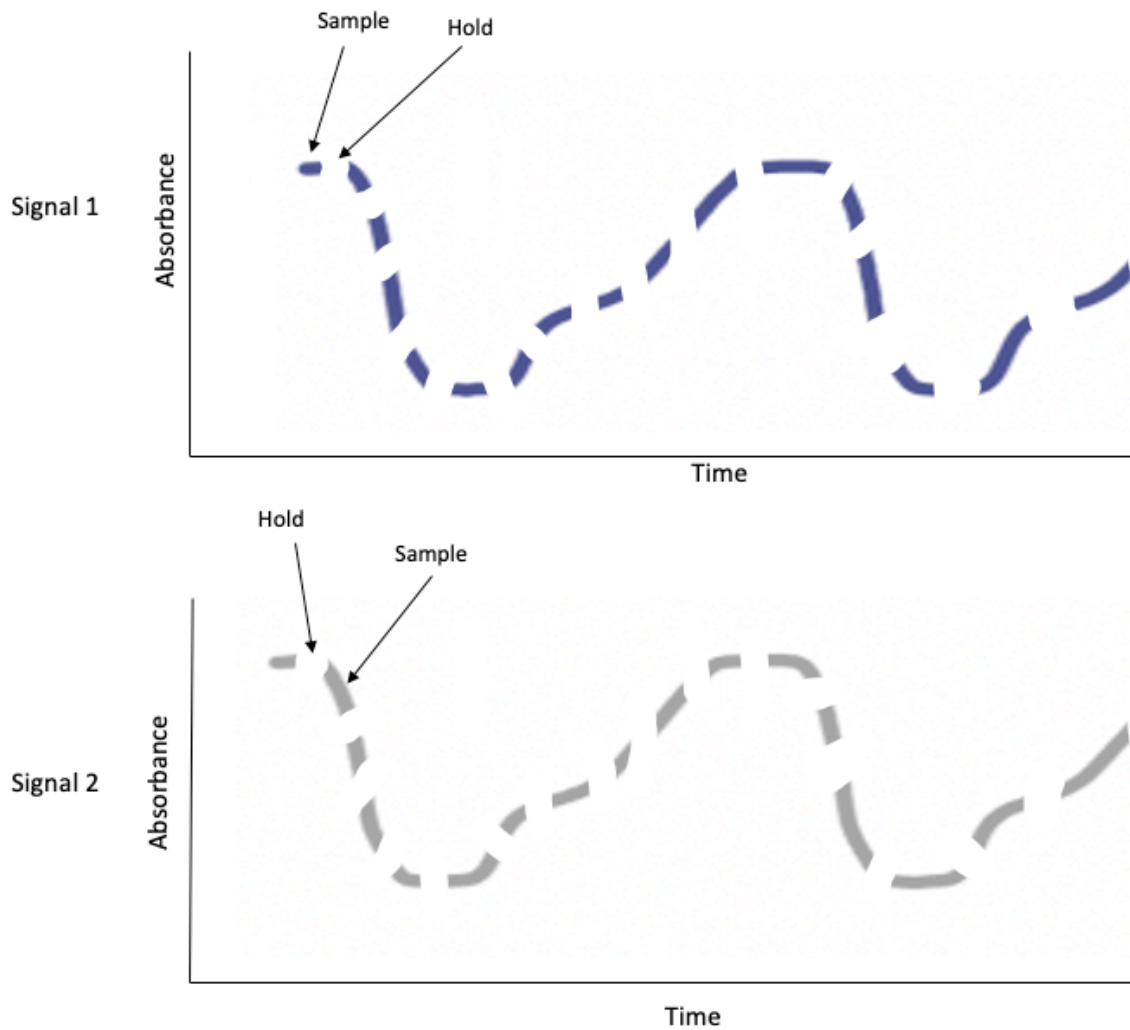
Figure 4.6: The sample and hold technique utilized for a PPG sensor with two LEDs and one photosensor, the first signal (signal 1) is the phototransistor signal when the first LED is powered, and signal 2 is the signal from the phototransistor when the second LED is powered. The software relays which LED is powered so that the incoming signal from the phototransistor is categorized with the correct wavelength. The separate signals can then be stitched together on separate graphs as separate signals.

If the sample and hold technique can be executed at a high enough frequency then the PPG signals can be stitched, meaning the missing data ignored and the data for each signal is connected to make a complete waveform instead of having gaps in the signal. Because the data is being stitched together and gaps ignored it is critical the sample and hold switching happens at a high rate. The calculation of SpO_2 requires the AC (peak) and DC (valley) of the IR and red

signals at the same time point, utilizing the sample-and-hold technique and the stitching of signals supplies these data points, for both wavelengths.

4.2.2   LabVIEW Software Signal processing

The signal coming in for the phototransistor via the analog input +1 on the myDAQ, must be manipulated to separate out the IR and red signals and evaluate the HR and SpO_2 values. Below figure 4.7 is the LabVIEW program designed to collect the PPG signals from the phototransistor and process the data. The first aspect of the program is the signal acquisition from the myDAQ indicated by figure 4.7-A, signal from the phototransistor is acquired by the myDAQ and processed in LabVIEW at a rate of 10kHz.

The signal is then processed using a relay switch figure 4.7-B, the relay switch in LabVIEW is similar to a sample-and-hold circuit, where the signals will only be acquired while the relay is enabled. As discussed in the previous section the LED driver circuit local variable control component enables and disables the relay switch. For example, when the red LED is on the local variable control will signal the red-relay to turn on and the signal from the phototransistor will be collected, and vice versa for the IR LED.

Once the signal for the IR and red LEDs are collected separately, there are passed through a bandpass filter in the LabVIEW software figure 4.7-C. The bandpass filter is a signal filtering control that is built into the software controls, the filtering is used to eliminate background noise and extract only the heart rate signal. A bandpass filter operates by extracting only the desired frequencies within the signal, defining a low pass frequency and a high pass frequency. A study was done to evaluate the optimal low pass filter (LPF) for calculating the AC/DC ratio of a PPG signal. The study indicated that lowering the frequency of the LPF resulted in a ratio with lower signal to noise and decreased standard deviations (SD)[34]. The bandpass filter utilized for the PPG sensor was set to 0.5Hz to 3Hz to extract only the frequency of signal needed.

After the signal is filtered the smoothed data is processed in an amplitude measurement component of the software, this component is continuously evaluating the amplitude between the positive peak and the negative peak. By measuring the peak-to-peak components of the PPG signal the ratio of AC/DC is extracted for both the IR and red signals. As discussed in previous sections the AC/DC ratio is what is utilized in the calculation of the SpO_2 percent. The ratios are stored and collected for evaluation figure 4.7-E where the ratio of the IR signal will be divided by the ratio of the red signal, to get the final ratio to evaluate the blood oxygen percentage.
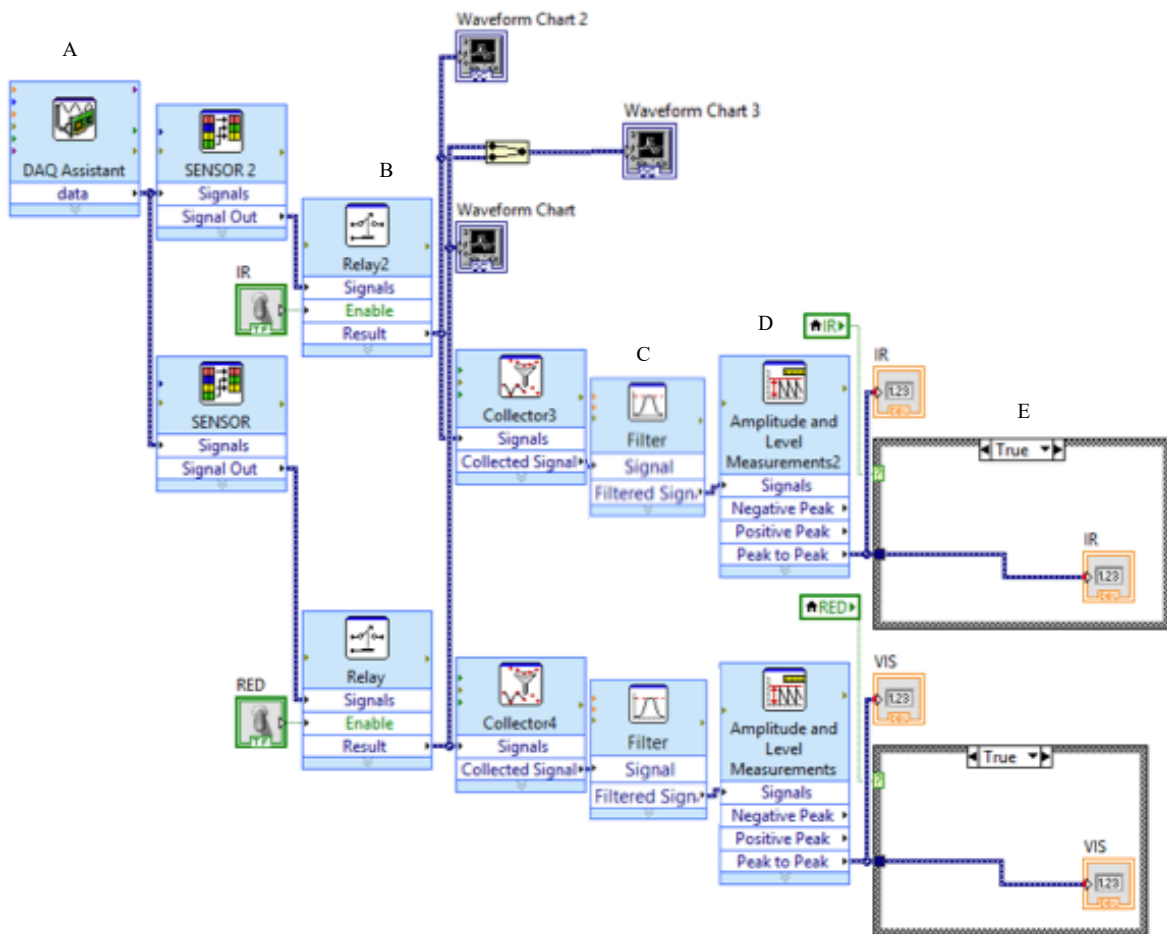
Figure 4.7: LabView software signal manipulation and processing, starts with (A) the DAQ assistant express VI relays the incoming data from the phototransistor from the NI MyDAQ to the LabVIEW software (B) the data from the is split into two signals using LabVIEW express VI relays. The two signals are then collected and Filtered (C) the filter is a band pass filter with a HPF at 0.5Hz and a LPF at 3HZ. The last express VI (D) selects the peaks and valleys of the signal correlating to the AC and DC components.

Figure 4.8 applies the same signal processing from 4.7 but the signal is acquired in a case structure to cycle through sensor states. The three states utilized in the case structure below are, "RED", "IR" and "DARK", each case is a different sensor state. This provides information about the background signal which is important for evaluation of the signal for example the background or "DARK" signal might be different if you are in a bright room or apply more pressure to the sensor. Figure 4.8 is divided into two sections A and B; figure 4.8-A controls the state and signal type being processed in section B. Figure 4.8-A cycles through three states "DARK", "RED" and "IR" for each state a different combo box (figure 4.8-B.1) is enabled. When figure 4.8-A is in the "DARK" state the combo box is in the "DARK" state and turns off both of the LEDs. When figure 4.8-A is in the "RED" state the combo box drives the red LED on and the IR LED off, and the "IR" state turns the IR LED on and the red LED off. For each state, the correlating signal from the PPG sensor is collected, after collection the data is passed to a relay switch to collect the IR and red LED signal figure 4.8 – B.2. The peaks of the signal are determined and passed through the SpO_2 equation (figure 4.8-B.3). The SpO_2 equation was discussed in section 5.3, and is the linear correlation between the ratio of signals and the SpO_2 value.
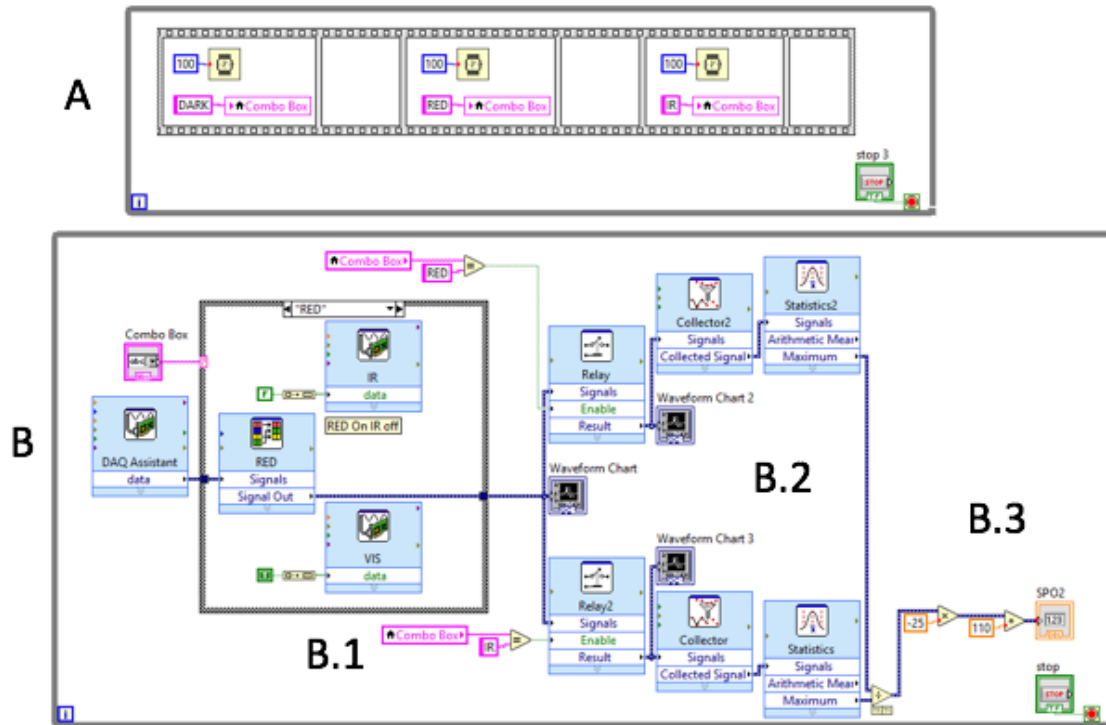
Figure 4.8: The PPG sensor signaling structure that controls the state of the LEDs and the collection of signal (A) the case structure responsible for controlling the state of the signal evaluation which cycles through dark, red and IR states. These states are relayed to the signal evaluation structure (B) where the incoming signal from the sensor is passed into the case structure (B.1).the case structure controls the LED states and collects the signal. (B.2) processes the signals from the sensor and the last component (B.3) is the SpO2 evaluation.

The ratio of signals is defined by the equation below:

$$R = \frac{(A_{max}/A_{min})_R}{(A_{max}/A_{min})_{IR}} = \frac{(AC/DC)_R}{(AC/DC)_{IR}}$$

Equation 4.1

Where the R is equal to the ratio of the red signal AC/DC over the IR signal AC/DC. The ratio is then implemented into the linear SpO$_2$ equation (equation – 2.20) to calculate the blood oxygen percentage. The LabVIEW program is capable of implementing the calculated ratio into the SpO2 equation indicated in figure 4.8-B.3.

4.3   Virtual instrument Monitoring

The LabVIEW contains the ability to develop a graphical user interface (GUI) to allow user interaction with the software. The PPG sensor is equipped with the LabVIEW GUI capable of displaying and calculating the data. The graph on the left in figure 4.9 displays the raw unfiltered data that is collected by the sensor, on the right of this graph is the signal after being processed through a 0.5-3Hz bandpass filter. The user can turn on the device by pressing the switch to pulse oximeter, once the pulse oximeter is turned on the user can watch the graphs as the signal is collected. The RED and IR green buttons indicated at the top of figure 4.9 will turn on and off indicating which signal is being collected. The heart rate and SpO_2 value will be displayed in the box to the right. The user also has the ability to collect the data, after the user inputs the name and trial number as well as the path location, the blue button at the top of the GUI can be pressed and the data will be recorded for 15 seconds.
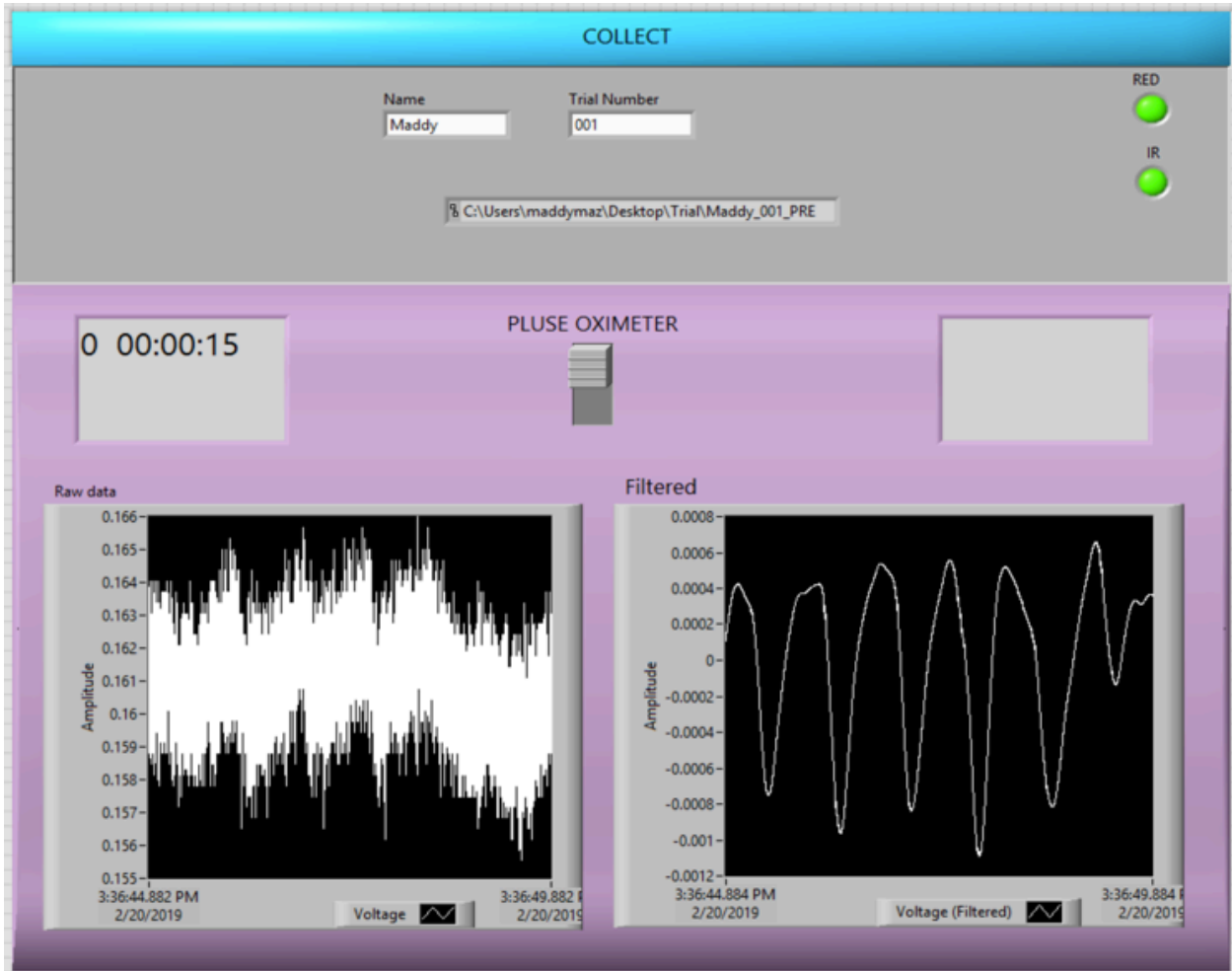
Figure 4.9: LabVIEW programing graphical user interface at the top of the GUI in brought blue is the collect button once this is pressed the program will collect the PPG signal data for 15 seconds. In this GUI you can enter the name and trial number as well as the location to store the results. On the left side of the GUI is the unfiltered raw data and on the right is the filtered data after manipulation.

CHAPTER 5

5.0   MECHANICAL SIGNAL OPTIMIZATION

The goal of this thesis was to implement the PPG sensor into the cap of the Electronic Tuning fork (ETF). The ETF is placed on the bottom of a patient's foot and vibrates to indicate neuropathy, or lack of feeling. The ETF is a hand-held rectangular instrument with a small cap located at the base of the device which comes in contact with the foot figure 5.1.

Figure 5.1: Electronic Tuning Fork utilized in this thesis, the device is 12 inches long and fits in your hand. The device is used for measuring diabetic foot neuropathy and the cap (indicated in figure) is placed on the bottom of your foot.

The PPG sensor for this thesis was logistically designed to fit in the cap of the ETF, to advance patient care by providing doctors with multiple biological vitals using a single device. Figure 5.2 illustrates the ETF cap dimensions, and the maximum usable area to build the PPG sensor. The sensor's physical design was optimized to fit in the ETF cap and come in contact with the patient, to take their vitals during a test.
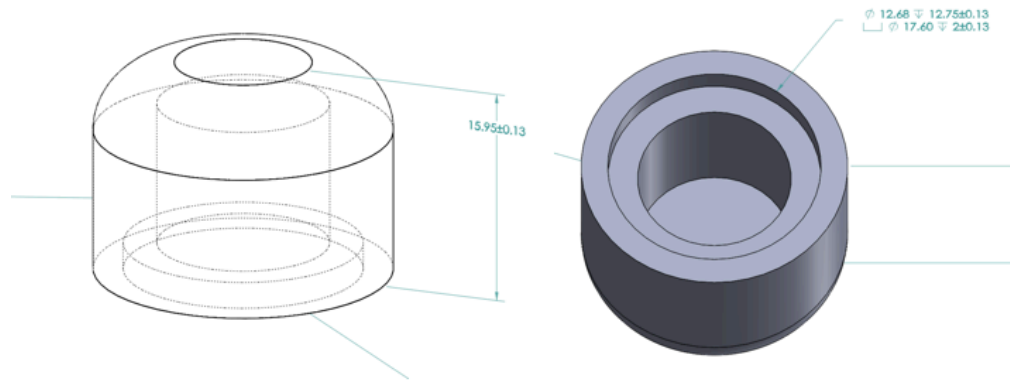
Figure 5.2: The cap from the ETF has a height of 15.95mm and an inner diameter of 12.6mm. The PPG sensor must fit within the cap, so the dimensions are critical to design.

After development of a PPG sensor dimensionally compatible with the ETF cap and capable of calculating SpO_2 the objective was to optimize the PPG signal from the sensor by altering the light attenuation using mechanical structures.

A normal pulse oximeter utilizes transmission based signaling, eliminating factors that can negatively impact the signal in a reflective PPG sensor. The type of sensor and the implementation of the sensor in this thesis allows for variation of applied pressure and movement. Although reflective based sensors have variations in signal due to pressure changes and movement, they are more optimal due to reduced limitation of use. One study that compared the contact pressure of reflective pulse oximeters to accuracy of results, found that the increased pressure of a sensor applied to the forehead, 12 and 27 kPa, resulted in a decrease in error and improved measurement accuracy for both SpO_2 and heart rate[41]. In contrast the study did determine that less applied pressure, 4kPa, caused both the SpO_2 and heart rate results to decrease in accuracy, from insufficient contact and movement. Movement from the patient or doctor can allow more or less light to reach the sensor therefore interfering with the PPG signal received. The goal is to design an overlay on the surface of the PPG sensor PCB to optimize the signal. The overlay is capable of directing the light through the tissue to amplify the signal and reduce the signal to noise ratio, which compares the signal intensity to the background noise from a signal.

5.1   Signal to Noise Ratio

The signal to noise ratio(SNR) is a critical metric of any signal. It calculates a value representing the amount of background noise in relation to the desired signal. Because of the PPG sensors variation from pressure and light perfusion the SNR is an important metric to indicate how the device is performing. The SNR formula is indicated by equation 5.1

$$SNR = \frac{\mu_{signal}}{\sigma_{signal}}$$ *Equation 5.1*

Where μ is the average signal value and σ the standard deviation of the signal. An example of a PPG signal with noise is illustrated in figure 5.3. As the amplitude is changing over time, there are minimal variations in amplitude throughout the signal, which is the noise.
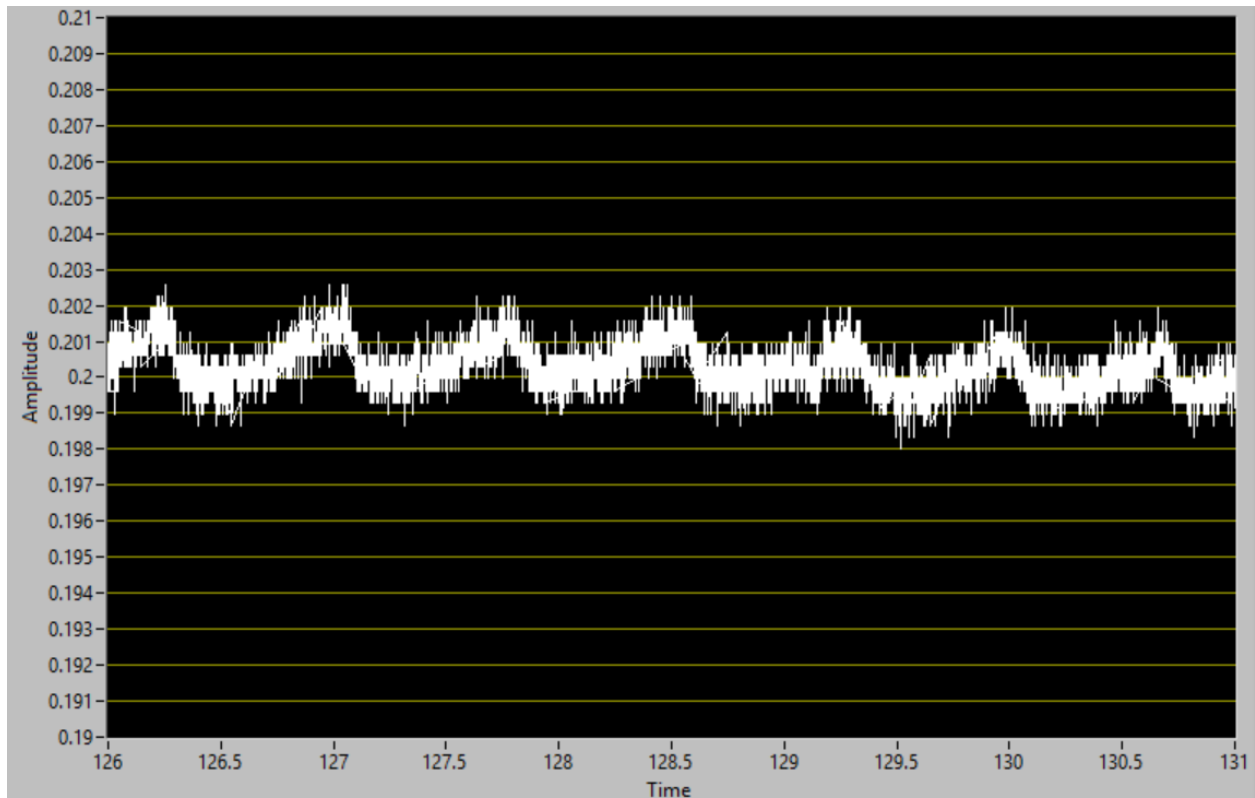
Figure 5.3: Example of a PPG signal containing noise, where the small variations in amplitude represent noise in the signal and the larger changes in amplitude are the desired signal.

The PPG signal fluctuates in amplitude, representing the pulsatile signal of blood perfusion. As discussed in previous sections the PPG signal has an AC and DC component, representing the

peak and valley respectively. Both components can have fluctuating SNR because they represent different parts of the tissue. Evaluating both the AC and DC components of the signal that SNR ratio becomes:

$$SNR = \frac{\mu_{AC} - \mu_{DC}}{\sigma_{AC-DC}}$$
Equation 5.2

Where the SNR becomes the average AC signal minus the average DC signal over the standard deviation of AC minus DC, and the equation for the standard deviation becomes:

$$\sigma_{AC-DC} = \sqrt{\sigma_{AC}^2 - \sigma_{DC}^2}$$
Equation 5.3

Where the standard deviation of the signals is the sum of squares of the components.

The SNR is an important component to optimize the PPG signal, the goal is to decrease the ratio having a high signal and low noise. The filtering discussed in the previous section will remove some of the noise from the PPG signal, but the signal can be further optimized by evaluating the SNR of the raw signal. As the various cap structures are utilized the SNR of the raw signal can be evaluated to determine how well the cap is optimizing the data.

5.2   Structures

Three caps were designed to fit over the PPG sensor and direct the LED and phototransistor different directions to optimize the PPG signal. The three designs can be seen in figure 5.4, where all caps were designed with a crevice in-between the LEDs and phototransistor intended to allow more tissue to fill between the optical components. The goal was to design the cap to maximize the amount of light from the LEDs to interact with the tissue and return to the phototransistor. The first cap design, figure 5.4-A, is designed with the outlet for the LEDs and the inlet for the phototransistor directed straight up, this is the control design, the middle of the cap is carved out to maximize the tissue between the components. The second cap design, figure

5.4-B, has the outlets for the LEDs directed inwards and the phototransistor inlet directed inwards. The concept behind the second cap design is for more light reflected off the tissue to reach the phototransistor, hence both components directed toward the midline. The third and final cap design, figure 5.4-C, is constructed to direct the light and phototransistor away, the concept for this design is to allow the light to travel further into the tissue before returning to the phototransistor. The third design is constructed to reduce signal to noise ratio and eliminate light bleeding for the LEDs to the phototransistor before reaching blood components.
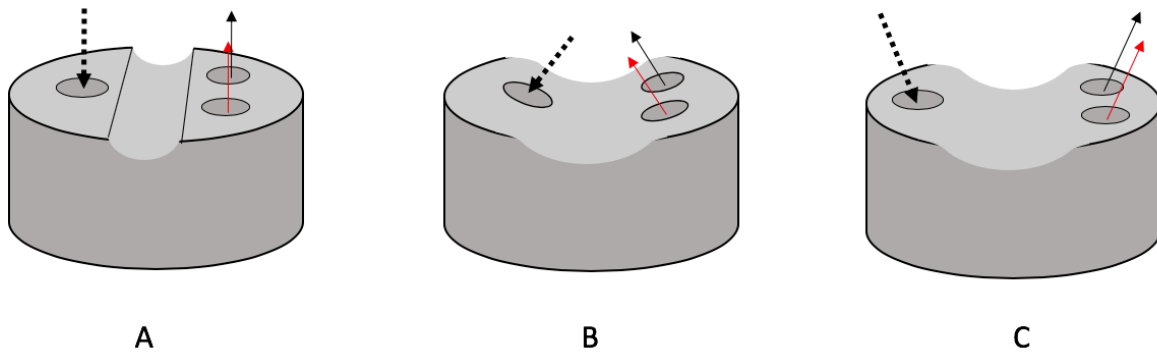
Figure 5.4: Initial cap overlay designs, constructed to direct light and optimize PPG signal all constructed with the same dimensions as the (A) is designed to project light from the LEDs directly out

The caps were designed using Solidworks© a CAD (computer-aided design) modeling software. After design the caps were printed using Ultimaker 2+™ a 3D-printer capable of printing approximately 2.58mm. Due to the size and complexity of the caps constructed for the PPG sensor and the limitations of the 3D printer, the caps designed to direct light outward and inward, figure 5.4-B&C, could not be printed successfully. Although the cap design with the light attenuation directed straight, figure 5.4-A, was able to be printed the pulsatile signal was not detected when this cap was utilized on the sensor.

The above cap designs were simplified to determine why there was no signal seen when using the first cap designs figure 5.4-A and if a similar cap could help determine the problem and

optimize the signal. Figure 5.5 shows the next stage of caps designs tested on the PPG sensor. The first is the PPG sensor contains a signal divider between the LEDs and the phototransistor, the second contains a full cap encompassing all the components, and the third is a sensor with no obstruction to the optical components.
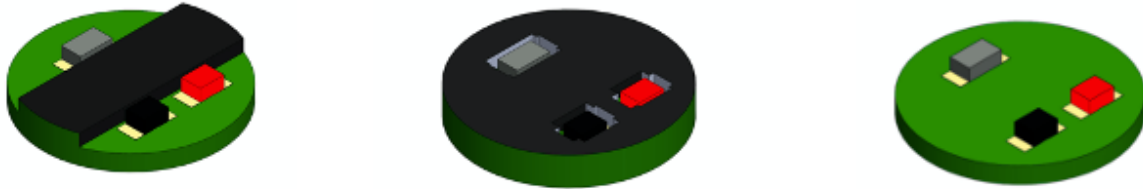
Figure 5.5: The two modified versions of the PPG sensor and the bare PPG sensor for testing.

The final cap designs tested are illustrated in figure 5.5. All of the caps are constructed using Solidworks© and 3D-printed on the Ultimaker 2+™ using black PLA material.

The first design is the "Middle Divider", figure 5.6, designed with a divider between the LEDs and the phototransistors on the PPG sensor. The divider design is constructed with intentions of eliminating light bleeding from the LEDs into the photosensor without first entering the tissues. The black middle divider will force the LED emission into the tissues, in turn causing the only light reflected from the blood to hit the phototransistor. The middle divider is constructed as a rectangle with dimensions of 11mm x 3.5mm x 2mm to fit between the components on the sensor, and the 2mm height is greater than the height of the optical components, to eliminate any light attenuating over.
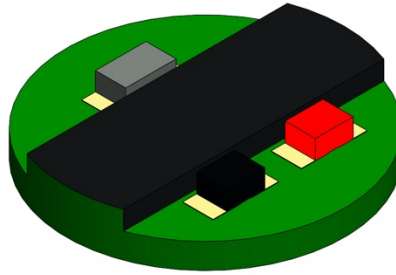
Figure 5.6: Middle Divider cap design

The "Full Cap" illustrated in figure 5.7, is constructed with the same dimensions as the PPG sensor, with cut outs for each of the optical components. The full cap design surrounds each component with a 2mm height, the cap will not only eliminate all light bleeding from the LEDs but also eliminate any ambient light hitting the photosensor.
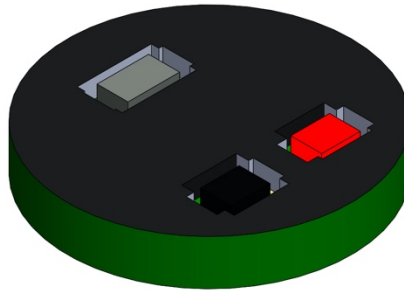
Figure 5.7: Final cap design

The final test will be the PPG sensor with no physical additions to the surface, figure 5.8, this is the control design and there is no attempt to optimize the light attenuation. The PPG signal collected from the phototransistor will be the raw signal, when a finger is placed directly on the surface.
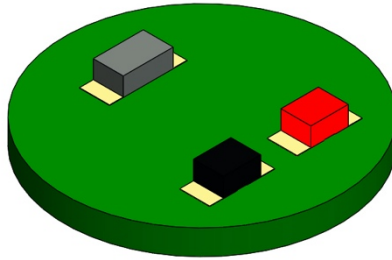
Figure 5.8: No Cap

The Middle divider and the final cap design are constructed to optimize the light reaching the sensor. The goal is to not only increase the light attenuation into the tissues, but also the reflected light from the tissues to the phototransistor. These designs attempt to force the light from the LEDs into the tissues and eliminate bleeding of light to the phototransistor. The full cap design also aims to decrease any light sources in the testing area that might attempt to affect the signal received by the phototransistor.

5.2   Test Methods

The caps are constructed to optimize the light attenuation from the tissues to the phototransistor on the sensor. The goal is to increase the amount of light from the LEDs reaching the blood and the amount of light reflected back to the phototransistor. Each mechanical cap was added to the sensor and secured to ensure no movement during the testing. The right index finger was applied to each sensor with comparable force, and data from the PPG sensor was collected. The subject was asked to place a digit on the sensor for approximately 10 seconds to ensure heart rate could be easily identified in the signal and calculated. The signal received from the PPG sensor was not filtered, to allow for optimization of the raw signal. The voltage variation was analyzed to determine which design optimized the signal. During the testing the PPG waveform signal was acquired using only the IR LED, because of its higher attenuation through the tissue and stronger signal projection. The PPG sensor was controlled through the NI myDAQ, powering the LED and controlling the phototransistor. The data was collected through the myDAQ and the signal

was visualized using the LabVIEW software. The signal evaluated was the raw signal collected directly from the phototransistor, where the amplitude reflects the voltage variation.

5.2   Results

The amount of light attenuation into the tissues and reflected back to the phototransistor can be determined by evaluating the raw voltage signal from the PPG sensor. The waveform represents the blood perfusion as a result of the heartbeat, and the extent of the signal can be a result of light perfusion through the tissues.

5.2.1   Proposed Results

The waveform signal produced from the PPG sensor, describes how the light is attenuating through the tissue and reaching the phototransistor. The signal from the phototransistor is collected in LabVIEW and a graph of the waveform is displayed. The signal amplitude, and the AC signal height, range of peaks and valleys in the pulsatile signal, provide information about movement of light from the LEDs to the phototransistor. High amplitude signals indicate that the phototransistor is receiving a large quantity of light, this could be caused by high reflection of light off the tissue or bleeding of light from the LEDs directly to the phototransistor. On the contrary low amplitude signals indicate minimal light is hitting the sensor.

When the light from the LEDs is hitting the tissue and reflecting back to the phototransistor, it is optimal, and the PPG signal will look like figure 5.9. In this graph the PPG waveform has a high amplitude and a high signal height. The high amplitude represents the phototransistor is receiving a large quantity of light, and the high signal height indicates that the light is reflected from blood volume changes.
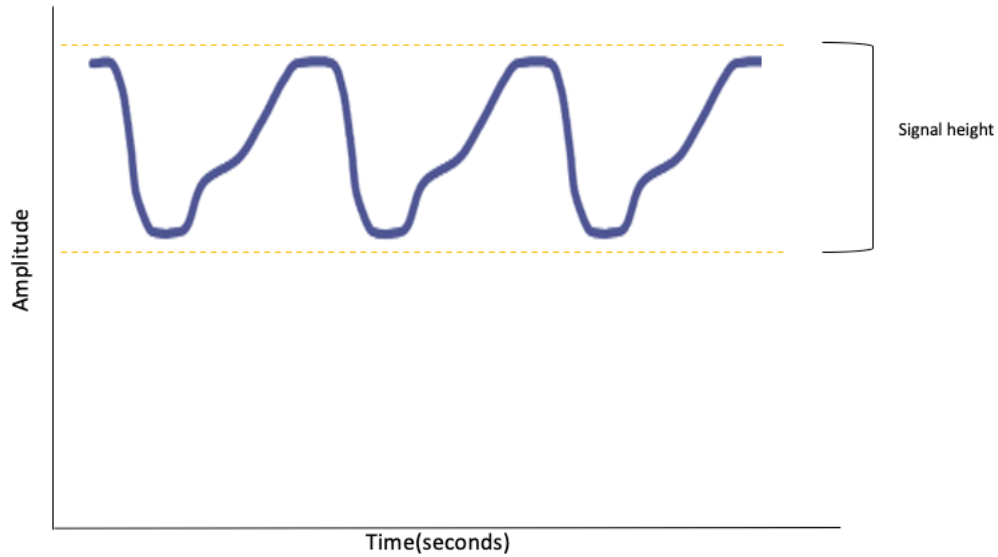
Figure 5.9: PPG signal with high amplitude and heigh signal height, this is the optimal signal output for a PPG sensor, because it reflects the light hitting the blood vessels in the tissues and reflecting back to the photosensor.

In figure 5.10 the PPG signal contains a high amplitude, but the signal height is small. The high amplitude illustrates the high incidence of light hitting the phototransistor, but the low signal height indicates the light is not reflected off the blood. In this instance there is a great deal of light hitting the phototransistor but not a lot of the light is reflected off the blood in the tissues.
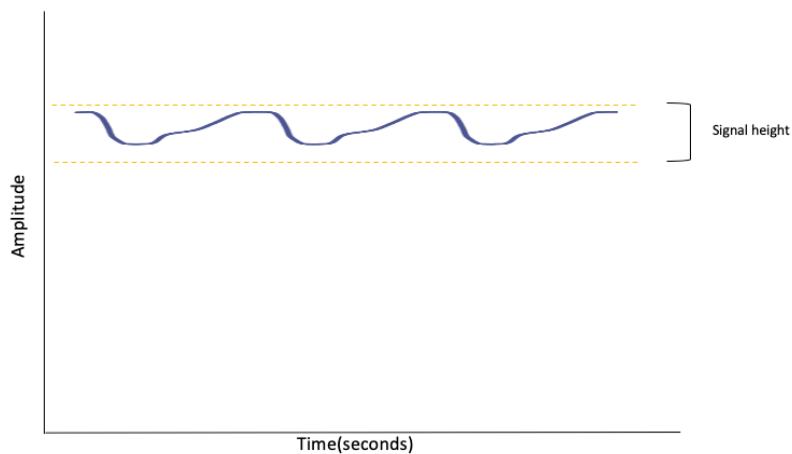
Figure 5.10: PPG signal where the amplitude is high, but the signal height is low, indicating high amount of light reaching the phototransistor but not high light attenuation through the tissues.

94

If the signal received from the PPG sensor, has a low amplitude and a low signal height, seen in figure 5.11. In this instance the extent of light hitting the phototransistor is low, represented by the low amplitude, and the light that is hitting the phototransistor is not reflected off the blood in the tissues. Light from the LEDs is not hitting the blood and picking up variations in blood volume and the phototransistor is not receiving any reflected light.
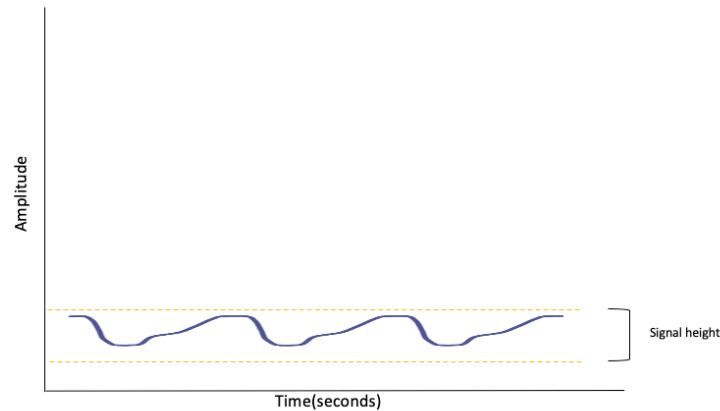
Figure 5.11: PPG signal where the amplitude is low and the signal height is minimal, indicating less light reaching the phototransistor and no light attenuating through the tissue.

When designing these caps, the goal is to optimize the raw signal from the phototransistor on the PPG sensor, to do this the signal should look like figure 5.9 where the amplitude is high, and the signal height is high. This signal illustrates high attenuation light through the tissues and increased light reflecting back to the PPG sensor.

5.2.2   Design Results

The two PPG sensor cap designs and the stand-alone PPG sensor that were tested can be seen in figures 5.6-8.

5.2.2.1 Middle Divider Cap Design

The first cap tested was the middle divider seen in figure 5.6, the part was made to fit between the LEDs and the phototransistor on the PPG sensor, and block excess light hitting the phototransistor from the LEDs. After the LED was eliminated the index finger was placed on the sensor and the data from the phototransistor was collected from the myDAQ and recorded using the LabView software. The results can be seen in figure 5.12, the graph indicates the amplitude of signal is 0.1, this is the voltage that is received from the phototransistor, representing the light hitting the sensor.
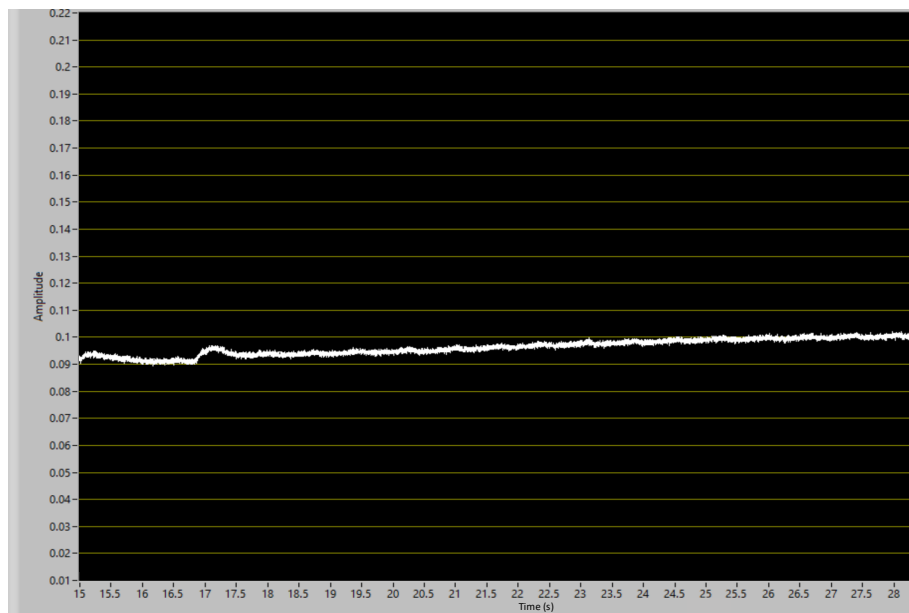
Figure 5.12: Middle divider cap design with an amplitude of 0.1v.

5.2.2.2 Full Cap Design

The next cap test is the full cap design, as seen in figure 5.7, is designed with the intent to fully encompass the sensor components. The cap is constructed to perfectly sit on top of the PPG sensor with cutouts for the LEDs and the phototransistor. The signal from the PPG sensor with the full cap design can be seen in figure 5.13, where the amplitude is low, approximately 0.05v.

The low amplitude indicates that there is minimal light hitting the phototransistor. When looking at the signal height it can be concluded that there is no visible heartbeat.
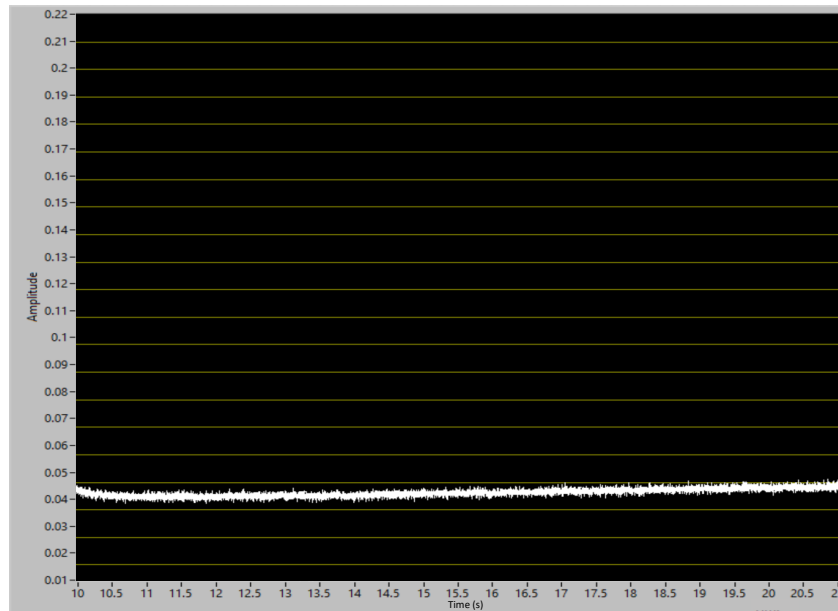
Figure 5.13: Full Cap design signal received from the PPG sensor with minimal amplitude at 0.04v.

The low amplitude indicates that the light coming from the LEDs is not penetrating into the tissues to pick up any signal involving blood perfusion. Because the phototransistor is not receiving any light signal there is no indication that the LEDs are not penetrating deep enough into the tissues. The signal height could be non-existent in the PPG signal because no light is hitting the phototransistor.

5.2.2.3 No Cap Design

For comparison, the same test was performed on the PPG sensor without any cap addition, design illustrated in figure 5.8. The signal results for the stand-alone PPG sensor can be seen in figure 5.14. The figure illustrates a high amplitude, of about 0.2v this indicates the

phototransistor is receiving high attenuation of light from the LEDs. Also indicated in figure 5.8 is the increased signal height, which is greater than the capped sensors.
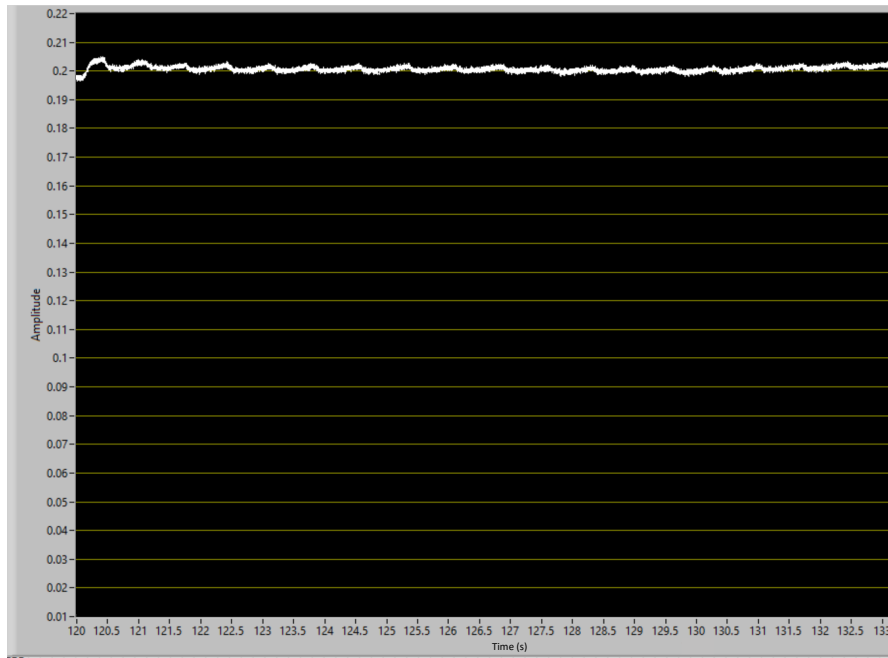
Figure 5.14: No Cap PPG sensor signal has a high amplitude of 0.2v.

The signal increase in decrease is related to the light variation from the blood volume changes. The raw PPG signal received when the index finger is laid directly on the PPG sensor has a high signal height and high amplitude, concluding the light reaching the phototransistor is reflecting from the vascular bed of the tissue.

Comparing the amplitude results for each sensor design, the middle divider PPG signal had an amplitude of 0.1v, the full cap, 0.05v, and the PPG sensor with no cap was 0.2v. Figures 5.12, 5.13 and 5.14 illustrate the amplitude recorded for the three sensors tested. The full cap design had the lowest amplitude indicating it was receiving the least amount of light from the LEDs, the middle divider had an amplitude between the full cap and no cap, thus receiving some light. The PPG sensor with no cap had the highest amplitude and was receiving the more from the LEDs. In

this instance it can be concluded that the PPG sensor with no cap is the most optimal for receiving more light, and the addition of the cap limits the sensor's ability to reflect and collect the light.

Comparing the signal heights which provide some indication as to how well the LEDs are projecting light in the tissue, is a factor that adds to the optimization of the signal. For each cap, figure 5.15, shows the pulsatile signal, demonstrating the extent of light reaching and reflected off the vascular bed. The full cap sensor, figure 5.15-A, has no pulsatile signal, and the phototransistor is not detecting light that is reflected from the blood perfusion. The middle cap design, figure 5.15-B indicates possible pulsatile signals from blood volume changes, the heartbeat is somewhat visible in the signal. The PPG sensor with no cap design, figure 5.15-A, has a high signal height, reflecting the light variations from the blood volume changes, the pulsatile PPG signal.
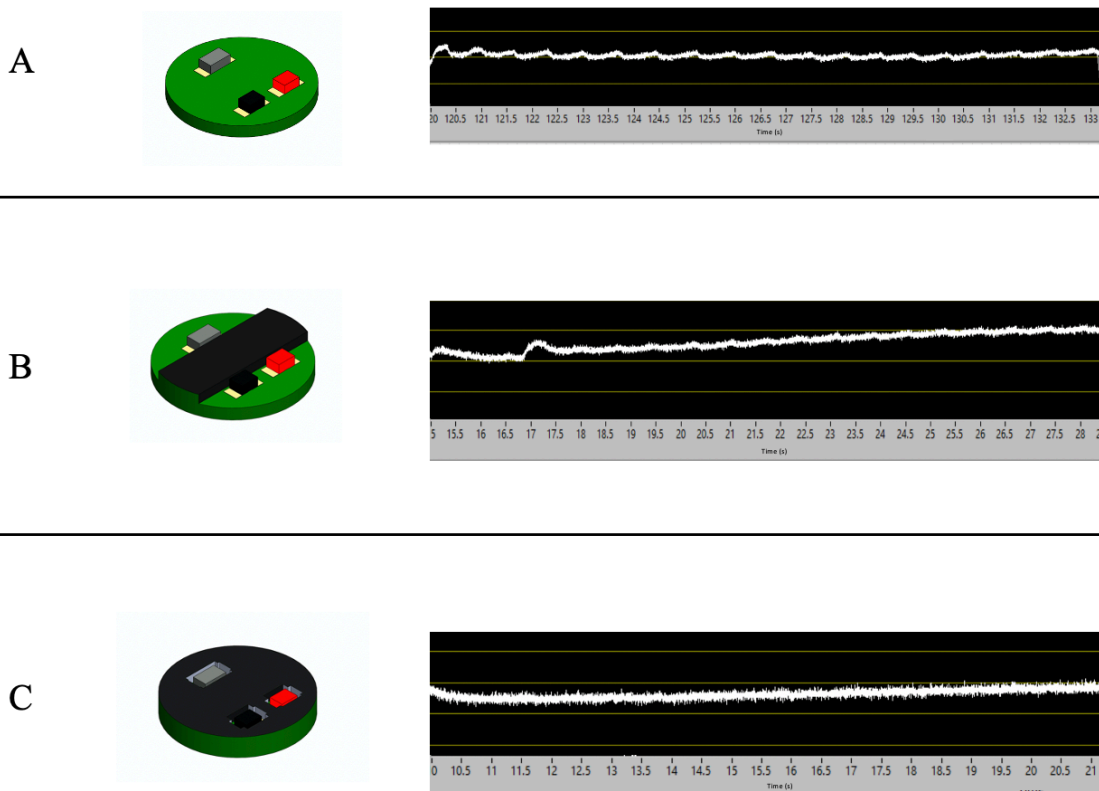
Figure 5.15: Signal height evaluation for the PPG sensor cap types. (A) the PPG sensor with no cap the correlating signal is significant, and the pulsatile signal can be clearly identified. (B) The PPG sensor with the middle divider, this signal contains minimal signal height, and the pulsatile signal can only somewhat be identified. (C) The PPG sensor with a full cap design has no signal height and the pulsatile signal is not present.

The PPG sensor cap designs did not reflect the desired outcome, both the full cap and middle divider indicated low light reaching the phototransistor, and light projection from the LEDs into the tissues was minimal. Compared to the PPG sensor with no cap the, two cap designs did not optimize the signal outcome like initially intended. It was concluded that the most optimal signal would be produced from a PPG sensor with no cap design, and the best results would come from placing the tissue directly on the sensor.

5.3   Theory

The question is why did the PPG sensor with no cap produce a better raw PPG signal than the sensors with the cap designs. The theory is skin from the fingertip is falling between the phototransistor and the LEDs, seen in figure 5.16. The PPG sensor is designed with 4mm of space between the phototransistor and the LEDs, when the subject places the finger over the sensor skin falls between the components.
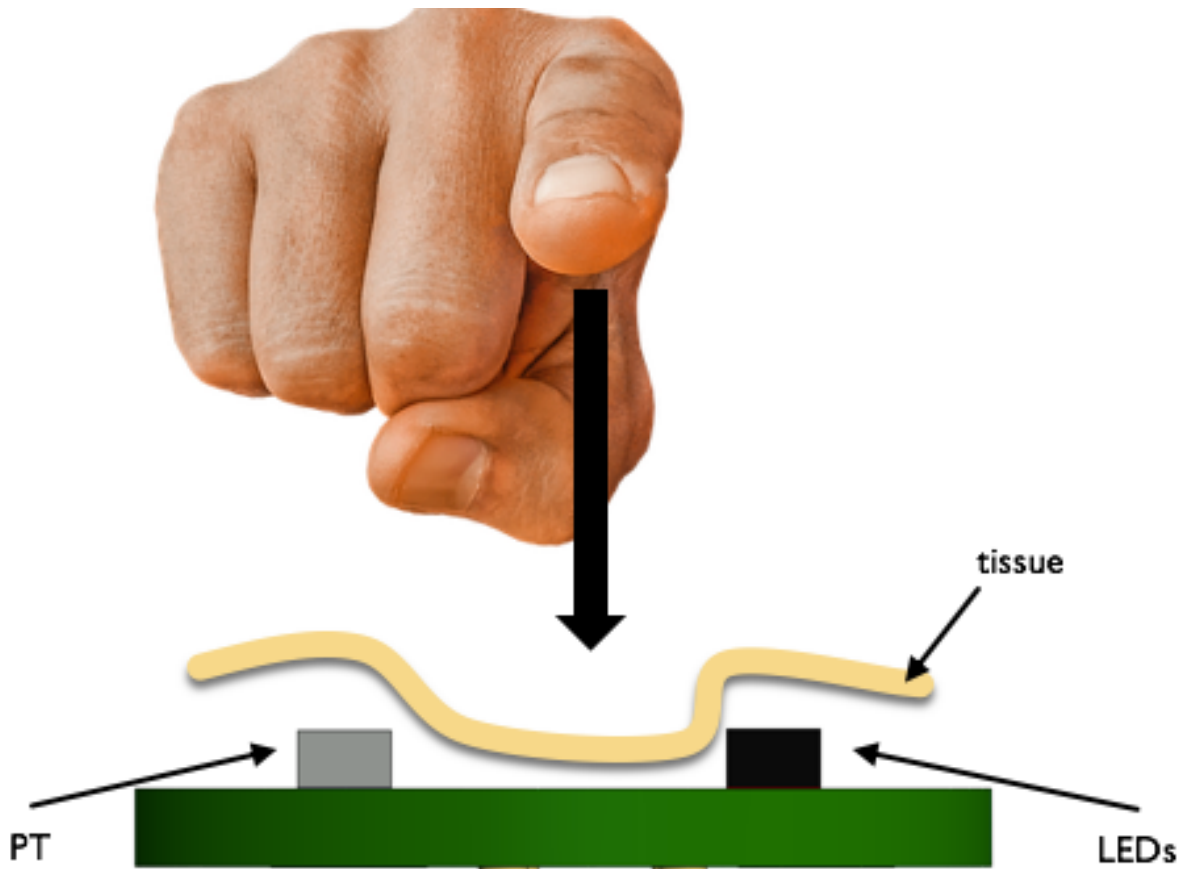
Figure 5.16: The designed PPG sensor cross section with a finger being placed over the sensor to show how the tissue of the finger can seep between the phototransistor (PT) and the LEDs on the sensor when there is no cap or mechanical obstruction between the components.

This changes the PPG sensor from a reflective based PPG sensor to a transmission-based sensor, discussed in chapter 2.3.4. In a transmission-based sensor the light from the LEDs attenuates

101

through the tissues to the phototransistor opposite. In this case the light projected from the LEDs is forced to pass through the tissues and absorb into the blood, because the phototransistor is on the opposite side the light that is not absorbed is directly projected to the phototransistor. This optimizes both the light signal attenuation through the tissue, and the reflected light reaching the transistor. For concept to be functional the skin depth capable of fitting between the components must contain blood vessels with blood perfusion. The skin that the light attenuates through must have information about blood volume changes. To calculate if this is possible, the LED height and the vascular tissue bed depth must be compared.

The PPG sensor that was tested is PPG sensor 2, discussed in chapter 3.2, and the optical components utilized are discussed in chapter 3.2.1. Both the IR and red LED have a height of 1.6mm and the phototransistor has a height of 1.7 mm. There are other factors such as tension and resistance of the skin that most likely impact the amount of tissue capable of fitting between the components, but the maximum, due to the optical component height, is 1.7mm. Now that the height of tissue that can fit between the components is determined, the depth of the skin containing the capillaries must be within 1.6mm. A study was completed to test the extent of skin thickness in response to various physical circumstances, such as vibrational and thermal signals. The study evaluated the thickness of the epidermis layer using an ultrasound. Although the study was to evaluate the difference in epidermis thickness in response to thermal and vibrational signals, the skin thickness throughout the study did not exceed 1mm[42]. The average skin epidermis thickness on the right index finger was found to be 0.57 (+- 12 SD)[42]. Because the depth of tissue containing capillaries is approximately 0.57mm below the skin surface (0.69mm at max) and the height of the optical components is 1.6mm, the skin falling between the optical components on the sensor is completely possible. In this case the transmission of light, through the vascular tissue between the optical components to the phototransistor would be more direct, resulting in a high amplitude and signal height in the PPG signal.

CHAPTER 6

6.0   CONCLUSION

Throughout my master's thesis at the University of Maine, a reflective based photoplethysmography sensor was designed and developed. With the help of the electrical department and the bioengineering staff I was able to construct a working prototype capable of detecting heart rate and calculating blood oxygen saturation. There are a few topics I would like to reflect on within this project; first I would like to discuss testing that I would have performed had I been able to access the resources, second I will reflect on the aims of this thesis and my accomplishments within those aims, and finally I want to discuss future work for this device and potential prospective projects.

6.1   Testing Intentions

The intention was to proceed with additional testing, evaluating the heart rate and SpO_2 calculations from the designed PPG sensor to determine if the sensor was proficient. Because of restrictions due to the COVID-19 pandemic this testing was limited, and comparing blood oxygen percentages across multiple subjects was not feasible. It was intended to prove that the PPG sensor designed in this thesis was capable of acquiring heart rate data and calculating the SpO_2 value, within 2% SD of SaO_2 which is the claimed accuracy for most manufactured pulse oximeters[36]. The intention is to compare the PPG sensor's acquired heart rate and SpO_2 value to other on market pulse oximeters. The SpO_2 value is calculated from the heart rate, which directly correlates to the light attenuation through the tissues and back at the sensor. The PPG signal result of the light projecting through the tissue and reflecting back to the photosensor is illustrated in figure 5.10 and defined by a height amplitude with a high signal height.

6.1.1   Intended Heart Rate and SpO_2 Testing Methods

When determining the protocol for my PPG sensor evaluation I wanted to utilize similar techniques that have been executed in the literature, keeping in mind my intentions for the study. The amount of people, blood oxygen saturation, skin type, age, and health were all important

components to be considered when designing the study, and often incorporated into the work of others. Many studies compare a personally designed PPG sensor to other pulse oximeters on the market, as well as the results of an arterial blood gas test. Although an arterial blood gas test takes time, and blood oxygen saturation can change rapidly, many studies utilizing this as a comparative technique, record the time of blood withdrawal. Another study I found interesting, which tested the ability of a PPG sensor to calculate blood oxygen saturation, utilized an ice water bath to decrease the blood flow to the tissues[43]. This method changes the PPG signal but the SpO_2 value and the calculation of that percentage remains constant. The study evaluates the accuracy of the PPG sensor when the skin temperature is colder than normal. There are many studies in the literature that evaluate the accuracy of PPG sensors, and after thorough research of many, I was able to construct a comparable testing method for the sensor designed in this thesis.

The testing would have included approximately 10 subjects with SpO_2 values ranging from 75% to 100% , similar to a study done in 2018 that compared two reflective PPG sensors at various locations on the body[44]. The study utilized 10 patients with various SpO_2 values, ages, medical conditions and skin tones. The study compared the pulsatile signal of multiple PPG sensors, to the sensor designed in the study, by calculating and comparing the R-value. The designed sensor SpO_2 value was also compared with the other sensors testing in this study. My intention is to design my study similar to this with comparable parameters and evaluation methods.

Study objectives

- The objective is to investigate feasibility of thesis designed PPG sensor by measuring heart rate and calculating SpO_2 values taken from the foot of the patient.
- Compare pulsatile differences between thesis designed PPG sensor and comparable sensors to evaluate efficiency.

Intended Study Methods

- Acquire information about the subject age, gender, weight, skin tone, medical conditions and average blood oxygen saturation.

- Attach designed PPG sensor to the right foot on the bottom of the big toe (figure 6.1).
- Attach two different, commonly used transmission-based PPG sensors (pulse oximeters) to right and left index fingers.
- Attach and secure reflective-based forehead PPG sensor to subject's forehead.
- Acquire data through the NI myDAQ and LabVIEW software for all of the sensors utilized in the study, for a total of 3mins.
- Once 3mins is completed, remove all sensors
- Draw blood and run arterial blood gas test

Figure 6.1: Designed PPG sensor placed on the bottom of the big toe in the study for testing.

<u>Study Results Comparison</u>

To compare the performance of the designed PPG sensor to the other sensors tested the R-value will be calculated from the pulsatile signal. The R-value is a ratio of the peaks and valleys from the signal and represents the PPG waveform. The signal for all of the sensors is collected on LabVIEW, and the calculations of the R-value are executed in the software as well. An example of how this data is compared for each sensor is seen in table 6.1. The R-value is calculated by extracting the AC and DC component from the PPG signal and taking the ratio of the components with respect to the dark signal, discussed in section 2.4.3.

Table 6.1: Example of R-Value comparison table that would exist for the PPG sensor testing and evaluation

Subject ID	R-Value			
	Right Finger Transmission Pulse Oximeter	Left Transmission Pulse Oximeter	Commercial Forehead PPG Sensor	Right Transmission Pulse Oximeter
001				
…				
010				

The R-value is utilized in calculating the SpO_2 values, which would also be compared for each one of the sensors and the arterial blood gas test, an example of this data is seen in table 6.2.

Table 6.2: Example of SpO₂ comparison table that would exist for the PPG sensor testing and evaluation

Subject ID	SpO$_2$ Percentage				
	Arterial Blood Gas Test	Right Finger Transmission Pulse Oximeter	Left Transmission Pulse Oximeter	Commercial Forehead PPG Sensor	Right Transmission Pulse Oximeter
001					
…					
010					

Further analysis of the values would be to correlate the data in a graph and evaluate the performance of the designed PPG sensor. The results from the PPG sensor should correlate to the other devices tested and no outliers or variations in the data should be apparent. The PPG sensor would be deemed feasible if the sensor correlation was no greater than 2 standard deviations

from the correlation of the over PPG sensors. An example of the PPG sensor SpO$_2$ valves compared to the other sensors across the 10 patients can be seen in figure 6.2
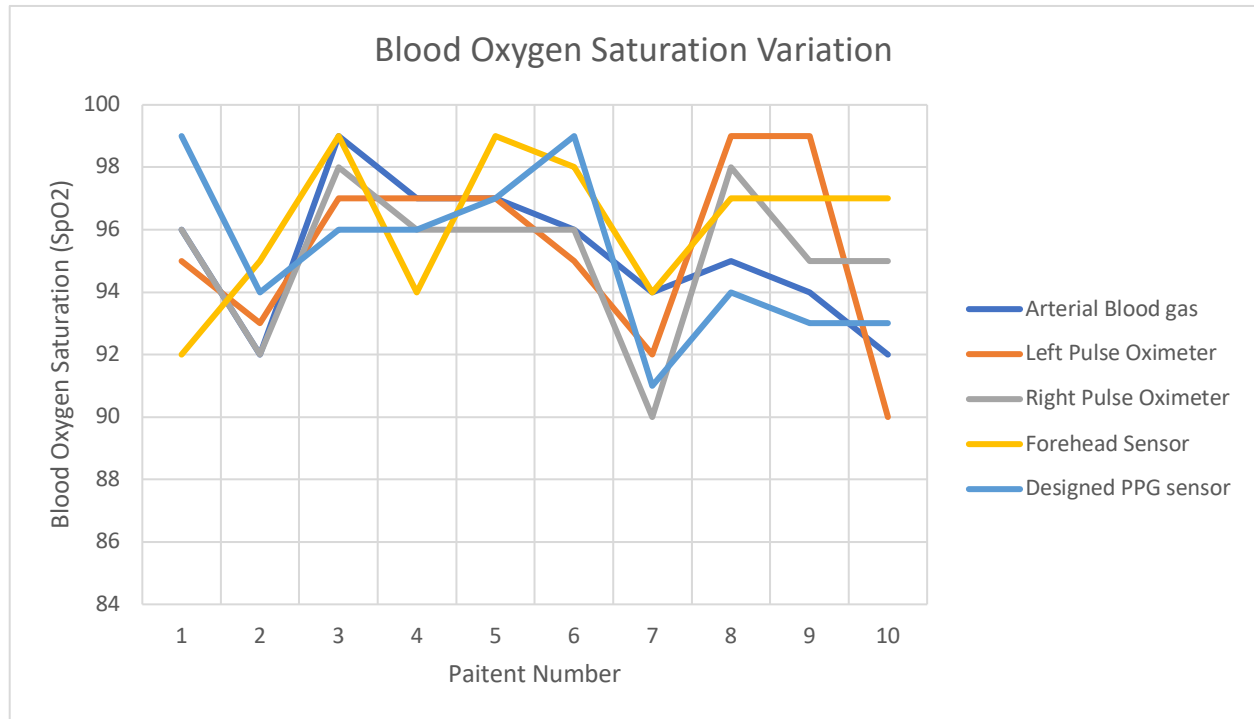
Figure 6.2: An example of a graph illustrating the results of the arterial blood gas test, left pulse oximeter, right pulse oximeter, forehead sensor, and the designed PPG sensor SpO$_2$, across the 10 patients

From the data collected on the SpO$_2$ results the percentage of error can be calculated using the equation below:

$$ERROR = \frac{|E-T|}{|T|} \ X \ 100\%$$

Where the percent error is the absolute value of the experimental results minus the theoretical results over the theoretical result time 100. The error represents how far the expected value is from the tested value. To compare the designed PPG sensor results to the other 4 methods of measuring blood oxygen in the study the experimental error is always the designed sensor results and the theoretical would be the compared sensors. Evaluation of error indicates how far the PPG sensor values differ from the other sensors, and example of a graph representing the percent error of the sensor is illustrated in figure 6.3
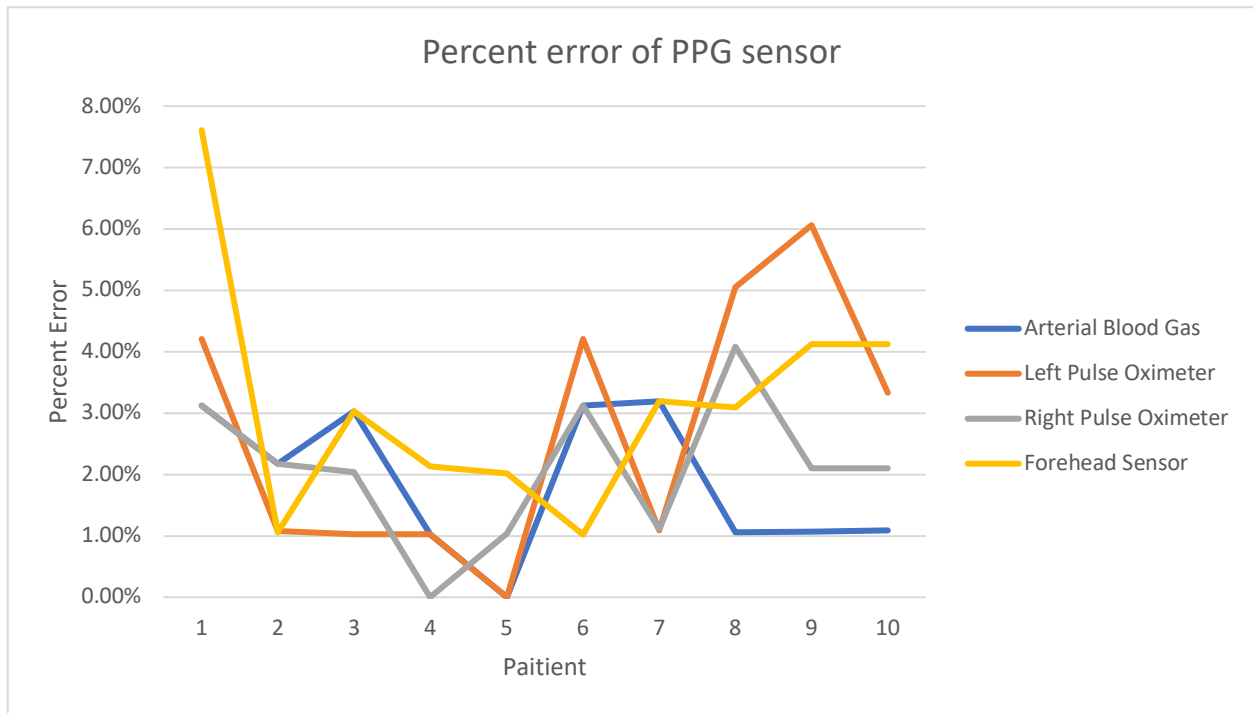
Figure 6.3: An example of the PPG sensor's calculated percent error of SpO₂ for each patient compared to the other sensors SpO₂ results.

6.2   Evaluation of Thesis Aims

The first aim in this thesis was to successfully design a reflective based PPG sensor capable of detecting blood oxygen saturation. The PPG sensor was designed with the intention of fitting into the cap of the ETF (figure 5.1 and 5.2), and thus constrained inside to 13mm in diameter. The size restriction was one of the most difficult aspects of this project, the initial thought was to fit the majority of the electronic components for the PPG sensor within the cap of the EFT. This is seen in the initial circuit board sensor design where the resistors needed in the circuit are equipped on the bottom of the PPG sensor. Upon further analysis of the electronics and what would be needed to fit and operate in the cap of the ETF it was determined, with the help of the electrical engineers, that the sensor could be reduced in size if constrained to only the core optical components on the PCB. Because the sensor has more components than just the core optical components, the intention was to wire the optical components in the cap through the base

109

of the ETF cap and onto the main control board, where more electronics could be constructed for the device. The intention was to design and optimize the PPG sensor outside of the ETF and then integrate the hardware and the electrical components into the device.

The second thesis aim was to optimize the PPG signal from the sensor by manipulating the design of the cap to enhance the light attenuation. This aim encompassed the majority of the work and analysis I performed with the sensor design. The intention was to optimize the PPG signal, as discussed in the previous sections the cap designs did not yield the initial intended result. The cap was initially designed to replace the entirety of the ETF cap and was constructed with those dimensions (figure 5.2). From the past chapters it is known that the initial caps, intended to replace the ETF cap, produced no signal and further design and testing was needed. The next stage of designs were not constructed with the intention of replacing the current EFT cap but to evaluate why the initial cap designs did not optimize the signal. The final caps designs provided useful information about the PPG sensor and its performance. It was determined that the signal from the PPG sensor was optimized when there was no cap or covering around the optical components, the PPG sensor with no cap produced the most optimal signal, and should be utilized as the final design in future testing.

6.3   Future Work

With the inability to complete all of the future work for this project due to time and unforeseen circumstances. I think it is important to express future work for this project and further functionality that can be incorporated into the PPG sensor and the ETF device. The intention of this thesis was to completely install the PPG sensor into the cap of the tuning fork. Future work would have encompassed installing the sensor in the ETF cap such that the installation caused no adverse effects to the original ETF vibrational functionality, and the PPG sensor was able to collect accurate data from the patient. Installing the PPG sensor into the ETF entailed working with the electrical engineering department to program a motherboard to control the device and integrate it into the ETF electronics.

6.3.1 Integration of Sensor into ETF

The intention of the thesis is to incorporate the designed PPG sensor into the ETF cap. The intention was to design the optimal reflective based PPG sensor that is compatible with the ETF design, once the PPG sensor was optimized it would be integrated into the device. First the PPG sensor would have to be strategically incorporated in the ETF cap with wiring to the main control board. The sensor and the wires would have to incorporate in the device and not cause any negative effect on the vibrational signal. Because the goal is to take the electronic tuning fork, which has the ability to vibrate and test diabetic neuropathy, and add the ability to monitor blood oxygen saturation, any obstruction to its initial function would be adverse. The intention was to install the PPG sensor into the cap of the ETF with wiring that travels through the cap and up to the motherboard. The electronics in the motherboard of the ETF would be designed to control the sensor and relay SpO_2 data through the ETF monitor.

Future work is needed to integrate the sensor into the ETF cap. The thesis work involved, constructing different ETF cap designs to optimize the PPG signal, but It was determined that the most optimal PPG sensor was the sensor without any obstruction to the optical components. Work is needed to incorporate the sensor into the the ETF cap without inhibiting the emission and detection aspects of the sensor. Integration must involve containing the sensor within the ETF cap and keeping the LEDs and the photosensor exposed to be placed directly on the skin. The electronic tuning fork is a medical device that must be used between patients so some type of protective layer must be incorporated to the sensor. This protective layer will act as a barrier between the sensor and the tissue, but it is critical that this addition does not affect the sensor emissions.

6.3.2 Signal Optimization for Integration

Currently the PPG sensor is designed where the electronic components are controlled via the LabVIEW software and NI myDAQ but to integrate into the ETF an external motherboard would have to be utilized to control and collect data from the sensor. The intention was to use the NI myDAQ and LabVIEW software to optimize the LED control and signal manipulation for the

PPG sensor, and then convert that into electronics. All of the components of the sensor control and signal processing within the software must be analyzed to determine the most optimal settings for acquiring the PPG sensor. This entails optimizing; the frequency of signal acquisition, rate of LED state switching, length of time LED signal acquired, high pass filter, lowpass filter and, extent of signal collection needed for SpO_2 evaluation. The LabVIEW and NI myDAQ control system should be utilized to evaluate the effect of changing each signal manipulation component.

The first component is the rate of frequency of signal acquisition, this is dependent on the rate of acquisition of the phototransistor, and the NI myDAQ in this case. Future work will involve converting the signal components to electrical parts, so the frequency of acquisition will not be restricted to the rate of the DAQ, but rather the rate of the electrical components and motherboard.

The next signal component to be optimized is the rate of LED switching and the time each LED signal should be acquired. The sample and hold technique, utilized in the PPG sensor, is optimized by increasing the rate of attenuation between the LED states, because the PPG signal will have smaller gaps in the data between "switching". The rate at which the LEDs can be switched to power on and off is only restricted by the time of acquisition of the phototransistor, or the rise and fall time. For the particular phototransistor utilized in the sensor the rise time is 0.11ms, and represents the time it takes for the phototransistor to respond to the light, and the fall time is 0.22ms and is the time it takes the phototransistor to stop responding to light. Those two characteristics of the phototransistor must be accounted for when optimizing the rate of the LED switching.

Most all PPG sensors utilize high and low pass filters to extract the pulsatile signal and remove noise. The filters are utilized to eliminate the high and low frequency signals from the pulsatile signal of the heart rate. The high and low pass filters needed for a PPG sensor can be determined with an understanding of a normal heart rate signal. The current PPG sensor designed utilizes

112

high and low pass filters of 3Hz and 0.5Hz, respectively, and were determined as a result of biological heart rate. The lowpass filter at 0.5Hz would correlate to a heart rate of 30bpm, which is not biologically possible, and the high pass filter of 3Hz correlates to a heart rate of 180bpm. For future work these filters could be optimized to be more inclusive or exclusive of the PPG signal representing the heart rate.

The final signal component is the minimum amount of data needed to calculate the SpO_2. As discussed in previous chapters the SpO_2 calculation relies on the AC and DC components of a PPG signal. As we know the AC and DC components of the signal correlate to the systole and diastole cycles of the heart beating, and thus to make one SpO_2 calculation the heart must complete one cycle. Although this is the minimum time and signal needed to make the blood oxygen calculation, more data utilized for the calculation has been known to produce more accurate results. This is a component of the signal processing that could be optimized in future work to produce more accurate SpO_2 results.

Each signal processing component should be tested by changing their values and evaluating how the PPG signal amplitude, signal height and SNR change in response to the changes. The LabVIEW software and NI myDAQ provides easy control of the signal components allowing future work developing a more optimized signal. Once each component is optimized to produce the desired PPG signal, the control and signal manipulation, the device will be converted to electrical components and a central processing unit (CPU).

6.3.3   Electrical Integration

Future work will require working with the electrical engineering department to take my LabVIEW software and component control and build that into an external motherboard to be installed in the ETF. The external motherboard is capable of controlling the LEDs as well as acquiring and evaluation the PPG signal to calculate the SpO_2 value. As I do not know much about the electrical conversion from signal manipulation, additional help from others with a more

in-depth knowledge of electronics would be needed. The components such as high pass filter and signal control can be built into electrical components on a PCB. Future work would involve investigating the most optimal way of taking the components determined from the LabVIEW software and converting them into electronic components that can be incorporated into the ETF device.

The PPG sensor control and signal evaluation components would have to be combined on a signal PCB that could be incorporated into the ETF. This would require further evaluation of the ETF and how the device operates. The frequency at which the device controls the components would need to be determined as well as the voltage that is supplied from the batteries to the electrical components. The PPG installation would require variations to the sensor electronics depending on the supply voltage and the device frequency. Once the PPG electronics are optimized to incorporate with the device, further electronic integration is needed to merge the ETF screen to project the results from the PPG sensor. An analog to digital converter would be required to process the signal and produce a result that could be utilized and integrated into the ETF screen.

6.3.4   Final Sensor Integration

Once all aspects of the sensor have been optimized the integration into the ETF must be finalized. First the sensor must be mechanically integrated into the ETF cap. This includes installing the sensor so that the optical components are exposed on the tip of the cap. They sensor must fit sufficiently in the cap such that it can be placed on the tissue of a patient with mild pressure applied. The exposed sensor requires a covering to facilitate sanitary exchanges from patient to patient. The sensor covering will also illuminate electronic exposure and decrease failures as a result of exposure to the elements. Once integrated and the sensor signal processing components are optimized the sensor must be converted to a motherboard and central processing unit. The motherboard of the sensor must be compatible with the ETF electronics, operating at the same voltage, and small enough to fit within the sensor. Wiring from the PPG sensor in the

cap to the mother board integrated into the ETF device, must be done such that there is no effect on the vibrational mechanics of the tuning fork.

After all of the mechanical and electrical integrations are completed the final processes requires alterations to the ETF. The tuning fork operates with a single function, performing the vibrational sensation test. The ETF must be altered to incorporate blood oxygen saturation monitoring functionality. Future work would involve integrating a new "Mode" into the tuning fork so the user could change the evaluation method. If the examiner wanted to test the blood oxygen saturation, there would be a button to do so and the device would turn on the sensor to collect PPG data. The signal acquired from the sensor would be evaluated in the ETF and projected on the device's display monitor. This would be the finial component needed to integrate the sensor into the electronic tuning fork such that the device could monitor blood oxygen saturation and peripheral neuropathy on the same handheld device.

REFERENCES

[1]   A. R. M. Forkan and I. Khalil, "A Probabilistic model for early prediction of abnormal clinical events using vital sign correlations in home-based monitoring," *2016 IEEE Int. Conf. Pervasive Comput. Commun. PerCom*, 2016, doi: 10.1109/PERCOM.2016.7456519.

[2]   I. J. Brekke, L. H. Puntervoll, P. B. Pedersen, J. Kellett, and M. Brabrand, "The value of vital sign trends in predicting and monitoring clinical deterioration: A systematic review," *PLoS One*, vol. 14, no. 1, pp. 1–13, 2019, doi: 10.1371/journal.pone.0210875.

[3]   J. Kellett and F. Sebat, "Make vital signs great again – A call for action," *Eur. J. Intern. Med.*, vol. 45, pp. 13–19, 2017, doi: 10.1016/j.ejim.2017.09.018.

[4]   U. R. Acharya, K. P. Joseph, N. Kannathal, C. M. Lim, and J. S. Suri, "Heart rate variability: A review," *Med. Biol. Eng. Comput.*, vol. 44, no. 12, pp. 1031–1051, 2006, doi: 10.1007/s11517-006-0119-0.

[5]   S. Fischer, T. E. Stewart, S. Mehta, R. Wax, and S. E. Lapinsky, "Handheld Computing in Medicine," *J. Am. Med. Informatics Assoc.*, vol. 10, no. 2, pp. 139–149, 2003, doi: 10.1197/jamia.M1180.

[6]   A. S. John and C. P Price, "Existing and Emerging Technologies for Point-of-Care Testing," *Clin. Biochem. Rev.*, vol. 35, no. 3, pp. 155–167, 2014, doi: 10.3923/ajps.2011.133.139.

[7]   Y. Du and M. L. Wang, "State of the Art and New Perspectives for Non-Invasive Point-of-Care Testing," *Int. J. Biosens. Bioelectron.*, vol. 1, no. 1, pp. 9–11, 2016, doi: 10.15406/ijbsbe.2016.01.00002.

[8]   U.S Department of Health and Human Services Centers for Disease Control and Prevention, "National Diabetes Statistics Report," 2020.

[9]   J. J. Duby, R. K. Campbell, S. M. Setter, J. R. White, and K. A. Rasmussen, "Diabetic neuropathy: An intensive review," *Am. J. Heal. Pharm.*, vol. 61, no. 2, pp. 160–176, 2004, doi: 10.1093/ajhp/61.2.160.

[10]   R. Pop-Busui *et al.*, "Diabetic neuropathy: A position statement by the American diabetes association," *Diabetes Care*, vol. 40, no. 1, pp. 136–154, 2017, doi: 10.2337/dc16-2042.

[11]   A. J. M. Boulton *et al.*, "Comprehensive foot examination and risk assessment," *Diabetes Care*,

vol. 31, no. 8, pp. 1679–1685, 2008, doi: 10.2337/dc08-9021.

[12]   Centers for Disease Control and Prevention, "Long-term Trends in Diabetes," *CDC's Div. Diabetes Transl.*, 2014.

[13]   K. S. Saladin, *Anatomy & physiology : the unity of form and funtion.* Boston: McGraw-Hill Higher Education, 2010.

[14]   P. Tate and R. R. Seeley, *Seeley's principles of anatomy*. New York: McGraw-Hill, 2009.

[15]   T. Ysehak Abay, "Reflectance Photoplethysmography for Non-invasive Monitoring of Tissue Perfusion," University of London, 2016.

[16]   J. A. Collins, A. Rudenski, J. Gibson, L. Howard, and R. O'Driscoll, "Relating oxygen partial pressure, saturation and content: The haemoglobin–oxygen dissociation curve," *Breathe*, vol. 11, no. 3, pp. 194–201, 2015, doi: 10.1183/20734735.001415.

[17]   M. Elgendi, "On the Analysis of Fingertip Photoplethysmogram Signals," *Curr. Cardiol. Rev.*, vol. 8, no. 1, pp. 14–25, 2012, doi: 10.2174/157340312801215782.

[18]   P. L. Ricketts *et al.*, "Non-Invasive Blood Perfusion Measurements Using a Combined Temperature and Heat Flux Surface Probe," *Natl. Institutes Heal.*, vol. 23, no. 1, pp. 1–7, 2011, doi: 10.1161/CIRCULATIONAHA.110.956839.

[19]   Rachel Hajar, "The Pulse from Ancient to Modern Medicine: Part 3," *Hear. Views*, vol. 18, no. 2, pp. 109–14, 2017, doi: 10.4103/HEARTVIEWS.HEARTVIEWS.

[20]   K. D. Kochanek, S. L. Murphy, J. Xu, and E. Arias, "National Vital Statistics Reports Deaths: Final Data for 2017," 2019. [Online]. Available: https://www.cdc.gov/nchs/products/index.htm.

[21]   F. Sessa *et al.*, "Sessa2018," vol. 10, no. 2, pp. 166–177, 2018.

[22]   D. G. Katritsis, B. J. Gersh, and A. J. Camm, "A Clinical Perspective on Sudden Cardiac Death," *Arrhythmia Electrophysiol. Rev.*, pp. 203–209, 2016, doi: 10.15420/aer.2016.

[23]   T. I. Papon, I. Ahmad, and N. Saquib, "Photoplethysmographic Analysis of Optical Signals : A Single Device to Measure All the Vital Signs," Bangladesh University of Engineering and Technology, 2015.

[24]   J. L. Moraes, M. X. Rocha, G. G. Vasconcelos, J. E. Vasconcelos Filho, V. H. C. de Albuquerque, and A. R. Alexandria, "Advances in Photopletysmography Signal Analysis for Biomedical Applications," *Sensors (Switzerland)*, vol. 18, no. 6, pp. 1–26, 2018, doi: 10.3390/s18061894.

[25]   B. B. Hafen and S. Sharma, "Oxygen Saturation," *NCBI Bookshelf. A Serv. Natl. Libr. Med. Natl. Institutes Heal.*, pp. 1–5, 2020.

[26]   B. R. O'Driscoll, L. S. Howard, J. Earis, and V. Mak, "BTS guideline for oxygen use in adults in healthcare and emergency settings," 2017. doi: 10.1136/thoraxjnl-2016-209729.supp1.

[27]   R. Sarma, C. I. Prickett, and J. L. Johnson, "Assessment of Clinical Laboratory Techniques in the Measurement of Oxygen Saturation in Whole Blood," *Med. J. Aust.*, vol. 2, no. 16, pp. 585–586, 1974, doi: 10.5694/j.1326-5377.1974.tb71020.x.

[28]   J. G. Webster, *Design of Pulse Oximeters.* Bristol Philadelphia: Institute of Physics Publishing, 1997.

[29]   P. Bosc Author, W. K. Smith, and P. C. Miller, "A Modified Van Slyke Method for the Determination of Dissolved Oxygen and Total Carbon Dioxide in Water," *Source Physiol. Zool.*, vol. 46, no. 3, pp. 186–207, 1973.

[30]   J. W. Severinghaus, "The invention and development of blood gas analysis apparatus," *Anesthesiology*, vol. 97, no. 1, pp. 253–256, 2002, doi: 10.1097/00000542-200207000-00031.

[31]   A. Jubran, "Pulse oximetry," *Crit. Care*, vol. 19, no. 1, pp. 1–7, 2015, doi: 10.1186/s13054-015-0984-8.

[32]   F. Huang, P. Yuan, K. Lin, H. Chang, and C. Tsai, "Analysis of Reflectance Photoplethysmograph Sensors," *World Acad. Sci. Eng. Technol.*, vol. 59, pp. 1266–1269, 2011.

[33]   Z. Bai, X. Chen, and J. Li, "A Miniaturized Single-Chip Oximetry Module Utilizing Reflectance Photoplethysmography," *2017 10th Int. Congr. Image Signal Process. Biomed. Eng. Informatics*, vol. 2018-Janua, pp. 1–5, 2018, doi: 10.1109/CISP-BMEI.2017.8302250.

[34]   N. Stuban and M. Niwayama, "Optimal filter bandwidth for pulse oximetry," *Rev. Sci. Instrum.*, vol. 83, no. 10, pp. 1–6, 2012, doi: 10.1063/1.4759491.

[35]   Y. Arora, S. Ramasahayam, and S. R. Chowdhury, "An Optimal Reflection Photoplethysmographic Sensor System Based on Skin Optics," *IEEE Sens. J.*, vol. 18, no. 17, pp. 7233–7241, 2018, doi: 10.1109/JSEN.2018.2850893.

[36]   M. Nitzan *et al.*, "Calibration-free pulse oximetry based on two wavelengths in the infrared - A preliminary study," *Sensors (Switzerland)*, vol. 14, no. 4, pp. 7420–7434, 2014, doi: 10.3390/s140407420.

[37] T. Tamura, Y. Maeda, M. Sekine, and M. Yoshida, "Wearable photoplethysmographic sensors— past and present," *Electronics*, vol. 3, no. 2, pp. 282–302, 2014, doi: 10.3390/electronics3020282.

[38] Y. Mendelson and B. D. Ochs, "Noninvasive Pulse Oximetry Utilizing Skin Reflectance Photoplethysmography," *IEEE Trans. Biomed. Eng.*, vol. 35, no. 10, pp. 798–805, 1988, doi: 10.1109/10.7286.

[39] J. Allen, "Photoplethysmography and its application in clinical physiological measurement," *Physiol. Meas.*, vol. 28, no. 3, 2007, doi: 10.1088/0967-3334/28/3/R01.

[40] Y. Mendelson, "Pulse oximetry: Theory and applications for noninvasive monitoring," *Clin. Chem.*, vol. 38, no. 9, pp. 1601–1607, 1992, doi: 10.1093/clinchem/38.9.1601.

[41] R. P. Dresher and Y. Mendelson, "Reflectance forehead pulse oximetry: Effects of contact pressure during walking," *Annu. Int. Conf. IEEE Eng. Med. Biol. - Proc.*, pp. 3529–3532, 2006, doi: 10.1109/IEMBS.2006.260136.

[42] R. Lundström, H. Dahlqvist, M. Hagberg, and T. Nilsson, "Vibrotactile and thermal perception and its relation to finger skin thickness," *Clin. Neurophysiol. Pract.*, vol. 3, pp. 33–39, 2018, doi: 10.1016/j.cnp.2018.01.001.

[43] K. Budidha and P. A. Kyriacou, "The human ear canal: Investigation of its suitability for monitoring photoplethysmographs and arterial oxygen saturation," *Physiol. Meas.*, vol. 35, no. 2, pp. 111–128, 2014, doi: 10.1088/0967-3334/35/2/111.

[44] A. Kiruthiga *et al.*, "Reflectance Pulse Oximetry for Blood Oxygen Saturation Measurement from Diverse Locations-A Preliminary Analysis," *2018 IEEE Int. Symp. Med. Meas. Appl.*, pp. 1–6, 2018, doi: 10.1109/MeMeA.2018.8438781.

BIOGRAPHY OF THE AUTHOR

Madeline Mazjanis was born in York, Maine on April 27th 1995. She was raised in Portland, Maine and graduated from Deering High School in 2013. She attended the University of Maine where she graduated in 2017 with a Bachelor's degree in Bioengineering. She returned to the University of Maine in January of 2018 and entered the Biomedical Engineering graduate program. After completing her graduate courses, she joined IDEXX to begin her carrier as a Systems Engineer. She has been working and completing her thesis for the past year. Madeline is a candidate for the Master of Science degree in Biomedical Engineering from the University of Maine in December 2020.